Supercritical Fluid Assisted Recovery of Organometallic Catalysts from Polymers

by

Lijuan Yang

A thesis
presented to the University of Waterloo
in fulfillment of the
thesis requirement for the degree of
Doctor of Philosophy
in
Chemical Engineering

Waterloo, Ontario, Canada, 2012

AUTHOR'S DECLARATION

I hereby declare that I am the sole author of this thesis. This is a true copy of the thesis, including any required final revisions, as accepted by my examiners.

I understand that my thesis may be made electronically available to the public.

Abstract

The recovery of organometallic catalysts from polymer matrices is of great importance in promoting the application of homogeneous catalysts in industry. Such a green recovery technique will not only popularize the techniques of green catalytic hydrogenation of polymers by Rempel's group, but also consummates the technique of heterogenization of organometallic catalysts. The high value product of hydrogenated nitrile butadiene rubber (HNBR) with dissolution of Wilkinson's catalyst [$RhCl(TPP)_3$] was selected as the model polymer matrix for developing a green separation technique.

The supercritical carbon dioxide ($scCO_2$) soluble fluorous Wilkinson's catalyst [$RhCl(P(p\text{-}CF_3C_6H_4)_3)_3$] was synthesized and shown exhibit a very limited activity in the catalytic hydrogenation of bulk HNBR. Its recovery from a HNBR matrix using $scCO_2$ however failed. In spite of the assistance of the $scCO_2$ dissolvable chelating ligand thenoyltrifluoroacetone (TTA), the weak compatibility of $scCO_2$ with rhodium complexes failed again as an extraction solvent for the HNBR matrix. Inspired by the merits of CO_2-expanded liquids (CXLs) and the versatility of CO_2 in changing the physical properties of polymer melts, CXLs were tested as extracting solvents for separation of Wilkinson's catalyst from bulk HNBR. CO_2-expanded water (CXW) and CO_2-expanded alcohols including methanol and ethanol (CXM and CXE) were examined with the assistance of a variety of chelating agents. The investigated chelating agents include ethylenediaminetetraacetic acid (EDTA), ethylenediaminetetraacetic acid disodium salt ($EDTA\text{-}Na_2$), diethylenetriamine (DETA), N,N,N',N',N''-pentamethyldiethylenetriamine (PMDETA), and N,N,N',N'-tetramethylethylenediamine (TMEDA). CXM and PMDETA

were recognized as the optimal combination of extracting solvent and chelating agent for recovery of Wilkinson's catalyst from HNBR.

An extraction system consisting of CXM and PMDETA was carefully investigated with respect to the effects of temperature and pressure on the extraction performance over the temperature range of 40 to 100 °C and the pressure range of 20 to 200 bar. Increasing temperature effectively increased the extraction rate and became less influential when the temperature was above 80 °C. Increasing pressure at a fixed temperature was found to improve the extraction rate followed by suppressing it. Nevertheless, further increasing the pressure to an extreme high value above the respective critical point was able to promote the extraction rate again. The complex effects of pressure were thoroughly investigated by the means of analyzing the dissolution behavior of CO_2 in HNBR and the variation of the extraction phase composition at different operational conditions. 0.14 g/mL was determined as the CO_2 density by which the optimal pressure at a fixed temperature can be estimated. Based on a careful interpretation of the experimental results, an extraction mechanism was illustrated for interpreting the present extraction system. Additionally, the reactions involved in the extraction process were illustrated to reveal the principal challenges present in the extraction process and pointed out the potential solution for eliminating the obstacles. Two special operations-sequential operation and pressure varying procedure were tested for their effectiveness in enhancing the extraction ratio. A pressure varying procedure was found to be beneficial in further improving the extraction ratio, while sequential operation did not show any promise in enhancing the recovery. At last, the developed technique was shown to be highly efficient in applying it to HNBR particles coagulated from the HNBR latex. A residue

of 59 ppm rhodium was obtained after 9 hours of operation. This study establishes a technology platform for separating the expensive catalyst from the polymer matrix, using "green" CO_2-expanded liquids.

Acknowledgements

Grateful appreciation is given to my supervisors: Professor Garry L. Rempel and Professor Qinmin Pan for their instructive guidance, generous financial support, and patience. I want to gratefully acknowledge my indebtness to them. I believe this indebtness will work as an impetus for my future research and serving our community.

Many thanks are given to the colleagues whom I worked with in the past four years. It is a pleasant experience to work and progress with them. They are Jialong Wu, Hui Wang, Karl Liu, Allen Liu, Enefiok Akpan, Ting Li, Ray Zou, Yan Liu, David Nissim, and Jungho Kang.

Special thanks also go to the staffs of the Chemical Engineering Department of University of Waterloo for their help in safety issues, instrument using, for their patience and help. They are Rick Hecktus, Ralph Dickhout, Lorna Kelly, and Rose Guderian.

I am very pleased with the encouragement I received from the friends I made in Kitchener-Waterloo. They are Pam and Don Harrison, Jim and Leona Mason, Krystal Lowes and Liya Zhang. With them, life has been very enjoyable here in Kitchener and Waterloo.

I gratefully acknowledge my indebtness to my family: my parents and my sister. With love, understanding and endurance, they helped me complete my Ph. D studies.

Lijuan Yang, May 2012, Waterloo, Canada

Table of Contents

AUTHOR'S DECLARATION ii

Abstract iii

Acknowledgements vi

Table of Contents vii

List of Figures xii

List of Tables xvi

Chapter 1 General Introduction 1

1.1 Organometallic catalyst and its recovery 1

1.2 Organometallic complex recovery from a polymer matrix 2

1.3 Application of supercritical fluid techniques for catalyst recovery 4

1.4 Layout of the thesis 6

Chapter 2 Literature Review 9

2.1 Chemical properties and catalytic reactions of Wilkinson's catalyst 9

2.1.1 Stoichiometric reactions of Wilkinson's catalyst 10

2.1.2 Catalytic reactions using Wilkinson's Catalyst 15

2.2 Development of organometallic catalyst recovery technology 15

2.2.1 Ion exchange resin adsorption 16

2.2.2 Biphasic catalysis via organometallic catalyst 17

2.3 Application of $scCO_2$ in recovery of organometallic catalyst from polymer matrix 25

2.3.1 Introduction to supercritical fluids 26

2.3.2 Strategies to increase an organometallic compound's solubility in $scCO_2$ 29

2.3.3 Application of $scCO_2$ for polymer processing 31
2.4 Application of CXLs in recovery of organometallic catalysts from polymer matrices 32
2.4.1 Introduction of CXLs 33
2.4.2 Properties of CXM 34
2.5 Summary 35
Chapter 3 Research Methodology and Approaches 37
3.1 Materials 37
3.1.1 Chemicals in catalysts preparation and catalytic hydrogenation 37
3.1.2 Chemicals in sample preparation 38
3.1.3 Chemicals in extraction 38
3.1.4 Chemicals in digestion and inductively coupled plasma analysis 38
3.2 Experimental procedures 39
3.2.1 Fluorinated Wilkinson's catalyst synthesis and bulk hydrogenation 39
3.2.2 Preparation of the extraction samples 39
3.2.3 Extraction using $scCO_2$ or CXLs 40
3.2.4 Digestion procedure 42
3.2.5 ICP analysis and extraction ratio calculation 43
3.3 Verification of the procedures involved in CXM extraction 44
3.3.1 The distribution of Wilkinson's catalyst in HNBR films 44
3.3.2 Different MEK evaporation approaches 45
3.3.3 Different sampling methods 47
3.3.4 Different post-treatment methods applied on the digestion solutions 50

3.3.5 Matrix effects on the ICP analysis 53
3.3.6 Duplication and error analysis 56
3.4 Summary 59
Chapter 4 Recovery of Rhodium Catalysts Using Supercritical Carbon Dioxide 60
4.1 Fluorinated analogue of Wilkinson's catalyst 60
4.1.1 Solubility of the fluorinated Wilkinson's catalyst in $scCO_2$ 62
4.1.2 NBR bulk hydrogenation with the fluorinated Wilkinson's catalyst 63
4.1.3 Recovery of the fluorous Wilkinson's catalyst using $scCO_2$ 65
4.2 Recovery of rhodium catalysts using $scCO_2$ and chelating ligands 67
4.2.1 Extraction of $RhCl_3$ from aqueous solution using $scCO_2$ and TTA 68
4.2.2 Extraction of rhodium catalysts from their crystals using $scCO_2$ and TTA 70
4.2.3 Extraction of rhodium catalysts and from a NBR matrix using $scCO_2$ and TTA .. 71
4.3 Extraction of $RhCl_3$ using CXLs 71
4.3.1 Extraction of $RhCl_3$ using CXW 72
4.3.2 Extraction of $RhCl_3$ using CXLs and chelating ligands 75
4.4 Summary 79
Chapter 5 Recovery of Wilkinson's Catalyst Using CXLs 81
5.1 CO_2-expanded water 81
5.2 CO_2- expanded alcohols 86
5.3 Characterization of the complex of Wilkinson's catalyst and PMDETA 89
5.4 Study on the usage of PMDETA 92
5.5 Study on the application of the amount of methanol in each run 95

5.6 Investigation of the thickness of the HNBR film 95
5.7 Investigate of the function of CO_2 97
5.8 Summary 99
Chapter 6 Tunability of the Process via Changing Temperature and Pressure 101
6.1 Experimental data collection 102
6.2 Function of temperature 103
6.2.1 Experimental results 103
6.2.2 Analysis of the effects of temperature 109
6.3 Effect of CO_2 pressure 112
6.3.1 Experimental results 112
6.3.2 Phase behavior of HNBR/CO_2 and methanol/CO_2 117
6.3.3 Identification of the extraction phase 126
6.3.4 Variation of the extraction phase polarity 131
6.4 Interpretation of the tunability 132
6.4.1 Optimal Pressure of CO_2 135
6.5 Extraction mechanisms 138
6.6 Reactions and Challenges 142
6.7 Summary 145
Chapter 7 Two Special Operational Procedures 147
7.1 Varying pressure procedure 147
7.2 Sequential Extraction 148
7.3 Application on the HNBR particles coagulated from the HNBR latex 151

7.4 Summary 152
Chapter 8 Conclusions and Recommendations for Future Research 153
8.1 Conclusions 153
8.1.1 Recovery of rhodium catalysts using $scCO_2$ 153
8.1.2 Recovery of Wilkinson's catalyst using CXLs and chelating agents 154
8.1.3 Function of temperature and pressure 154
8.1.4 Extraction mechanism involved 155
8.1.5 Identification of the major obstacle 156
8.1.6 Milestones and contributions 157
8.2 Recommendations for future research 158
8.2.1 Further investigation on the $scCO_2$ system 158
8.2.2 Further investigation of CXM system 159
8.2.3 Recovery of the catalyst in a latex system 160
Nomenclature 161
Appendix A Original Experimental Data 165
Bibliography 175

List of Figures

Figure 2-1. Some chloro ligand substitution reactions. 11

Figure 2-2 Some TPP displacement reactions 13

Figure 2-3 Silica-based PPh_2-containing ion exchangers, bearing different spacer lengths... 16

Figure 2-4 Molecular Structure of TPPTS 20

Figure 2-5 Schematic pressure-temperature phase diagram for a pure component showing the supercritical fuid (SCF) region 27

Figure 2-6 Illustration of the generation of a CXL 33

Figure 3-1 Schematic Diagram of the Extraction Apparatus 42

Figure 3-2 Extraction sample characterized by scanning electron microscope (SEM) 45

Figure 3-3 Static extraction profiles of CXM and PMDETA on HNBR/Wilkinson's catalyst films at 40 °C and 100 bar collected via different methods 48

Figure 3-4 Spike recovery of 10 spiked samples and the average spike recovery obtained from them 55

Figure 4-1 FT-IR of $RhCl(TTFMPP)_3$ and TTFMPP 62

Figure 4-2 Conventional Wilkinson's Catalyst (1) and Modified Catalyst (2) 62

Figure 4-3 Equipment illustration and pressure varying procedure in rhodium extraction 69

Figure 4-4 Extraction Ratio vs TTA Loading 70

Figure 4-5 Ligand Function Confirmation 77

Figure 4-6 Extraction Efficiency of Different Initial Concentration 79

Figure 5-1 Molecular structures of EDTA, EDTA disodium salt dihydrate, DETA, TMEDA and PMDETA in the order of a, b, c, d, and e. 83

Figure 5-2 A. draw of the molecular structure of the Wilkinson's catalyst; B. draw of the molecular structure of the coordination complex formed by PMDETA and most of the metals. 90

Figure 5-3 Static extraction profiles of CXM and different loadings of PMDETA on HNBR/Wilkinson's catalyst films at 40 °C and 100 bar 93

Figure 5-4 Static extraction profiles of CXM and PMDETA on HNBR films with thickness of 0.3 or 0.6 mm under various pressures (20, 40, 60, 100, 150 and 200 bar) at 80 °C 96

Figure 5-5 Static extraction profiles of methanol, PMDETA and compressed CO_2 or N_2 on HNBR films under different pressure of 20 and 60 bar at 80 °C..... 98

Figure 6-1 Static extraction profiles of Wilkinson's catalyst using CXM and PMDETA from HNBR films at different temperatures of 40, 50, 60, and 80 °C at atmospheric pressure.... 104

Figure 6-2 Static extraction profiles of Wilkinson's catalyst from HNBR films using CXM and PMDETA at different temperatures of 40, 50, 60, 70, 80, 90, 100 °C under a fixed pressure: a. 20 bar, b. 40 bar, c. 60 bar, d. 100 bar, e. 200 bar. 108

Figure 6-3 Static extraction profiles of Wilkinson's catalyst from HNBR films using CXM and PMDETA under different pressures of 20, 40, 60, 100 and 200 bar at a fixed temperature: a. 40 °C, b. 50 °C, c. 60 °C, d. 70 °C, e. 80 °C, f. 90 °C, g. 100 °C. 115

Figure 6-4 Saturation mass ratios of CO_2 to HNBR as a function of pressure at different temperatures of 40, 50, 60, 70, 80, 90, and 100 °C, simulated using the PC-SAFT equation of state and parameters (M_w=100,000, m=0.0263, σ(Å)=4.0217, ε/k(K)=249.5, k_{ij}^0= -0.3840, k_{ij}^1= 0.5263, and k_{ij}^2= 0.6120) based on von solms' report 122

Figure 6-5 Isothermal phase equilibrium for binary system of MeOH+CO_2 simulated by PC-SAFT using the parameters (m=1.5255, σ=3.2300, ε/k=188.9, κ^{AB}=0.035176, ε^{AB}/k=2899.5, k_{ij}^{0}=0.0354, k_{ij}^{1}=-5.8339): a. simulation results for temperatures from 40 to 100 °C, b. comparion of the simulation results and the literature reports at temperatures of 40, 80 and 100 °C. 125
Figure 6-6 Isothermal vapor and liquid equilibrium (VLE) phase compositions of CO_2 and methanol at different temperatures of 40, 50, 60, 70, 80, 90, and 100 °C and the feeding mole fraction of CO_2 based on CO_2 and methanol under various experimental pressures at the respective same temperature. 130
Figure 6-7 Mole fractions of CO_2 (denoted by x) in the extraction phase as a function of the feeding pressure at various temperatures, and the solvent polarity of CXM (characterized by π^*) as a function of the mole fraction of CO_2 at 40 °C from the literature 132
Figure 6-8 Static extraction profiles of Wilkinson's catalyst from HNBR films using CXM and PMDETA under different pressures of 20, 40, 60, 80, 100 and 200 bar at 100 °C. 136
Figure 6-9 Density of CO_2 at different temperatures of 40, 50, 60, 70, 80, 90, and 100 °C and pressure range from 0 to 200 bar. 137
Figure 6-10 Schematic diagram illustrating the extraction process: (a) extraction vessel; (b) one single polymer strip selected for the mass transfer investigation; (c) methanol (MeOH) expanded by CO_2; polymer plasticized by CO_2; PMDETA absorbs on the surfaces of the polymer and reacts with Wilkinson's catalyst distributed on the polymer surfaces; (d) Wilkinson's catalyst diffusing from the interior of the polymer towards its surfaces; (e) Wilkinson's catalyst coordinates with the functional groups of the polymer and is retained in

the polymer matrix; (f) separation of Wilkinson's catalyst terminated and the volume of polymer recovered after the CO_2 release. 140
Figure 6-11 Schematic diagram illustrating the events taking place in the extraction process: (a) reactions within HNBR; (b) diffusion of Wilkinson's catalyst and PPh_3 in HNBR; (c) PMDETA complexation of Wilkinson's catalyst on the interfaces of HNBR and CXM 144
Figure 7-1 Extraction profiles collected under the square-wave pressure varying between 50 and 100 bar, or under a constant pressure of 60 or 100 bar at 80 °C. 148
Figure 7-2 Extraction profiles obtained at 80 °C and 60 bar by static operation and sequential operation (Runs 0, 1, 2 and 3 represent 0, 3, 6 and 9 h extraction, respectively) 150
Figure 7-3 Sequential extraction results on the HNBR particles coagulated from its latex at 80 °C and 60 bar (Runs 0, 1, 2, and 3 represent 0, 3, 6, and 9 h extraction, respectively) ... 151

List of Tables

Table 2-1 Critical Data for selected Substances 28

Table 3-1 Experimental parameters and extraction results obtained under various pressures (20, 40, 60,100 and 200 bar) at 80 °C on samples dried by two different methods 46

Table 3-2 Experimental parameters and extraction results obtained at 40 °C and 100 bar with two different sample collecting approaches 49

Table 3-3 Experimental parameters and ICP analysis results obtained on the digestion solutions from the same HNBR matrices but with different post-treatments 51

Table 3-4 Experimental parameters and ICP analysis results obtained on 10 random samples and their spikes 54

Table 3-5 Extraction results obtained in two times operation at 90 and pressure from 20 to 200 bar 56

Table 4-1 Experimental parameters and results obtained for bulk hydrogenation with different catalysts and ligands..... 64

Table 4-2 Experimental parameters and results obtained for the $scCO_2$ extraction of rhodium catalyst from HNBR at 70 °C and 270 bar in 2 h 67

Table 4-3 Experimental parameters and results obtained for the extraction of $RhCl_3$ from its aqueous solution under 150 bar at 60 °C 70

Table 4-4 Experimental parameters and results obtained for the extraction of $RhCl_3$ from NBR using CXW 73

Table 4-5 Experimental parameters and results obtained for the extraction of $RhCl_3$ from NBR using CXW, analyzed by ICP..... 74

Table 4-6 Extraction Routes Description 76

Table 4-7 Extraction Routes Description 78

Table 5-1 Experimental conditions and performance of various chelating ligands on removal of Wilkinson's catalyst from HNBR using CXW 82

Table 5-2 Applicable physical or chemical properties of the chelating ligands investigated. 83

Table 5-3 Experimental conditions and performance of various chelating ligands on removal of Wilkinson's catalyst from HNBR using CXM and CXE 87

Table 5-4 Physical and chemical properties of Wilkinson's catalyst and PMDETA 90

Table 5-5 Titration of PMDETA with Wilkinson's catalyst 92

Table 5-6 Experimental parameters and extraction results obtained at 40 °C and 100 bar with different loadings of PMDETA 92

Table 5-7 Experimental parameters and extraction results obtained with different usages of methanol at 80 °C and 60 bar 95

Table 6-1 Pure-component parameters of the PC-SAFT equation of state for HNBR, MeOH and CO_2 121

Table 6-2 Interaction parameters to correct cross-dispersive interactions for CO_2 (*i*) + HNBR (*j*) or MeOH (*j*) systems 121

Table 6-3 Published phase equilibrium data for the binary system of MeOH+CO_2 124

Table 6-4 Critical points of the binary system of MeOH+CO_2 at different temperatures 124

Table A-1 Experimental parameters and extraction results obtained under 20 and 60 bar at 80 °C with N_2 added into the system 165

Table A-2 Experimental parameters and extraction results obtained under various pressures (20, 40, 60, 100, 150 and 200 bar) at 80 °C on the samples with a thickness of 0.3 or 0.6 mm 165
Table A-3 Experimental parameters and extraction results obtained under various pressures (0, 20, 40, 60, 100, 200 bar) and temperatures (40, 50, 60, 70, 80, 90, and 100 °C)..... 168

Chapter 1
General Introduction

1.1 Organometallic catalyst and its recovery

Homogeneous catalysis using transition metal complexes is an area of research that has grown enormously in recent years. Organometallic catalysts consist of a central metal surrounded by ligands and prominently feature with high selectivity arising from the large variety of ligands that can be used. High selectivity provides a great advantage to green chemistry in terms of reducing waste, reducing the work-up equipment of a plant, and ensuring a more effective use of the feed stocks. Besides, homogeneous catalysts are more reactive than heterogeneous catalysts as a result of the elimination of mass transfer concerns that are involved in the heterogeneous catalytic process.

However the primary disadvantage of homogeneous transition metal catalysts that has prevented them from extensive application is the difficulty of separating the catalyst from the product. Heterogeneous catalysts are either automatically removed in the process (e. g., gas-phase reactions in fixed-bed reactors), or they can be separated by simple methods such as filtration or centrifugation. In the case of homogeneous catalysts, more complicated processes such as distillation, liquid–liquid extraction, and ion exchange must often be used [*1*]. One of the effective measures to improve the separability of a homogeneous catalyst is heterogenizing it into an independent phase which is immiscible with the phase that contains the reactants and products. The phase for heterogenization of a homogeneous catalyst can be water, a fluorous compound, an ionic liquid, or a solid [*2*]. For the heterogenization via solid supports, most of the time, the organometallic catalyst precursor is required to be anchored on to the surface of the solid by a coordinative interaction.

1.2 Organometallic complex recovery from a polymer matrix

Polymer resins have been widely used by different means targeted for the homogeneous catalyst recovery: absorbing organometallic catalysts from the product stream after completion of the reaction or by heterogenizing a homogeneous organometallic catalyst before the reaction. However, the polymer resins suffer from a limited lifetime and their performance always decreases upon subsequent usage. Hence, an effective separation technique is urged to be developed for recovery of the metal values from the polymer resins so as to reduce the investment involved in using a precious metal based organometallic catalyst.

Although the organometallic catalyst heterogenization technique is a very effective strategy for realizing ease of catalyst recovery, its application range is restricted to the substrates of gaseous reagent or small molecule chemicals so that the mass transfer problems related to a heterogeneous catalysis process can be well circumvented. When the organometallic catalyst heterogenization technique is applied to polymeric systems, it suffers not only from mass transfer problems due to the high viscosity of the polymer solutions, but also from catalyst leaching problems arising from frictions between the polymer molecule and the anchored organometallic complex.

Hydrogenated nitrile butadiene rubber (HNBR) is an extremely useful commercial product with many important applications in the automotive, oil, and atomic energy industries, making the hydrogenation of NBR an active area for research [*3-7*]. Therban® HNBR is one of the most competitive commercial HNBR products with high quality and less extraneous components. The production of Therban® HNBR is carried out in solution and is

catalyzed by the costly Wilkinson's catalyst, i.e. tris(triphenylphosphine) chloro rhodium(I) [$RhCl(TPP)_3$], and involves a large amount of toxic organic solvent, i.e. monochlorobenzene (MCB) [*3*]. Hydrogenation of nitrile rubber in latex form has been appraised of being of high practical importance in the commercial production of HNBR, since its precursor NBR is usually synthesized by emulsion polymerization [*4*]. This allows for a direct preparation of HNBR from the latex without isolation of NBR and substantially reduces the costs involved by using an organic solvent and its subsequent removal. In addition, bulk hydrogenation of nitrile rubber has been reported as another alternative approach for production of HNBR without using any organic solvent [*5*]. The catalyst systems utilized in these two processes are either Wilkinson's catalyst itself or one of its water soluble analogues, which constitute a significant investment as it is required to recover the rhodium in the catalyst. The effective removal of Wilkinson's catalyst from the HNBR melt is considered to be essential for the overall success of these hydrogenation processes.

Compared to the polymer melt, polymer resins are more favored as a matrix from which to separate the organometallic complex, because it is usually commercially manufactured in the form of beads with porous internal structure. Therefore, the metal value recovery from such a polymer resin matrix is expected to be easier than that from the polymer melt, i.e. HNBR. HNBR with dissolution of Wilkinson's catalyst was hence used as the model polymer for developing this organometallic complex separation technique. The objective of this project is thus to develop an effective and green catalyst recovery system for removal of Wilkinson's catalyst from the HNBR melt and to try to understand the mechanism involved, and ultimately to optimize the extraction operation conditions. The

success of this technique will not only benefit the metal value recovery from the resin beads, but also lead to a great revolution of the hydrogenation process for other polymers as well.

According to the best of our knowledge, there has been no literature reported regarding the removal of Wilkinson's catalyst from an HNBR melt. Nevertheless, there have been typically two options for recovery of metal values from the resins: elution and fuming. Elution is a method by which the resin is chemically striped of the metal and recycled. "Fuming", on the other hand, is a method of recovering the metal by thermally decomposing the resin matrix to yield a metallic concentrate. The method of "fuming" is obviously not a good reference for the investigated system, because it decomposes the matrix. Meanwhile, the elution method suffers from extensive organics consumption and incomplete recovery of the metal values. The conventional elution method will not be a good candidate for separation of the rhodium complex from HNBR melts either, because Wilkinson's catalyst is dissolved in the HNBR melts and more serious mass transfer resistance is encountered within the HNBR melts than in the polymer resin beads.

1.3 Application of supercritical fluid techniques for catalyst recovery

Supercritical fluids (SCF), especially supercritical carbon dioxide ($scCO_2$) has been used in a variety of chemical processes as a versatile alternative solvent being inertial, non-toxic, and environmental benign. The dissolution of CO_2 into a polymer matrix will induce the plasticization of polymers and impose effects on a few of their physical properties [*6-11*]. Those effects include reduction of glass transition temperature (T_g) [*7, 9*], depression of viscosity [*8, 10*], and enhancement of permeability [*9, 11*]. The diffusion of additives through polymers is significantly improved by adding CO_2 and thus provides an advantage to

processes requiring delivery of additives in or out of the polymer. In addition, the change in the extent of these physical properties can be manipulated through adjusting temperature and pressure. For instance, increasing temperature and pressure generally decreases the viscosity of polymer melts and increases their permeability [*9*].

Although using $scCO_2$ has the benefit of regulating the physical properties of the polymer matrix, the non-polar solvent property of $scCO_2$ greatly restricts the solubility of most organometallic complexes in it. Fortunately, a novel green CO_2-expanded liquids (CXLs) technique has the best solution for both worlds by providing adequate solvation power towards the organometallic complex and reserving the regulation ability to the physical properties of the polymer matrix as well [*12*]. CXLs can be continuously tuned from the neat organic solvent to supercritical carbon dioxide ($scCO_2$) through changing the CO_2 composition, as modulated by adjusting the operating pressure of CO_2 [*13*]. Most rhodium catalysts are only sparsely soluble in $scCO_2$, whereas adequate solubility of them in CXL can be easily obtained. By taking advantage of the large solubility, homogeneous catalysis can be carried out in CXLs with CO_2 pressures an order of magnitude lower than those required in $scCO_2$ [*14, 15*]. Additionally, the tunable properties of CXL provide the feasibility of catalyst recycle following the extraction from the polymer matrix. Furthermore, the addition of a cosolvent, i.e. ethanol was able to enhance the benefits offered by CO_2 in enhancing the diffusion of additives inside the polymer melts due to the improved interactions between the solvent and the polymer [*16*]. The combination of tuning CO_2 and adding cosolvent provides for more controllable process parameters and allows for the impregnation of thermally labile and metastable materials under lower temperature and pressure.

1.4 Layout of the thesis

In this thesis, the work reported is that done for developing an effective and green technique for separation of organometallic catalysts from polymers with assistance of $scCO_2$.

In Chapter 1, the general background on homogeneous catalysts, i.e. organometallic catalyst and its recovery is presented along with the development of the polymer selective catalytic hydrogenation technique to introduce the motivation and objectives related to this research work. The benefits of using $scCO_2$ for polymer processing were briefly introduced as well as the merits of CXLs for serving two purposes - increased compatibility with organometallic complexes and regulation on the physical properties of polymers - to examine the feasibility of applying CXLs in recovering organometallic complexes from polymers. Thus the layout of the thesis is now presented.

In Chapter 2, a literature review that has been carried out to explore the problems involved in the research work is presented. The literature review work covers several topics as follows. In the first section, the chemical properties of Wilkinson's catalyst are reviewed so as to know the proper chelating agents that can be used for forming chelating complexes with Wilkinson's catalyst. In the second section, the methods used for recovery/recycle of a homogeneous catalyst are reviewed with the objective of knowing the significance involved in recovery of organometallic complexes from a polymer matrix. In the third section, the application of SCF technology in polymer processing is reviewed. In the last section, the features and applications of CXLs are reviewed.

In Chapter 3, the experiment procedures involved in the research work are reported. The reported procedures include extraction sample film preparation, $scCO_2$ and CXLs

extraction, sample collecting, digestion, and ICP analysis. In addition, the verification of some procedures involved in CXM extraction is reported.

In Chapter 4, the trials to extract rhodium catalysts including Wilkinson's catalyst and rhodium trichloride from polymers, i.e. NBR and HNBR using $scCO_2$, are reported. The efforts were made from two aspects. One is to modify the rhodium catalyst; the other one is to modify the extraction solvent, i.e. $scCO_2$. $ScCO_2$ soluble catalyst was synthesized and tested in terms of its catalytic hydrogenation activity and separability from the HNBR matrix. On the other hand, the $scCO_2$ dissolvable chelating ligand thenoyltrifluoroacetone (TTA) was employed to conduct the extraction. The observations obtained from both aspects illustrated that the mass transfer resistance within the HNBR matrix is much higher than expectation and $scCO_2$ itself has inadequate solvency power toward those rhodium organometallic complexes. CXLs and chelating ligand were hence investigated in respect to their efficiency in improving the extraction results.

In Chapter 5, the efforts made to extract Wilkinson's catalyst from HNBR using CXLs and chelating agents are reported. The recipe and the operational conditions involved in the extraction process consisted of a CXL and a chelating agent are investigated. Besides, the loading amount of the optimal extraction system consisted of CXM and PMDETA was carefully investigated, as well as the thickness of the extraction sample film of HNBR and the importance of compressed CO_2 in the extraction system.

In Chapter 6, an investigation of the tunability of the extraction process regulated by adjusting temperature and pressure is presented in detail. The extraction results were studied as the function of operational temperature and pressure. The regulation of pressure on the

extraction process was studied in terms of its effects on the matrix and the extraction phase. The Perturbed Chain Statistical Associating Fluid Theory (PC-SAFT) equation of state was employed to study the dissolution behavior of CO_2 in HNBR and the transformation of the extraction phase at various operational conditions. The polarity variation of the extraction phase was used to interpret the extraction results. Based on a comprehensive understanding of the extraction data, an extraction mechanism was proposed to explain the extraction process. Additionally, the extraction process related to this specific system of Wilkinson's catalyst and HNBR was determined as controlled by chemical reactions and the challenges involved were thus explicitly illustrated. Some suggestions were put forward to enhance the recovery of rhodium in HNBR.

In Chapter 7, the efforts made to further improve the recovery of Wilkinson's catalyst from HNBR are presented. A varying pressure procedure was applied to further improve the extraction ratio, as well as a sequential operation. The varying pressure procedure showed promise in enhancing the extraction ratio, whereas the sequential operation failed to do that. At last the extraction technique was tested by applying on the HNBR particles coagulated from the HNBR latex.

In the final Chapter of the thesis (Chapter 8), all conclusions drawn from the research work are listed, while some recommendations for future work are proposed based on the discussions presented in the previous chapters.

Chapter 2
Literature Review

The literature review work carried out covers several topics as follows. In the first section, the chemical properties of Wilkinson's catalyst were reviewed to know the proper chelating agents that can be used for forming chelating complexes with Wilkinson's catalyst. In the second section, the methods used for recovery/recycle of homogeneous catalysts were reviewed to reveal the significance involved in recovery of an organometallic complex from a polymer matrix. In the third section, the application of SCF technology in recovery of organometallic compounds from polymers is reviewed. Finally, the application of CXLs is reviewed with evaluation of its feasibility in recovering organometallic complexes from polymers.

2.1 Chemical properties and catalytic reactions of Wilkinson's catalyst

Wilkinson's catalyst is the common name for chlorotris(triphenylphosphine)rhodium(I), a coordination compound with the formula $RhCl(TPP)_3$ (TPP = triphenylphosphine). It is named after the late organometallic chemist and 1973 Nobel Laureate, Sir Geoffrey Wilkinson who popularized its use. The discovery of Wilkinson's catalyst has been treated as a major breakthrough in the history of selective hydrogenation. This catalyst offers remarkable activity toward hydrogenation of carbon-carbon double bonds (C=C) in the presence of other reducible functional groups. The main criterion for NBR hydrogenation is the selectivity toward reduction, in order to maintain the oil resistance and other physical properties of the hydrogenated product. In the presence of a nitrile group, which can inhibit

the catalytic activity during hydrogenation, Wilkinson's catalyst is capable of retaining its high activity without any pronounced difference.

2.1.1 Stoichiometric reactions of Wilkinson's catalyst

2.1.1.1 Chloro ligand substitution

The chloro ligand may be substituted by a wide variety of anions. The reactions can conveniently be classified into those in which the triphenylphosphine (TPP) ligands are retained and those in which they are lost, together with the chloro ligand as follows.

The simplest substitution reactions are those in which the chloro ligand is replaced by a pseudohalide ligand. The reported chloro ligand substitution reactions are summarized by Jardine and are shown in Figure 2-1 [*17*]. The recovery of Wilkinson's catalyst from solution can be realized via the replacement of the chloro ligand by a reaction on an anion-exchange resin in the cyanide form with an ethanol/dichloromethane solution of $RhCl(TPP)_3$ to give the cyano complex $RhCN(TPP)_3$ [*18*]. In addition, the reaction of tetraphenylarsonium cyanate with $RhCl(TPP)_3$ is solvent dependent. Polar solvents such as acetonitrile favor the formation of the *N*-bonded isomer, i.e. $Rh(NCO)(TPP)_3$. If the reaction is run in less polar ethanol, the formation of the *O*-bonded isomer, i.e. $Rh(OCN)(TPP)_3$ is favored [*19*].

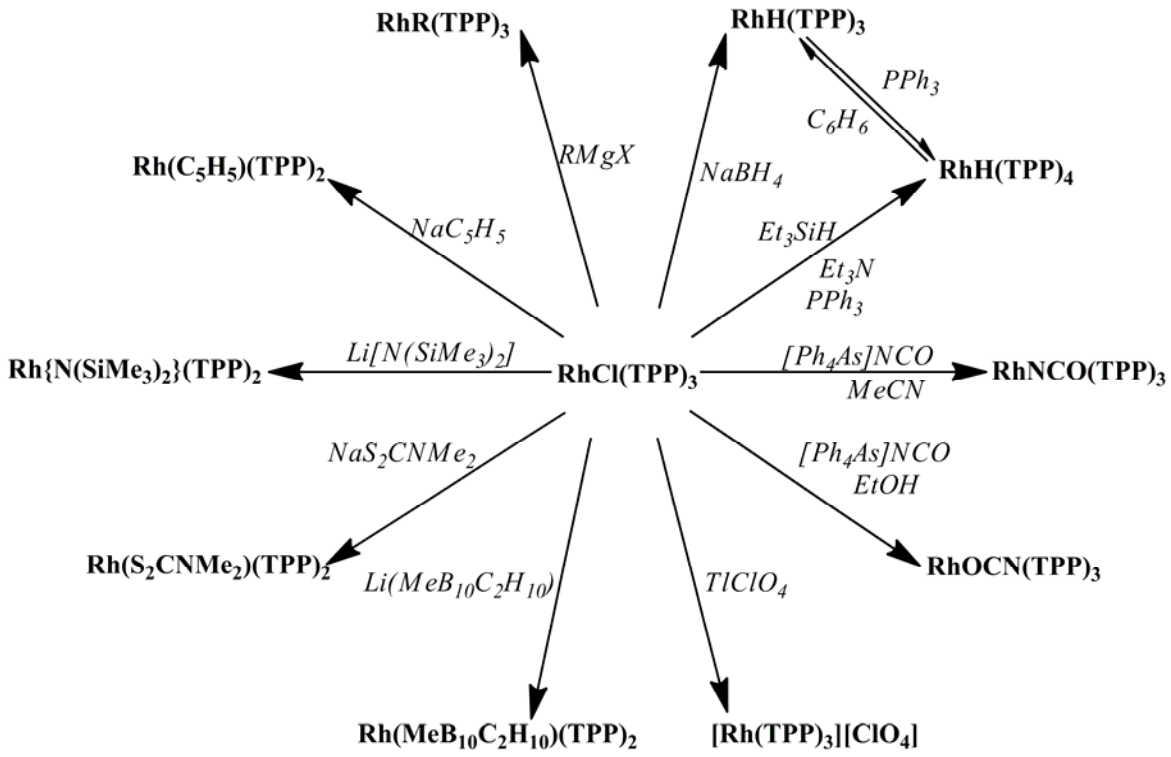

Figure 2-1. Some chloro ligand substitution reactions.

If $RhCl(TPP)_3$ is allowed to react with potentially bidentate uninegative anions, complexes of the general formula $RhX(TPP)_2$ usually result. Disulfur anions particularly give complexes of this type. For example, reactions with ammonium dialkyldithiophosphinates or dialkyldithiophosphates form $Rh(S_2PR_2)(TPP)_2$ and $Rh[S_2P(OR)](TPP)_2$ complexes, respectively [*20*]. The reaction of $RhCl(TPP)_3$ with lithium carboranes can prepare different carborane complexes [*21, 22*]. The reaction of $RhCl(TPP)_3$ with lithium bis(trimethylsilyl)amide in tetrahydrofuran can produce the stable, green, three-coordinate complex $Rh[N(SiMe_3)_2](TPP)_2$ [*23*]. In a similar way, the $Rh[N=C(CF_3)_2](TPP)_2$ complex can be prepared from $Me_3SnN=C(CF_3)_2$ in excellent yield and from $LiN=C(CF_3)_2$ in poor yield [*24*].

2.1.1.2 TPP displacement

$RhCl(TPP)_3$ undergoes dissociation of its TPP ligands, especially in the presence of reagents which have strong coordinating ability with the central rhodium [*25, 26*]. Nevertheless, in the absence of all reagents apart from the pure solvent of low coordinating power, the dissociation of a TPP ligand occurs only to a small extent (ca. 5%) at room temperature or below [*25, 27*]. In the absence of oxygen the salmon pink dinuclear complex $[RhCl(TPP)_2]_2$ can be formed [*17, 26*]. The reactions reported involving only the substitution of TPP ligand are summarized by Jardine and are shown in Figure 2-2 [*17*].

Tertiary phosphines other than TPP replace the TPP ligands in a stepwise fashion, and these reactions are generally slow. By this process RhCl(TPP)n ($n \leq 2$) fragments can be bound to a phosphinated polymer [*28-31*] or to silica surfaces [*32*]. Additionally, soluble high molecular weight catalysts can be obtained similarly from reaction of $RhCl(TPP)_3$ and non-cross-linked phosphinated polystyrene [*33*] or oligomeric phosphines [*34*]. Alternatively the triphenylphosphine ligands can be exchanged entirely for three diphenyl(sodium *m*-phenylenesulfonate) phosphine ligands to give a water soluble homogeneous hydrogenation catalyst [*35*]. Yellow crystals of trans-$RhCl(TPP)_2(PF_3)$ can be obtained from the reaction of phosphorus trifluoride (PF_3) and chlorotris(phenylphosphine)rhodium(I) in dichloromethane [*36*].

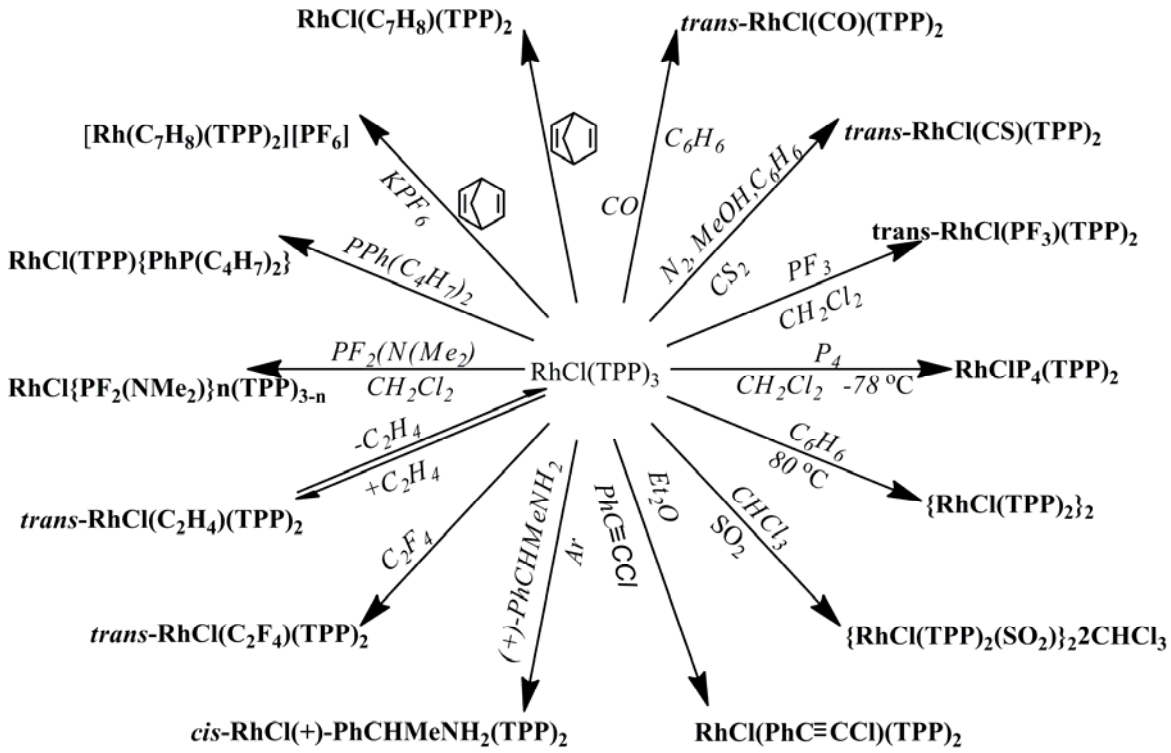

Figure 2-2 Some TPP displacement reactions

Compared to monodentate tertiary arsines and stibines, which have been scarcely reported to replace the TPP, many compounds containing nitrogen donor atoms were found capable of displacing the TPP of Wilkinson's catalyst. For example, at room temperature under an inert atmosphere both (±)-$PhMeCHNH_2$ and benzo[*c*]cinnoline give cis-bis(triphenylphosphine)rhodium complexes [*17, 37*]. The pyrrolidine complex $RhCl(TPP)_2(C_4H_9N)$ can be synthesized in a sealed-tube reaction between the ligand and $RhCl(TPP)_3$ at 80 °C [*38*].

$RhCl(TPP)_3$ reacts with carbon monoxide in solution to produce a very stable complex of trans-carbonylchlorobis(triphenyl-phosphine)rhodium(I) [$RhCl(CO)(TPP)_2$] [*26*]. A very

similar reaction occurs with carbon disulfide, giving the first thiocarbonyl complex to be isolated, trans-$RhCl(CS)(TPP)_2$ [*39-41*].

The complexity constants of most monoalkenes are so low at equilibrium that it is not possible to isolate their complexes even when the parent complex is allowed to react with neat alkene. Ethene has been shown to react reversibly with the parent complex, but tetrafluoroethene is not lost from its alkene complex $RhCl(TPP)_2(C_2F_4)$. Thus whereas the ethene complex is stable in solution only under an ethene atmosphere, the tetrafluoroethene complex is sufficiently stable in the solid state. Additionally, monotriphenylphosphine alkadiene complexes could be obtained if chelating alkadienes were used instead of alkenes. Although many alkynes react exothermically with the complex $RhCl(TPP)_3$, as $RhCl(TPP)_3$ is a polymerization catalyst for alkynes it is often difficult to isolate a pure product.

In line with above, there are generally three types of ligating agents that can react stoichiometrically with Wilkinson's catalyst. The first type mainly consists of some pseudohalides, e.g. cyanide and cyanate which substitutes the chloro ligand of Wilkinson's catalyst. The second type includes some bidentate uninegative anions such as the disulfur anions, which generates complexes of $RhX(TPP)_2$ by reacting with Wilkinson's catalyst. The third type comprises tertiary phosphines other than TPP, N-donor ligand, carbon monoxide and alkenes, which is able to substitute the TPP ligand of Wilkinson's catalyst. Moreover, many of the reported stoichiometric reactions were affected by the effect of the properties of the reaction medium.

2.1.2 Catalytic reactions using Wilkinson's Catalyst

2.1.2.1 Hydrogenation

Wilkinson's catalyst was the first effective homogeneous hydrogenation catalyst for alkenes or alkynes to be discovered. Compared to heterogeneous hydrogenation catalysts which are usually naked transition metals or their oxides, Wilkinson's catalyst presents great advantages in several aspects. First Wilkinson's catalyst has high selectivity toward C=C or C≡C bonds in the presence of other functionalities. Wilkinson's catalyst is able to hydrogenate insoluble or macromolecular substrates like rubbers and other polymers. Moreover, Wilkinson's catalyst can be used to catalyze the hydrogenation of long-chain unsaturated fatty acids in phospholipids biolayers by dissolution in tetrahydrofuran swollen lipid micelles suspended in water, whereas the metallic heterogeneous catalysts cannot even pass through the cell walls in the biochemical systems [*42*].

2.1.2.2 Other catalytic reactions

In addition to its catalytic function for hydrogenation of alkenes and alkynes, Wilkinson's catalyst has also been demonstrated to be efficient for catalyzing many other reactions such as dehydrogenation [*43*], hydrogen transfer [*44*], hydroformylation [*45*], carbonylation [*46*], hydrosilylation [*47*] , isomerization [*48*], and oligomerization [*47*].

2.2 Development of organometallic catalyst recovery technology

Despite their many advantages, such as selectivity, versatility, and activity, organometallic catalysts suffer from one serious inherent disadvantage, namely, the difficulty of separating the catalyst from the product. Heterogeneous catalysts are either automatically removed in the process (e.g., gas-phase reactions in fixed-bed reactors), or they can be separated by

simple methods such as filtration or centrifugation. In the case of homogeneous catalysts, more complicated processes such as distillation, liquid-liquid extraction, and ion exchange must often be used [*49*]. Mainly two classes of recovery methods are reviewed. They are ion exchange resin adsorption and biphasic catalysis.

2.2.1 Ion exchange resin adsorption

Ion exchange has been proved to be a highly efficient technique for the recovery of low concentrations of metal ions. Often rhodium complexes can be separated by passing the solution down a column of alumina [*50*] or silica gel [*51*], in which TPP may still stay in the product and contaminate it. Jurjen et. al. [*52*] reported the recovery of Wilkinson's catalyst with silica-immobilized P-donor ligands. In their research, monodentate PPh_2-containing ion exchangers with various spacer arms of C_n (see Figure 2-3) were tested on their applicability as ion exchangers in the recovery of Wilkinson's catalyst. Ion exchangers containing N-only donor ligands were reported to be very suitable for the recovery of trivalent rhodium, i.e., Rh^{3+} in $RhCl_3 \bullet 3H_2O$ [*53*]. However, these N-only ion exchangers were not considered as good candidates for recovery of Wilkinson's catalyst, because their strong binding of rhodium precluded the desorption of Rh^+ from the ion exchangers [*52*].

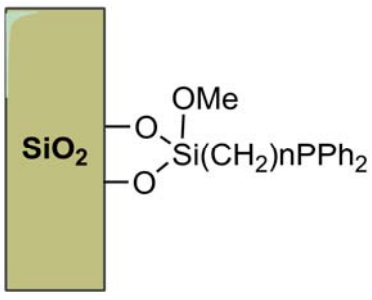

Figure 2-3 Silica-based PPh_2-containing ion exchangers, bearing different spacer lengths.

2.2.2 Biphasic catalysis via organometallic catalyst

To avoid difficult separations, many workers have attempted to combine the desirable features of homogeneous catalysts with the ease of removal associated with heterogeneous catalysts. Biphasic catalysis is considered as a most promising strategy for increasing the separability of organometallic catalyst. In a biphasic catalytic system, the organometallic catalyst can be immobilized in various phases such as solid, water, fluorous compounds, and ionic liquids.

2.2.2.1 Immobilization on solids

The catalyst precursor can be anchored onto an insoluble material, so that the catalyst can be quantitatively separated by filtration and recycled [*54-56*]. Preformed, molecular homogeneous chemical catalysts (usually metal complexes or organometallic compounds) are most conveniently anchored to diverse materials through covalent or non-covalent bonding. This approach hereinafter is referred to as heterogenization of homogeneous catalysts [*57, 58*]. A variety of solids, often being highly sophisticated, have been exploited for this purpose, including inorganic (silica, clays, zeolites, metal oxides, heteropolyacids, etc.) [*59, 60*], organic (carbon, polymer resins, dendrimers, polymeric ligands, polyeletrolytes, etc.) [*61-63*], and hybrid materials [*64-66*].

The fragment $RhCl(TPP)_2$ of Wilkinson's catalyst with one TPP ligand dissociated was combined with phosphinated cross-linked polystyrene polymers or divinylbenzene-styrene copolymers [*28-31, 33, 67*]. The immobilized catalysts were easily removed from the reaction mixture and could be used many times with little loss of activity. Moreover, the immobilized catalysts showed selectivity for the olefin's molecular size. This selectivity was

due to a restriction in the size of the solvent channels leading to the catalytic site by the crosslinks in the polymer beads [*28-31, 67*]. The isocyano polymer (acrylic polymer) bound Wilkinson's catalyst was also synthesized and investigated on its hydrogenation activity, selectivity, and stability [*68, 69*].

In addition, silica was reported as a support for immobilization of phosphine rhodium complexes and homogeneous Ru catalysts [*32, 70-73*]. In the work of Lei et. al., a trimethoxysilane functionalized TPP was coordinated to rhodium(I) and the resulting rhodium complex was covalently bound to a mesoporous SBA-15 support, which was reported with excellent activity, selectivity, stability, and reusability [*71*]. Moreover, the phosphinated silica, the benzoylthiourea [*74*] or thiourea [*75*] functionalized silica xerogel or silsesquioxanes were synthesized as supports for the heterogenization of Rh(I) catalysts. A novel clay catalyst containing a heterogenized Rh(I) phosphine complex (Rh-bentonite) has been prepared via ion exchange of a Hungarian Na^+-bentonite with Wilkinson's complex [$RhCl(TPP)_3$]. It was established that the active species $[Rh(TPP)]^+$ was situated on the external surfaces of the resin, which was found to be efficient in the liquid-phase hydrogenation of 1-octene, cyclohexene, norbornadiene, 1,5-cyclooctadiene, phenylacetylene and cyclohexene-3-one [*76*].

Except for these common supports mentioned above, some other solid materials have been investigated as a matrix for heterogenization of Rh(I) complexes as well as the catalytic activity of the anchored Rh(I) matrix [*77*]. Carbon nanotubes with an oxidized surface were also applied as supports for immobilization of Wilkinson's catalyst [*78*]. The cross-linked polymer obtained by reaction of $Rh(cod)(AAEMA^-)$ ($AAEMA^-$ =deprotonated form of 2-

(acetoacetoxy)ethyl methacrylate) and suitable acrylamides as comonomers and cross-linkers was investigated in respect to its catalytic activity for hydrogenation of olefins, unsaturated aldehydes and ketones, nitrobenzene and nitriles [*79*].

The main problems are still catalyst "bleeding" and the relatively low stability and high sensitivity to poisoning of the heterogenized complexes, which greatly restricted their application in the viscous reaction media. Besides, the catalytic performance of these heterogenized catalysts may vary enormously depending on the immobilization method and the support. Thus, it is of outmost importance to get a systematic picture of favorable and unfavorable factors and to test different support materials in developing such an effective catalyst process with high activity and stability.

2.2.2.2 Immobilization in water

Water-organic biphasic catalysis were established in the "Ruhrchemie/Rhône-Poulenc process" (RCH/RP) [*80*]. The catalyst applied is $RhHCO(TPPTS)_3$ [TPPTS=tris(sodium-m-sulfonatophenyl)phosphine], the water soluble analogue of $RhHCO(TPP)_3$, where TPP is substituted by TPPTS.

The structure of TPPTS is shown as below in Figure 2-4. Up to now, TPPTS has been developed as the best water soluble ligand in respect to its simultaneous water-solubility, high activity, high selectivity, and competitive price [*81, 82*]. Similarly, $RhCl(TPPTS)_3$, the water soluble analogue of $RhCl(TPP)_3$ has been synthesized and applied for biphasic catalytic hydrogenation of various substrates including polymers [*83-85*], and esters [*86*].

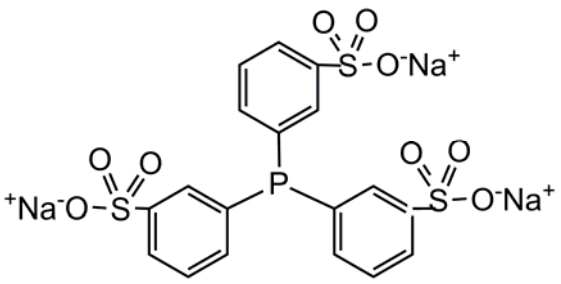

Figure 2-4 Molecular Structure of TPPTS

The water-organic biphasic catalysis system significantly enables the ease of precious metal catalyst recycle by phase separation [*87*]. These are very elegant in that a water soluble catalyst is kept completely separate from the lypophilic product, except under conditions of fast stirring. A stop in stirring leads to rapid phase separation and the product can be collected by decanting. Such processes have been commercialized for short chain substrates, which have significant solubility in water, but it has been observed that the rate of reaction when using a longer chain, less hydrophilic substrates are too low to be of commercial interest, presumably because mass transport limitations dominate the reaction.

2.2.2.3 Immobilization in fluorous compounds

Fluorous biphasic catalysis was introduced by Horváth and co-workers in 1994 [*88*]. He coined the term "catalysis in the fluorous biphase" and the process uses the temperature dependent miscibility of fluorinated solvents (organic solvents in which most or all of the hydrogen atoms have been replaced by fluorine atoms) with normal organic solvents, to provide a possible answer to the biphasic hydroformylation of long-chain alkenes. With the catalyst immobilized in the fluorous phase, the substrate can be introduced either in solution, e.g. with toluene, or neat [*89*]. When heated, the two phases form a single homogeneous

phase, which allows the substrate to be in intimate contact with the catalyst at all times. With the addition of reacting gases, reaction will occur at this elevated temperature and the catalyst and product are easily separated by cooling the mixture and decanting the product allowing easy reuse of the catalyst phase.

It has generally been accepted that if the reaction can be carried out under homogeneous conditions, then it should be possible to fluorinate the ligands and perform the reaction under fluorous biphasic conditions [*90-92*]. Nevertheless, the position of these perfluoroalkyl modifying "ponytails" on the aryl ring, especially *o*- and *p*- positions of the ring, had a great effect on the metal complex, because the strongly electron withdrawing effect of the fluorine atoms affects the behavior of the phosphorus atom [*93, 94*]. The most common practice for reducing the electronic effect is to add a spacer group, e.g. aryl or alkyl group between the phosphorus and the fluorine tail [*95*]. The spacer group can act as a shield to the phosphorus and metal centre from the powerful electron withdrawing effect of the perfluoroalkyl tail. C_2H_4, $O(CH_2)_n$ (n = 1 or 5) [*96*], and $SiCH_2CH_2$ [*97, 98*] have been revealed as good spacer groups for insulation of the effects of the fluorous substituent on the aryl groups. The fluorous analogues of Wilkinson's catalyst that have been designed and reported in terms of their catalytic application in hydrogenation are listed as below.

The Wilkinson's complex of $RhCl[P(CH_2CH_2(CF_2)_5CF_3)_3]_3$ was applied by Horváth and co-workers for hydrogenation of a range of alkenes [*99*], in which perfluoro(methylcyclohexane) (PFMC) and toluene provided the fluorous phase and organic phase respectively. The catalyst activity reported did not compare to those found for the best homogeneous catalysts. Besides, another range of fluorinated ligands have been reported for

producing the fluorous Wilkinson complexes by Horváth and co-workers [*100*]. The fluorous ligand P(*p*-$C_6H_4OCH_2C_7F_{15})_3$ was revealed to have adequate rates in a toluene/hexane/perfluoro-1,3-dimethylcyclohexane (PFDMCH) solvent system. No free ligand was observed in the organic phase and recharging the reactor with further fractions of substrate resulted in no effect on the catalytic activity, demonstrating a high catalyst stability and recovery.

The fluorous biphasic catalytic system is a very attractive solution to the problem involved in homogeneous catalyst recycles. In principle, all the homogeneous catalysts can be fluorinated by means of fluorine substitution or addition of a fluorinated "ponytail". However, there is still a long way to go for the industrial application of this technique, taking into account the fact that the fluorous versions are always not as reactive as the conventional homogeneous catalysts and the leaching of active species, e.g. rhodium and the phosphine into the organic phase is inevitable. This restricted its application to systems containing long chain or macromolecular substrates, in which conventional organic solvent has to be used for dissolving the substrate. Moreover, the fluorous compounds are always very expensive and the high investment also discouraged their development.

2.2.2.4 Immobilization in ionic liquids

Ionic liquids (ILs) are low melting point (<100°C) salts of organic cat ions that are finding increasing interest as solvents for organometallic catalysis [*101, 102*]. ILs exhibit no detectable vapor pressure below the temperature of their thermally decomposition. The most common cations that used so far for formation of ILs include imidazolium, pyridinium, ammonium and phosphonium, whereas a wide spectrum of anions can be used such as Cl^-,

Br^-, $[BF_4]^-$, $[PF_6]^-$, $[AlCl_4]^-$,$[Al_2Cl_7]^-$, $[HSO_4]^-$, $[RSO_4]^-$, $[RSO_3]^-$, $[CF_3COO]^-$, and $[(CF_3SO_2)_2N]^-$ [*103*]

Many transition metal complexes dissolve readily in ILs, thus enabling their use as solvents for transition metal catalysis. There are many good reasons for applying ILs as alternative solvents in transition metal catalyzed reactions. One very important advantage is the possibility of tuning their solubility [*104*] and acidity/coordination properties [*105*] by varying the nature of the anions and cations systematically. With an IL system displaying partial solubility of the substrates and poor solubility of the reaction products, the product is removed by simple phase decantation, whereas the IL containing the catalyst can then be recycled.

Despite most transition metal catalysts easily dissolve in an IL without any special ligand design, modifying the active organometallic catalyst precursor with ionic ligand achieved great success to prevent catalyst leaching under the conditions of intense mixing in continuous liquid-liquid biphasic operation. It was found that modification of neutral phosphine ligands with cationic phenylguanidinium groups constitutes a very powerful tool for immobilizing Rh complexes in ILs [*106*]. In the biphasic Rh-catalyzed hydroformylation experiment using [BMIM][PF6] as the catalyst solvent, this ligand reduced Rh-leaching to about 0.07% of the Rh used in the experiment. The ionic catalyst solution could be recycled 10 times without significant loss in activity. Alternative methods of immobilizing phosphine ligands by attaching them to ionic groups similar to the IL cation have been reported. Both pyridinium-modified phosphine ligands [*107*] and imidazolium modified phosphine ligands [*108, 109*] have been synthesized and applied in Rh-catalyzed hydroformylation.

Most catalytic reactions in the ILs media suffer from the problems of mass transfer limitation ascribed to the high viscosity of ILs. The $scCO_2$/ILs system however provides a promising solution to overcome the encumbrance of mass transfer limitation. Being composed entirely of cations and anions, ILs generally show no detectable solubility in pure $scCO_2$. CO_2, however, has a remarkable affinity for ILs allowing high concentrations of CO_2 in the liquid phase, and thus rapid mass transfer between the two media [*110*]. On the other hand, catalyst leaching problem can be very well circumvented in the system of $scCO_2$/ILs, because ILs are known to be excellent solvents for many transition metal catalysts, whereas the solubility of most transition metal complexes in $scCO_2$ is poor (if not modified with e. g. phosphine ligands with fluorous "ponytails" [*111*]). However, product isolation from $scCO_2$ is always very simple, while from an ionic catalyst solution it may become more and more complicated depending on the solubility of the product in the IL and on the product's boiling point. These properties make IL/$scCO_2$ biphasic system highly attractive for application in catalyst immobilization, especially under continuous flow conditions.

Wilkinson's catalyst was used in 1-butyl-3-methylimidazolium hexafluorophosphate ([BMIM][PF_6]/$scCO_2$ for hydrogenation of alkenes and CO_2 [*112*]. Asymmetric hydrogenation of tiglic acid catalyzed by $Ru(O_2CMe)_2$·((R)-tolBINAP) in wet IL ([BMIM][PF_6] with added water) gave 2-methylbutanoic acid with high enantioselectivity and conversion. The product was extracted with $scCO_2$ giving a clean separation of product and catalyst [*113*]. The rhodium complex of [1-propyl-3-methylimidazolium]$_2$PhP[$C_6H_4SO_3$-3]$_2$ was dissolved in the IL of [BMIM][PF_6] for biphasic catalytic hydroformylation of octane in $scCO_2$ [*114*].

Potential problems common to all IL/ $scCO_2$ systems are the current cost and unknown toxicity of ILs. Although in an optimized system the IL should remain within the reactor, the absence of toxicity data may prove a hindrance to their acceptance for products used in the fine chemicals or pharmaceutical industries. With the number of successful examples increasing, it is expected that these general advantages of continuous flow multiphase catalysis in IL/$scCO_2$ will be exploited further making this a viable option for fine chemical production.

2.3 Application of $scCO_2$ in recovery of organometallic catalyst from polymer matrix

A lot of literature and patents are available regarding recovering metal values from polymer resins by "elution" or "fuming". The conventional "elution" process involves extensive use of organic solvents and constitutes a heavy environmental burden. The "fuming" method recovers the metal values through thermally decomposing the polymer resins, which damages the matrix and is not a method that can be used. Moreover, the polymer is considered as more difficult than polymer resins as a matrix from which the organometallic complexes are extracted. Therefore the conclusion is that almost no meaningful references appear in the open literature regarding recovery of organometallic catalysts from polymers. Based on the experience accumulated with SCFs, SCF technology is expected to provide a solution to the problem. Thereafter the literature of SCFs is reviewed with concentrating on the solvent power of $scCO_2$ and its application in processing polymers.

2.3.1 Introduction to supercritical fluids

Supercritical fluids (SCFs) are substances which are simultaneously heated above their critical temperature T_c and compressed above their critical pressure P_c, and which have density close to or higher than their critical density ρ_c (Figure 2-5 [*115*] and Table 2-1 [*116*]). SCFs fill the entire space available to them like gases, but at the same time can act as solvents for solids or liquids. Typical supercritical fluid properties of SCFs, sometimes termed a "hybrid of those of a liquid and a gas", include the ability to dissolve solids, miscibility with permanent gases, high diffusivity, low viscosity, etc. The unique combination of gas-like and liquid-like tunable properties provides alternative approaches for researchers to access new areas of chemistry by taking advantage of SCFs.

"Near-critical" is another frequently used term for description a fluid status in the field of SCF technology. A fluid is regarded as near critical when its density has changed sufficiently so that its property has become similar to that of a SCF. The transition from a dense liquid to a less dense SCF occurs over a distinct temperature range but not instantaneously. Therefore, for each substance, there exists a "near-critical" region at temperatures below T_c in which the density of the substance is already considerably reduced compared to the normal liquid but still denser than ρ_c. Because many of the potential benefits of a SCF are also retained in such a "near-critical" region, operations below T_c have been widely applied in many cases with exploitation of those advantages [*116*] .

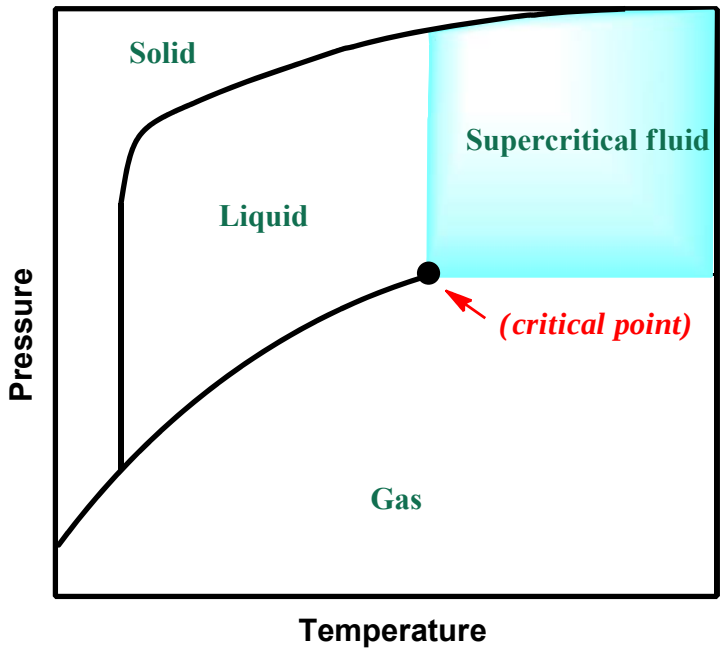

Figure 2-5 Schematic pressure-temperature phase diagram for a pure component showing the supercritical fuid (SCF) region [*115*].

CO_2 is by far the most widely used supercritical fluid. It has mild critical properties (T_c = 31.1 °C, P_c = 73.8 bar, ρ_c = 0.437 g/mL) [*116*], is non-toxic, non-flammable and can be handled safely on laboratory and industrial scales. Unlike classical organic solvents, CO_2 is not classified as a "volatile organic chemical" (VOC) and is considered environmental benign. However, using SCFs and $scCO_2$ in particular cannot always be economically justified based solely on replacing environmentally harmful solvents. Simplified reaction/separation schemes, lower energy requirements, improved product quality, or some combination of these is a process advantage as well.

Table 2-1 Critical Data for selected Substances [*116*]

Substance	T_c, °C	P_c, bar	ρ_c, g/mL
Ar	-122.4	48.6	0.53
CH_4	-82.6	46.4	0.16
Kr	-63.8	55.0	0.92
C_2H_4	10.0	51.2	0.22
Xe	16.7	58.8	1.15
C_2F_6	19.9	30.6	0.62
CHF_3	26.2	48.5	0.62
$CClF_3$	28.9	38.6	0.58
CO_2	31.1	73.9	0.47
C_2H_6	32.4	48.8	0.2
N_2O[a]	36.6	72.7	0.45
SF_6	45.6	37.2	0.73
Propane	97.2	42.5	0.22
H_2S[b]	100.4	90.1	0.35
NH_3	132.5	114.0	0.24
Pentane	197.1	33.7	0.23
^{i}PrOH	235.4	47.6	0.27
MeOH	240.6	79.9	0.27
EtOH	243.5	63.8	0.28
^{i}BuOH	275.1	43.0	0.27
Benzene	289.0	48.9	0.30
$C_2H_4(NH_2)_2$(en)	319.9	62.7	0.29
Pyridine	347.1	56.3	0.31
H_2O	374.2	221.2	0.32

Note: [a] Safety Warning! N_2O has similar critical parameters and rather better solvent properties than $scCO_2$ but there have been reports of explosions when scN_2O has been used with modest amounts of organic compounds. Therefore, scN_2O should only be used with extreme caution! [b] H_2S is highly toxic.

The schematic phase behavior of SCF depicted in Figure 2-5 is only valid for the pure compound. The phase behavior of mixtures is much more complex [*117*], being a function of composition, and the actual phase diagram can vary considerably even for seemingly similar components. Reaction systems contain at least three substances (substrate, product and

catalyst), but in most cases more components are present and a full description of the phase behavior is a challenging task [*118*]. On the other hand, this permits operating conditions where a condensed phase is in equilibrium with a compressed CO_2-rich phase at temperatures and pressures beyond the critical point of pure CO_2. Although the whole mixture is then not supercritical, the compressed CO_2 phase will behave like a supercritical fluid in exhibiting solvent properties. Any component in such a mixture will partition between the condensed and the supercritical phase, depending on its molecular structure as well as the pressure and temperature of the system. This rich phase behavior and the ability to control the partitioning of substrates and catalysts allow the design of integrated reaction/separation schemes that rely on CO_2 as the only mass separating agent.

For traditional solvents, the "solvent power" of a fluid phase is often related to its polarity. Compressed CO_2 has a fairly low dielectric constant under all conditions (ε =1.2-1.6), and has been widely believed to have "hexane like" solvent properties. However, this measure has increasingly been shown to be insufficiently accurate to define solvent effects in many cases [*119*]. According to the Hildebrand solubility parameter (δ) of CO_2 at various pressures, the solvent properties of a supercritical fluid depend most importantly on its bulk density, which depends in turn on the pressure and temperature [*111*]. In general higher density of the SCF corresponds to stronger solvation power, whereas lower density results in a weaker solvent.

2.3.2 Strategies to increase an organometallic compound's solubility in $scCO_2$

The solubility of a solute in $scCO_2$ is extremely dependent on its structure, with three features of paramount importance. As expected, compounds of low polarity are more soluble than

very polar compounds or salts. However, solubility also increases greatly with increasing vapor pressure of a substrate. To account for the contribution of volatility and solvation to the solubility process, Kurt Zosel coined the term "Destraktion" (from Latin *destillare* and *extrahere*) in his pioneering work on natural product extraction with SCFs [*120*]. Finally, some specific functional groups like perfluoroalkyl and polysiloxane substituents, or polyether/polycarbonate copolymers are known to give compounds a high affinity to compressed CO_2 that cannot be explained through simple polarity or volatility arguments [*119*]. These "CO_2-philic" substituents can lead to dramatic solubility enhancements, thus allowing control of the phase preference of reaction components at different stages of a reaction/separation process.

Many, if not most, organometallic complexes exhibit solubility in $scCO_2$, however, they are too low even for catalytic applications under single phase conditions. This applies particularly to the large class of catalysts bearing aryl phosphine ligands, a structural motif also found frequently in chiral ligands used in enantioselective catalysis. This problem can be overcome by the introduction of perfluoroalkyl groups into the ligand periphery of metal catalysts bearing this type of ligand [*121*]. Fluorinated groups can be introduced into ligand frameworks via relatively straightforward synthetic routes [*122-124*]. Moreover, the introduction of perfluoroalkyl groups into the ligand periphery of an organometallic complex can lead to a considerable increase in molecular weight and size of the catalytically active species. This has been utilized to separate "CO_2-philic" catalysts from the products in a continuous flow membrane reactor, in which the catalyst is a fluorous Wilkinson's complex containing the ligand $P(C_6H_4\text{-}p\text{-}SiMe_2CH_2CH_2C_8F_{17})_3$ [*125*]. This intriguing methodology is

appraised as being particularly useful where highly fluorinated polymers or copolymers are used to stabilize and solubilize organometallic or colloidal catalysts in $scCO_2$ as the reaction medium.

Many organometallic catalysts and especially many chiral catalysts are cationic and modification of the anion has been found to be very effective for enhancing their solubility in $scCO_2$. Tetrakis-(3,5-bis-trifluoroimethylphenyl)borate (BARF) was an early example of such an anion which has proven extremely useful for this purpose [*126*], and very pronounced anion effects on the activity and selectivity of the catalysts are observed in many other cases [*127, 128*]

2.3.3 Application of $scCO_2$ for polymer processing

The dissolution of CO_2 into a polymer matrix will induce the plasticization of polymers and impose effects on a few of their physical properties [*7-11*]. These effects include reduction of glass transition temperature (T_g) [*7, 9*], depression of viscosity [*8, 10*], and enhancement of permeability [*9, 11*]. The viscosity reduction greatly benefits the processes involving high molecular weight polymers where high viscosity is a major obstacle. It also facilitates the processing of temperature-sensitive polymers at low temperatures to prevent thermal degradation and save energy. The diffusion of additives through polymers is significantly improved by the addition of CO_2 and thus promotes the processes requiring delivery of additives in or out of the polymer, such as dyeing [*16*], impregnating biological agents [*129*] and fabricating polymer composites [*130*]. In addition, the alteration of these physical properties can be manipulated through adjusting temperature and pressure. For instance, increasing temperature and pressure generally decreases the viscosity of polymer melts and

increases their permeability. However, with increasing pressure under high pressure conditions, the decrement of diffusion and increment of viscosity could also be observed as a result of the combined effects of hydrostatic pressure and the polymer's high compressibility [*9*]. Moreover, the adding of a co-solvent, i.e. ethanol was able to enhance the benefits offered by CO_2 in enhancing the diffusion of additives inside of polymer melts due to the improved interactions between solvent and polymer [*16*]. The combination of tuning CO_2 and adding co-solvent provides more controllable process parameters and allows for the impregnation of thermally labile and metastable materials under lower temperature and pressure. On the other hand, the foaming effect accompanied by the releasing of CO_2 from the polymer results in a high-surface porous polymer and thus is expected to further accelerate the mass transfers inside [*131*].

2.4 Application of CXLs in recovery of organometallic catalysts from polymer matrices

In recent years, there has been a heightening interest in the fundamental and applied research of the use of CXLs for performing reactions [*12, 14, 132*], separations [*12, 14*], and other applications like particle formation [*133, 134*] and material processing [*134*]. Compared to $scCO_2$, CXL can dissolve organometallic complexes at mild pressure conditions. Meanwhile, the presence of CO_2 in polymers facilitates their processing by means of lowering their melting and glass transition temperatures, as well as increasing their permeability. By selection of a suitable solvent to be expanded by CO_2, the CXL generated can serve both purposes as dissolving the organometallic catalysts as well as retaining the intactness of polymers.

2.4.1 Introduction of CXLs

CXLs are solvent mixtures composed of compressed CO_2 dissolved in an organic solvent which can be continuously tuned from the neat organic solvent to $scCO_2$ by controlling the operating pressure of CO_2 (see Figure 2-6 Illustration of the generation of a CXL). A large amount of CO_2 in the CXL grants the mixture excellent transport properties and good solubility of most of the gaseous reagents, while the presence of a suitable amount of polar organic solvent favours the solubility of solids and liquid solutes [*13, 135*]. For example, most of the rhodium catalyst complexes are only sparsely soluble in $scCO_2$, whereas adequate solubility of them in CXL can be obtained to carry out homogeneous catalysis with CO_2 pressures an order of magnitude lower than those required in $scCO_2$ medium for dissolving rhodium catalyst complexes with fluorinated ligands [*14*]. Additionally, the application of CXLs in chemistry and reaction engineering is beneficial to the environment by reason of substantial replacement of organic solvents or volatile organic carbons (VOC) with environmental friendly dense-phase CO_2, which improves process safety and reduces the exposure to hazardous materials as well [*13, 136*].

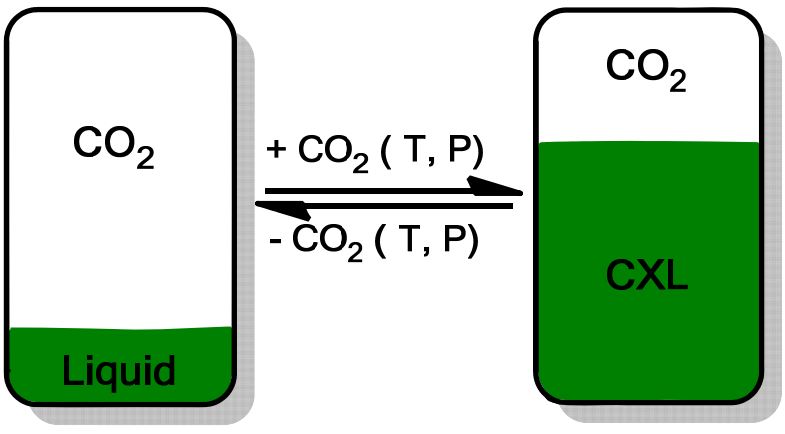

Figure 2-6 Illustration of the generation of a CXL

CXLs have been separated into three classes by Jessop and Subramaniam based on the liquids ability to dissolve CO_2 [*13*]. Liquids defined in Class I, such as water, lack a sufficient ability to dissolve CO_2, and thus do not expand significantly. Traditional organic solvents, like methanol and hexane, can dissolve large amounts of CO_2, so they do expand substantially and experience significant physical changes. These are Class II liquids, and the degree of their expansion is highly dependent on the mole fraction of liquid CO_2. In comparison, Class III liquids, such as liquid polymers, ILs, and crude oil, dissolve smaller amounts of CO_2, and so only expand slightly. This causes some properties to change drastically, such as viscosity, whereas others, such as polarity, do not.

2.4.2 Properties of CXM

As an alternative medium to the traditional organic solvents, CO_2 expanded methanol (CXM) is one of the most studied CXLs. Eckert and co-workers have conducted meaningful research on the characteristics and application of CXM. They measured the diffusivity of five different solutes in CO_2-expanded methanol at 40°C and 150bar; their diffusivity in CXM unexceptionally increased with CO_2 fraction addition, and the rate of increment was augmented as the CO_2 fraction grew [*137*]. In addition, they determined the solvatochromic solvent parameters ($E_T(30)$, α, β, and π^*) of CXM at 35°C and 40°C, and the entire range of solvent composition with six probe indicators [*15, 138-141*]. Their work shows that mixture polarity, indicated by π^*, decreases moderately while the CO_2 amount increases at the beginning, and drops dramatically when it is approaching the pure CO_2, which is supposed to be the vicinity of the critical point. Moreover, they investigated the cybotactic region of CXM with spectroscopy technique and molecular dynamic simulation, and explored the

presence of large solvent clustering near the electron withdrawing side of the probe Coumarin 153 [*15, 139*]. The differences between the local and bulk compositions can be exploited in the reactions affected by the transport properties and chemical transformations. The formation of alkylcarbonic acid in various CO_2-expanded alcohols at 25°C has also been investigated by Eckert group with spectroscopic method [*141*]. Their dissociation constants in CO_2-expanded alcohols have also been measured, which provides key parameters to design acid catalysis reaction in CO_2-expanded alcohols with utilization of the tunable proton concentration, and reversibility of the alkylcarbonic acid in them. CXM has been reported as catalytic media for the formation of cyclohexanone acetal and synthesis of methyl orange and iodobenzene with the in situ formed methylcarbonic acid as self-neutralizing catalyst [*142-144*]. Besides from the work of Eckert and co-workers on the fundamentals and applications of CXM, the application of CXM merely as an alternative media to conventional solvent produced promising results as well as the exploitation of the solubility of gaseous reagents and organometallic catalysts in the reaction phase to improve the reaction rate and selectivity [*145*].

2.5 Summary

The chemical properties of Wilkinson's catalyst are carefully reviewed so that a clear idea was obtained about the chelating agent that can substitute the ligands of the catalyst. Besides, the reactions occurring inside of the polymer matrix was clarified by the discussion of dissociation of the TPP ligand from Wilkinson's catalyst in the presence of other functionalities at elevated temperature. The review of the organometallic catalyst recovery technology acquainted the researcher about the concept of green catalysis and the

significance of recovering organometallic complexes from polymers. The review of $scCO_2$ technology informed the researcher of the advantage and disadvantage of using $scCO_2$ for recovering organometallic complexes from polymers. The review of the research progress about CXLs demonstrated the feasibility of employing CXL for solving metal complex recovery problems.

Chapter 3
Research Methodology and Approaches

The objective of this project is to set up an effective catalyst recovery or recycle system to recover the rhodium catalyst from rubbery polymers, i.e. NBR and HNBR, and try to understand the mass transfer mechanism and extraction dynamics revolved in the extraction process, ultimately to optimize the extraction operation conditions. Efforts have been made to approach the objective in two ways. One approach was to synthesize $scCO_2$ soluble catalyst with catalytic activity in selective hydrogenation of the C=C bond in NBR. The other approach was to employ a $scCO_2$ dissolvable chelating ligand to assist the separation of Wilkinson's catalyst. As it will be reported later that CXLs were found advantageous as alternative extraction solvents to overcome the poor solvent power of $scCO_2$. The experiment procedures involving sample preparation, sCO_2 extraction, CXL extraction, digestion, post-treatment of the digestion solution, and ICP analysis method are presented in this Chapter. Additionally, the verification of procedures involved in the extraction technique consisted of CXM and PMDETA were conducted and reported in this Chapter.

3.1 Materials

3.1.1 Chemicals in catalysts preparation and catalytic hydrogenation

Triphenylphosphine (TPP, 99%), tris(*p*-trifluoromethylphenyl)phosphine (TTFMPP, 97%), rhodium(III) chloride hydrate ($RhCl_3 \bullet 3H_2O$, 99.9%) were purchased from Aldrich and used without further purification. Wilkinson's catalyst and the fluorinated Wilkinson's [$RhCl(TPP)_3$] catalyst [$RhCl(TTFMPP)_3$] were prepared according to the literature [*39, 146*], whereas TPP was replaced by TTFMPP. The water soluble Wilkinson's catalyst [RhCl(dpm)] was offered by Allen in Rempel's group, in which 'dpm' is the abbreviation of the water

soluble ligand diphenylphosphinobenzen-m-sulphonate, i.e. ($P(C_6H_5)_2(m\text{-}C_6H_4SO_3H$). The ultra-high purity nitrogen (N_2, 99.999%) was supplied by Praxair Inc. (Mississauga, CA). The commercial NBR which contained 62% butadiene (80% trans, 15% cis, 5% vinyl C=C) and had an Mn=70,000 was provided by LANXESS Inc. (Leverkusen, Germany).

3.1.2 Chemicals in sample preparation

The bulk HNBR (Therban A 3406) with a degree of hydrogenation of greater than 99 mol% was provided by LANXESS Inc. (Leverkusen, Germany). Methyl ethyl ketone (MEK, 99%) and acetone reagent (≥99.5%) was purchased from Sigma Aldrich (Oakville, CA) and used as received.

3.1.3 Chemicals in extraction

Carbon dioxide (CO_2, 99.9%) and ultra-high purity nitrogen (N_2, 99.999%) were supplied by Praxair Inc. (Mississauga, CA). Methanol (reagent grade), ethanol (reagent grade), PMDETA (99%), N,N,N',N'-tetramethylethylenediamine (TMEDA, 99%), ethylenediaminetetraacetic acid (EDTA, 99%), ethylenediaminetetra acetic acid disodium salt (EDTA-Na_2, 99%), diethylenetriamine (DETA, 99%), and thenoyltrifluoroacetone (TTA, 99%) were purchased from Aldrich and used as received.

3.1.4 Chemicals in digestion and inductively coupled plasma analysis

Hydrochloric acid (HCl, 36.5-38 wt%) and nitric acid (HNO_3, 68.0-70.0 wt%) were purchased from Aldrich and used as received. Hydrogen peroxide (H_2O_2, 29-32 wt%) was provided by Alfa Aesar (Massachusetts, USA). 1000 ppm rhodium ICP standard (Rhodium trichloride in 3 wt% HCl) was supplied by Ricca Chemical Company (Oakville, CA). The

distilled water was obtained from the Department of Chemical Engineering, University of Waterloo, Canada.

3.2 Experimental procedures

3.2.1 Fluorinated Wilkinson's catalyst synthesis and bulk hydrogenation

The fluorinated Wilkinson's catalyst $RhCl(P(p\text{-}C_6H_4CF_3)_3)_3$ was prepared according to the literature [*39*] with TPP replaced by TTFMPP. The bulk hydrogenation was performed according to the standard procedure described in the patent granted to Rempel et. al. [*85*].

3.2.2 Preparation of the extraction samples

The extraction sample of HNBR film was prepared with rhodium concentration of approximate 700 ppm, which is determined based on the usage of Wilkinson's catalyst in the latex direct hydrogenation and bulk hydrogenation processes [*4*]. This pre-determined concentration was used to quantitatively analyze the extraction ratio after the recovery treatment. Unless otherwise indicated, the extraction sample of HNBR film with dissolution of Wilkinson's catalyst were all prepared according to the following procedure. 4.34 g of HNBR in small pieces was first dissolved into 65 mL of MEK to obtain a homogeneous solution. In the meantime, 0.027 g of Wilkinson's catalyst was dissolved into a new batch of 10 mL of MEK to obtain another homogeneous solution. These two resulting homogeneous solutions were mixed together and shaken for 20 min to form a homogeneous mixture of HNBR and Wilkinson's catalyst in MEK. The above mixture was then cast into a Petri Dish with a diameter of 110 mm and a HNBR film with dissolution of Wilkinson's catalyst was acquired with a thickness of 0.3 mm after slowly evaporating the MEK solvent at room temperature in a fume hood.

The preparation procedure for extraction sample of NBR film can refer to the preparation procedure of HNBR film as described above with several modifications. First, the solvent for dissolving NBR was acetone instead of MEK, when the catalyst that dissolved in it is $RhCl_3$. Second, the concentration of rhodium in NBR was not fixed at around 700 ppm as in the HNBR sample. The concentration of rhodium in each NBR sample was thereafter indicated cased by case.

In a typical experimental run, the sample films of HNBR or NBR were first cut into strips with a dimension of 2 mm×4 mm×0.3 mm.

3.2.3 Extraction using $scCO_2$ or CXLs

A commercial supercritical fluid extraction instrument R100 (Thar Technologies Inc. Pennsylvania, USA) was employed to carry out the extraction experiments. A schematic diagram of the extraction apparatus is illustrated in Figure 3-1. The R100 system has two high pressure vessels: one is the 150 mL high pressure reactor equipped with two visual quartz glass windows; the other one is the 500 mL extraction vessel. CO_2 and co-solvent can be delivered to either of the two reactors by regulating the specific manual valves installed in this system. Meanwhile, the R100 system is interfaced with a computer and controlled by the software named Processsuite (Thar Technologies Inc. Pennsylvania, USA), through which the operational temperature, pressure, and flow rates of CO_2 and co-solvent were set at the desired values. The temperature and pressure can be maintained at a preset value with an error of less than ±1 °C by a thermocouple and less than ±1 bar by a back pressure regulator, respectively. In a $scCO_2$ extraction process, the 150 mL high pressure reactor was employed. Around 0.2 g extraction sample of HNBR film was directly placed into the reactor and the

extraction was conducted with CO_2 and co-solvent introduced at constant pressure and temperature. In a CXL extraction process, the 500 mL extraction vessel was employed. Approximate 0.2 g HNBR extraction sample was sandwiched into a stainless steel mesh box before it was placed into a 100 mL wheaton glass bottle preloaded with 2.5 mL PMDETA and 15 mL methanol. The glass bottle was then set in a 500 mL extraction vessel of the R100 to carry out the extraction with its cover having a hole to allow CO_2 to pass through freely when the temperature reached the set value. The 500 mL extraction vessel was then sealed and the extraction was carried out with addition of CO_2 at certain pressures and temperatures. In both $scCO_2$ and CXL extractions, liquid CO_2 passed through a chiller and was cooled down before it was pumped into the extraction vessel by a high pressure liquid pump. Before CO_2 finally reached the extraction vessel, it was preheated by the heat exchanger, which was set at exactly the same temperature as the extraction vessel. Meanwhile, the pressure of the extraction system was maintained by the back pressure regulator automatically as soon as the pressure reached the set point. The time counting was started to record the extraction time once the operational temperature and pressure reached the preset values. When the required extraction time was reached, CO_2 was released by setting the working pressure of the back pressure regulator to 0. The extraction vessel was then opened to collect the samples. The extraction time was varied for the purpose of studying the extraction ratios as a function of operation time.

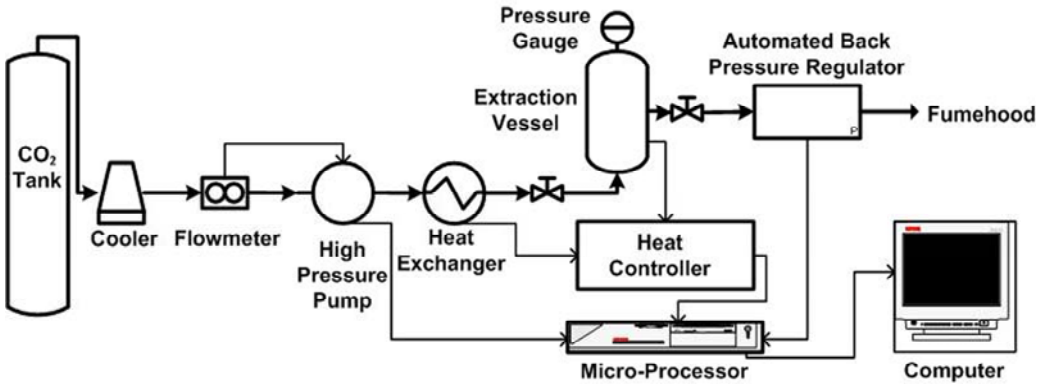

Figure 3-1 Schematic Diagram of the Extraction Apparatus

3.2.4 Digestion procedure

The superior resistance of HNBR to oxidative and thermal degradation leads to a great challenge existing in the digestion of the HNBR matrix in order to quantitatively determine the residual rhodium left in the matrix. A high pressure asher (HPA-S) manufactured by Anton Paar GmbH (Graz, Austria) was employed for sample digestion under a working pressure of up to 128±8 bar. The temperature profile applied for the HNBR digestion is the default program for difficult organic materials, which is able to run at 300 °C. The typical digestion operation is completed according to the following six steps. First, for a sample of known weight, 1 mL HCl, 5 mL HNO_3, and 1 mL H_2O_2 were all added into a quartz vessel in order; second, the quartz vessel with the sample and reagents were wrapped with the polytetrafluoroethylene (PTFE) strips and the quartz lids on the wrapping attachment purchased from the HPA-S; third, the wrapped quartz vessels were placed in the heating block inserted in the high-pressure heating vessel of the HPA-S; fourth, the high pressure heating vessel was topped with a lid and the pressure warning valve was closed; fifth, the nitrogen was charged into the vessel slowly and the pressure was ramped up to 100 bar; sixth, the program of Organic High was run to start the digestion process. The total digestion time

with this program was two hours including the time allowed for the temperature ramping. When the temperature of the system dropped to below 45 °C, the system pressure was slowly decreased to atmospheric pressure by slowly opening the outlet valve. The digestion solutions were placed in the fume hood for 12 h to remove the matrix effect from concentrated acids.

3.2.5 ICP analysis and extraction ratio calculation

Inductively Coupled Plasma with Optical Emission Spectrometer (ICP-OES) is one of the most reliable methods up to now to determine rhodium quantitatively [*147*]. The Prodigy high dispersion ICP-OES with state-of-the-art array detection (Teledyne Leeman Labs, New Hampshire, USA) was used for the rhodium analysis. A calibration curve was generated by the solutions of rhodium trichloride ($RhCl_3$) in 1M HCl with different concentrations of 0.1, 1, 5, 10 ppm rhodium. Electromagnetic radiation at 343.489 nm was applied to identify and quantify the rhodium.

Extraction ratio calculation

The extraction ratio was based on the results of ICP-OES analysis and calculated from Equation 3-1:

$$Extraction\ Ratio(\%) = \left[1 - \frac{W_d \times I}{W_m \times C}\right] \times 100\,\% \qquad \textbf{Equation 3-1}$$

where W_d and W_m represent the mass of diluted digestion solution and a digested matrix, respectively. I is the ICP-OES detection value in ppm. C is the initial concentration of rhodium in HNBR in ppm, which is calculated from Equation 3-2:

$$C = \frac{W_w \times 111221.71}{(W_w + W_h)} \qquad \textbf{Equation 3-2}$$

where W_w and W_h are the mass of Wilkinson's catalyst and HNBR, respectively. 111221.71 is a constant calculated based on the atomic and molecular weight of rhodium and Wilkinson's catalyst, which is calculated from Equation 3-3:

$$\frac{M_{Rh}}{M_w} \times 10^6 \qquad \textbf{Equation 3-3}$$

where M_{Rh} and M_W are the molecular weight of rhodium and Wilkinson's catalyst, respectively.

3.3 Verification of the procedures involved in CXM extraction

3.3.1 The distribution of Wilkinson's catalyst in HNBR films

In the procedure of extraction sample preparation, the HNBR and Wilkinson's catalyst were dissolved in the MEK, respectively, to form homogeneous solutions, the solutions then were put together to have homogeneous solution of Wilkinson's catalyst and HNBR in MEK. The procedure was designed to obtain extraction samples with Wilkinson's catalyst evenly distributed in the HNBR matrix. In order to verify the pattern of the allocation of the Wilkinson's catalyst in HNBR, Scanning electron microscope (SEM) was employed to characterize it. The image obtained by SEM is presented below in Figure 3-2. It can be seen

that no spots can be observed in the image presented. Therefore, the Wilkinson's catalyst appears homogeneously mixed with HNBR.

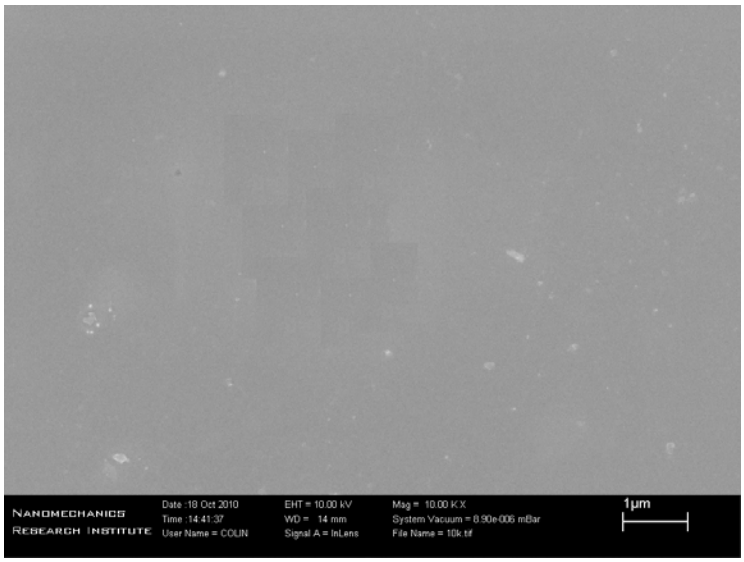

Figure 3-2 Extraction sample characterized by scanning electron microscope (SEM)

3.3.2 Different MEK evaporation approaches

The HNBR samples prepared for the extraction experiment are characterized according to the following two aspects: first, the Wilkinson's catalyst is homogenously mixed with HNBR; second, the Wilkinson's catalyst is evenly distributed in HNBR matrix. The first aspect is secured by the homogeneous solution formed with Wilkinson's catalyst and HNBR in MEK. However the second aspect was thought to be dependent on the drying method utilized to obtain the sample film. In the process of drying, too fast evaporation of MEK may induce phase separation and uneven distribution of Wilkinson's catalyst's depth-concentration in the sample film.

In order to investigate this potential indeterminacy, the sample film was dried by vacuum to increase the evaporation rate of MEK and magnify the effect observed. The time taken to dry one batch of sample by the manner of natural evaporation in the fume hood is around 3 h, while the time spent for a similar sample with vacuum evaporation is around 1hour. 3 h static extraction experiments were performed under different pressures of 20, 40, 60, 100 and 200 bar on samples dried by vacuum. The extraction results are presented in Table 3-1 as well as those obtained on the regular samples with identical extraction conditions and time.

Table 3-1 Experimental parameters and extraction results obtained under various pressures (20, 40, 60,100 and 200 bar) at 80 °C on samples dried by two different methods †

P (bar)	Ms (g)	C_0 (ppm)	Time (h)	M_d (g)	I (ppm)	Ext. (%)	Residue (ppm)
				Method I‡			
20	0.2003	700.1	3	23.1398	2.86	53	330.4
40	0.2002	694.3	3	24.9179	2.48	56	308.5
60	0.2007	701.5	3	23.0607	2.17	64	249.8
100	0.2035	705.2	3	20.3329	2.98	58	297.5
200	0.2001	705.0	3	25.5133	2.28	59	290.3
				Method II‡			
20	0.2002	683.1	3	23.8721	2.77	52	330.0
40	0.2004	664.2	3	24.5317	2.34	57	286.4
60	0.2001	683.1	3	24.9679	1.89	65	235.6
100	0.2000	664.2	3	24.9351	2.36	56	294.1
200	0.2004	664.2	3	24.9529	2.29	57	285.4

Note: † P stands for pressure, Ms for mass of polymer matrix, C for initial concentration of Wilkinson's catalyst in HNBR matrix, Time for extraction duration, I for ICP results, Ext. for extraction ratio, Residue for the concentration of Wilkinson's catalyst remaining in HNBR matrix after extraction treatment. ‡Method I are extraction results obtained on the sample dried by naturally evaporation of MEK in 3 h, Method Π are extraction results collected on the samples dried by vacuum in 1h.

From the data in Table 3-1, it can be seen that the extraction results of Method Π samples which are dried in a vacuum oven are very close to the extraction results obtained via Method I samples which are dried by naturally evaporation of MEK in the fume hood, when the extractions are completed at the same temperatures and pressures. Therefore, the drying process did not impede the distribution of the Wilkinson's catalyst in the HNBR matrix or the minor alteration of the Wilkinson's catalyst's distribution in the HNBR matrix did not influence the extraction results ascribed to the fact that the thickness of the HNBR film is only 0.3mm.

3.3.3 Different sampling methods

In order to explore the mechanisms involved in the extraction process, the extraction profiles describing the variation of the extraction ratio with time are necessary to be collected properly. Two approaches have been designed and tested to inspect their effects on the extraction profiles collected by the corresponding method. The two approaches for sample collection are described as follows: A. Five independent samples are settled in the extraction vessel all at once. The first sample is collected one hour after the extraction is started with both the temperature and pressure of CO_2 stabilized at the preset values. The other samples are collected one by one at a time interval of 1 h. The CO_2 is released and pressure drops to 0 when the sample is collected. In the mean time, the corresponding amount of methanol/PMDETA solution is decanted (17.5mL) together with each sample collected. Then the CO_2 will be recharged to the pre-set value to continue the extraction on the remaining samples. Therefore, the sample collected after the first one undergoes some pressure fluctuation when the samples prior it are collected. The extraction time applied on every

sample is counted from the start time to the sampling time. The time needed for one extraction profile using approach A is 5 h in total. B. The extraction samples are run independently. Only one single sample is put in the extraction vessel at one time. The extraction starts when the pressure and temperature of CO_2 reach their pre-set values, respectively. The extraction ends when CO_2 is released and the pressure drops to 0 bar and the sample is collected for analysis. The exact same procedure is duplicated on every investigated sample. Therefore, the pressure applied on every sample is ensured to be constant and there is no pressure alteration in the process of extraction. The time used to obtain one extraction profile with approach B is 15 h. The extraction results collected using the two different approaches are presented in Table 3-2 and Figure 3-3.

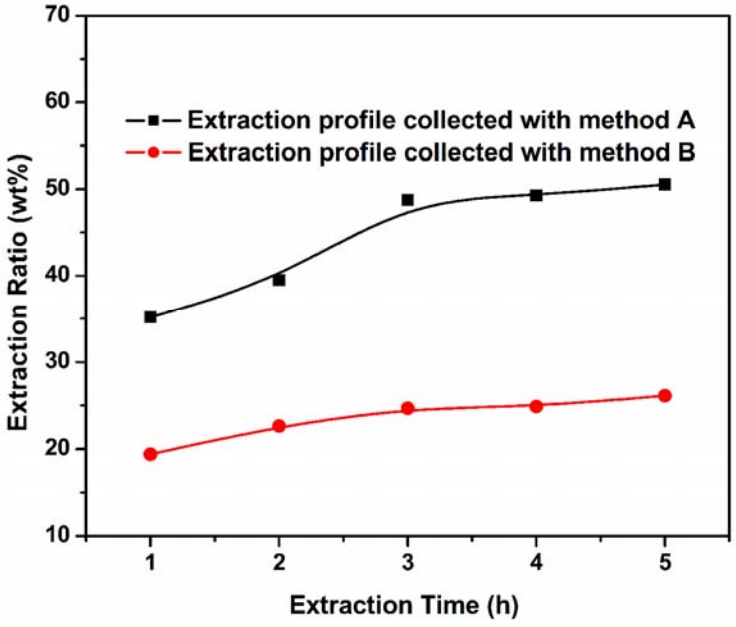

Figure 3-3 Static extraction profiles of CXM and PMDETA on HNBR/Wilkinson's catalyst films at 40 °C and 100 bar collected via different methods

Table 3-2 Experimental parameters and extraction results obtained at 40 °C and 100 bar with two different sample collecting approaches †

Ms (g)	C_0 (ppm)	Time (h)	M_d (g)	I (ppm)	Ext. (%)	Residue (ppm)
			Approach A‡			
0.2108	663.1	1	14.0089	6.47	35	429.8
0.2005	663.1	2	13.1939	6.10	39	401.2
0.2019	663.1	3	17.4142	3.94	49	339.6
0.2004	663.1	4	12.4230	5.42	49	336.2
0.2024	663.1	5	20.2507	3.27	51	327.7
			Approach B‡			
0.2003	703.5	1	20.1930	5.62	19	567.1
0.2004	703.5	2	22.1294	4.93	23	544.2
0.2002	703.5	3	23.7776	4.46	25	529.9
0.2003	703.5	4	21.4437	4.94	25	528.4
0.2003	703.5	5	22.4705	4.63	26	519.8

Note: † refer to the note of Table 3-1; ‡Approach A is extraction results obtained using the sampling method A; Approach B is extraction results collected with the sampling method B.

As shown in Table 3-2 and Figure 3-3, the extraction profiles collected by two methods A and B are notably different from each other. Method B is neat and fundamentally rigorous. The operational conditions including temperature, pressure, usage of methanol and PMDETA in every run are well known and under control. Therefore, the data collected with method B can be doubtlessly employed to investigate the reaction and mass transfer process happening at a specific temperature and pressure. In comparison, the situation in method A is much more complicated. First, the pressure applied on the second and after samples is not constant, they go through pressure variations as the sample before them are collected. Second, it is technically difficult to accurately decant a corresponding amount of methanol/PMDETA at the operational temperature i.e., 40 °C but not the room temperature, which affects the

amount of methanol/PMDETA applied for the later samples. Third, even for the first sample, the situation in method A is still different from it in method B. The usage of methanol/PMDETA in method A is four times more than that used in method B. This helps explains why higher extraction ratios were obtained with method A than with method B.

3.3.4 Different post-treatment methods applied on the digestion solutions

The procedure used to treat the digestion solution could affect the components of the solution matrix and therefore affects the detected ICP value. The digestion solutions for spike studies were processed with the method described as follows: after the digestion procedure, the digestion solution was placed in the fume hood for 12 h to allow for natural evaporation of NO_x, and after that the digestion solution was transferred to a vial and diluted using distilled water to a final volume of around 20 mL. The matrix effects of the solutions processed with this kind of post-treatment were verified by spiking the solutions and the average spike recovery is 84%. Three procedures have been employed for the post-treatment of the digestion solutions. Post-treatment 1: digestion solutions were diluted using distilled water to a total volume of around 20 mL right after the digestion. Post-treatment 2: digestion solutions were firstly placed in the fume hood for 12 h to allow for natural evaporation of NO_x, and then were diluted using distilled water to a total volume of around 20 mL. Post-treatment 3: digestion solutions were firstly heated to 180 °C for 2 h to remove most of the residue of the acids and then were diluted using distilled water to a total volume of around 20 mL. An HNBR film was prepared with a rhodium concentration of 683.1 ppm using the regular sample preparation procedure. Seven extraction samples with identical mass weight of 0.2000 g were obtained from different parts of the HNBR film. The samples were cut into

strips and digested directly without running any extraction process. Two of the seven digestion solutions were treated with the procedure of post-treatment 1; another three of them were treated with the procedure of post-treatment 2; and the other two were treated with the procedure of post-treatment 3. All the results are presented in Table 3-3.

Table 3-3 Experimental parameters and ICP analysis results obtained on the digestion solutions from the same HNBR matrices but with different post-treatments †

Post-Treatment	M_s (g)	C_0 (ppm)	M_d (g)	I (ppm)	L (wt%)	I_a (ppm)	L_a (wt%)
1	0.2000	683.1	24.8464	4.88	11	5.79	-5
	0.2000	683.1	22.6007	4.71	22	5.59	7
2	0.2000	683.1	23.9383	4.72	17	5.60	2
	0.2000	683.1	25.2082	4.57	16	5.42	0
	0.2000	683.1	22.6157	5.23	13	6.21	-3
3	0.2000	683.1	22.8145	5.60	6	6.65	-11
	0.2000	683.1	24.0804	5.79	-2	6.88	-21

Note: † Post-treatment stands for the treatment applied on the digestion solutions: 1, the digestion solutions were diluted with distilled water immediately; 2, the digestion solutions were placed in the fume hood to allow the naturally evaporating of NO_x in 12 h; 3, the digestion solutions were treated using a vaporization set-up to reduce the content of NO_x. M_s stands for the mass weight of the extraction sample, C for the initial concentration of rhodium in HNBR, M_d for the mass weight of the digestion solution, I for the ICP analysis result, L for the loss based on I, I_a for the adjusted ICP analysis result obtained through dividing the ICP results by 84%, L_a for the loss based on I_a.

The seven digested samples had the same pre-known concentration of rhodium, because they are cut from the same piece of HNBR film and no extraction operation had been carried out on them at all. The loss of rhodium is calculated from the total amount of rhodium in the HNBR sample to the total amount of rhodium in the digestion solution. The total amount of rhodium in the digestion solution can be calculated based on the mass weight of

the diluted digestion solution and the concentration of rhodium in the diluted digestion solution. The concentration of rhodium in the diluted digestion solution was indicated by the ICP value. According to the study results obtained on the matrix effects, the detected ICP value and the adjusted ICP values by the factor 84% are presented in the Table 3-3. In the meantime, the losses based on the detected and adjusted ICP values are shown in Table 3-3. The loss of rhodium could be induced from two resources: one is in the procedure of digestion, the other one could be the detected ICP value was effected by the matrix. As seen in Table 3-3, the loss of rhodium from the three post-treatments are different, the loss of rhodium by using post-treatment 3 is the smallest of the three investigated post-treatments. The loss of rhodium by using post-treatment 1 is larger and at the same time less stable than the loss incurred by using the other two. The loss of rhodium by using post-treatment 2 is relatively stable compared to the loss incurred by using post-treatment 1. These observations indicate that the loss of rhodium grows with the residue of acids in the solution. In post-treatment 2, the digestion solutions were placed in the fume hood for 12 h and cooled down to room temperature. The concentration of acids in the solution after 12 h was approximately the equilibrium concentration of acids in the solution and was kept at the same level for different samples but digested using the same recipe. This can explain why the loss of rhodium by using post-treatment 2 are relatively stable. Although the loss of rhodium from post-treatment 3 is the smallest, one more operational step is involved in post-treatment 3 and more risks have to be taken in the operations.

It can also be seen from Table 3-3 that the calculated loss of rhodium by the adjusted ICP value showed large difference among the three post-treatments. The calculated loss of

rhodium for the solutions treated by post-treatment 2 is the smallest, varying from -3 to 2 %, because the adjustment coefficient used was the spike recovery on the solutions processed with post-treatment 2. This means the calculated loss of rhodium based on the detected ICP value resulted of the effects from the matrix and no rhodium was lost in the process of digestion. In the meantime, the observations obtained here illustrated the effectiveness and reliability of our digestion procedure from a different perspective.

3.3.5 Matrix effects on the ICP analysis

The sample "matrix" is the bulk composition of the sample such as water, organic compounds, acids, dissolved solids, and salts. Matrix effects could influence the ability of an analytical method to qualitatively identify and quantitatively measure target compounds in environmental and other samples by indirectly affecting the intensity and resolution of the observed signals.

All the HNBR/Wilkinson's catalyst films were prepared with the same recipe; almost the same amount of HNBR/Wilkinson's catalyst film entered into each run of extraction experiment; equivalent dosage of mixture of acids and hydrogen peroxide (1 mL hydrochloric acid, 5 mL nitric acid and 1 mL hydrogen peroxide) was applied to digest the HNBR matrix after each extraction; and finally the digestion solutions were processed with a fixed procedure (set the digestion tubes in the fume hood overnight to let the NO_x evaporate naturally). Therefore, all matrixes of the solutions for ICP analysis are supposed to be the same, consisting of water, nitric acid, hydrochloric acid and phosphate of given proportions.

The method applied to investigate the matrix effect is to spike 10 samples with commercial available ICP standard of $RhCl_3$; recovery of the standard rhodium spiked

solution was examined. In every spiked ICP sample, 20 μL of 1000 ppm rhodium ICP standard was added as spike into a 5 mL ICP sample. The addition of rhodium concentration in the spiked sample was supposed to be 4 ppm. Both the ICP sample and the spiked ICP sample were measured by ICP-OES. The addition of rhodium concentration determined by ICP from the ICP sample to its accordingly spiked one was divided by 4 ppm to obtain the spike recovery. The spike recovery will be used to investigate the effect of matrices. The results are presented in Table 3-4 and Figure 3-4.

Table 3-4 Experimental parameters and ICP analysis results obtained on 10 random samples and their spikes†

M_s (g)	C (ppm)	M_d (g)	I (ppm)	I_s (ppm)	Recovery (%)
0.2001	684.0	23.8218	2.03	5.43	85
0.2001	684.0	25.1545	1.99	5.43	86
0.2002	698.8	24.3507	1.73	5.05	83
0.2000	698.8	22.6242	1.41	4.69	82
0.2003	684.0	24.2278	1.26	4.65	85
0.2003	684.0	24.5858	1.42	4.82	85
0.2000	683.1	24.8464	4.86	8.19	83
0.2000	683.1	22.6007	4.61	7.82	80
0.2000	684.0	24.6734	3.05	6.44	85
0.2004	684.0	25.795	4.53	8.06	88

Note: † refer to the note of Table 3-1, I for the ICP analysis result, I_s for the ICP analysis result of the spiked sample. Recovery stands for the spike recovery.

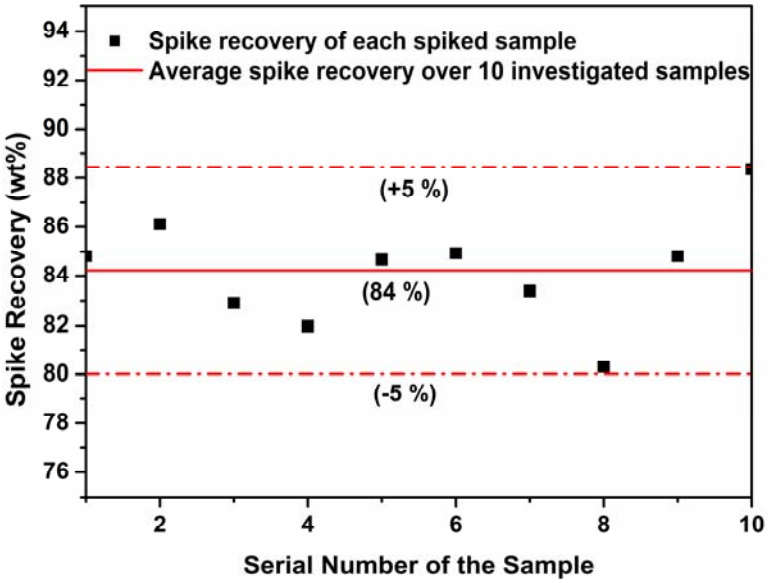

Figure 3-4 Spike recovery of 10 spiked samples and the average spike recovery obtained from them

As seen from the Table 3-4, the spiked solution samples have different rhodium concentrations varying from 1.2644 to 4.8567 ppm. This distribution range covers most of the concentrations of the solution samples for ICP analysis in our experiment. As shown in Figure 3-4, the spike recoveries are distributed from 80 to 88% and the average spike recovery over the 10 studied samples is 84%. All the spike recoveries obtained are scattered within the range of ±5% of 84%. Most of the spike recoveries are within the range of ±3% of 84%. The results obtained prove that the matrix effect arising from the residue of acids could be treated by recovery of 84% for all the solution samples. The results measured by ICP were divided by 84% to obtain the true concentrations of rhodium in the solution samples. These true concentrations of rhodium in the solutions were used to evaluate the extraction ratios.

In line with above, in the following experiments, all the digestion solutions were placed in the fume hood for 12 h to allow the natural evaporation of NOx before it was diluted with

distilled water. All the detected ICP values of the solutions processed using this procedure were adjusted by the coefficient of 84% and the adjusted ICP values were used to calculate the extraction ratio. Unless otherwise indicated, all the ICP values mentioned in this thesis present the ICP after adjustment.

Because the spike recoveries were mostly scattered from 82 to 86%, error bars were added on the extraction ratios presented in the subsequent Figures. These error bars were generated using extraction ratios calculated from ICP values, which were produced by dividing the measured ICP values with coefficients of 82% or 86%.

3.3.6 Duplication and error analysis

The extraction experiments were repeated two times for duplication test at temperature of 90 and pressure range from 20 to 200 bar. The second group experiments were carried out around half a year later after the first group. The experimental results are listed in Table 3-5.

Table 3-5 Extraction results obtained in two times operation at 90 and pressure from 20 to 200 bar

Group	P (bar)	M_s (g)	C (ppm)	Time (h)	M_d (g)	I (ppm)	Ext. (wt%)	Residue (ppm)
I	20	0.1999	701.0	1	23.7254	3.26	45	387.0
		0.1999	701.0	2	23.9156	2.85	51	340.6
		0.2001	701.0	3	22.9053	2.48	60	283.7
		0.2000	701.0	4	23.8377	2.15	63	256.1
		0.2003	701.0	5	23.6710	2.05	65	242.5
	40	0.2005	701.9	1	23.6970	3.30	44	390.3
		0.2001	701.9	2	22.5793	2.89	54	326.3
		0.2001	701.9	3	23.7949	2.47	58	294.0

		0.2002	701.9	4	22.0453	2.54	60	279.8
		0.1998	701.9	5	26.3290	1.94	64	255.6
	60	0.2000	708.3	1	24.5719	2.46	57	302.7
		0.2001	708.3	2	25.7181	1.88	66	241.8
		0.2000	708.3	3	24.8508	1.72	70	214.0
		0.2000	708.3	4	23.8200	1.74	71	207.4
		0.2000	708.3	5	24.1118	1.63	72	197.0
	100	0.2006	701.5	1	21.7484	3.56	45	385.8
		0.2003	701.5	2	24.0515	2.79	52	334.4
		0.2005	701.5	3	22.5802	2.72	56	305.9
		0.2004	701.5	4	23.9650	2.06	65	246.3
		0.1999	701.5	5	23.3366	2.16	64	251.7
	200	0.2002	708.3	1	25.2800	2.60	54	328.2
		0.2003	708.3	2	24.3141	2.44	58	296.2
		0.2000	708.3	3	24.4105	2.16	63	263.3
		0.2000	708.3	4	21.8629	2.41	63	264.0
		0.2002	708.3	5	21.4803	2.45	63	262.7
II	20	0.2005	700.1	1	23.9064	3.20	46	381.2
		0.2002	700.1	2	23.0818	2.86	53	330.0
		0.2005	700.1	3	22.5711	2.65	57	298.3
		0.2003	700.1	4	23.8750	2.36	60	281.5
		0.2003	700.1	5	23.9041	2.29	61	273.9
	40	0.2005	700.1	1	22.6772	3.14	49	355.7
		0.2003	700.1	2	24.6234	2.76	51	339.9
		0.200	700.1	3	24.3114	2.52	56	306.8
		0.2003	700.1	4	24.6745	2.27	60	279.1
		0.2005	700.1	5	23.3089	2.19	64	255.1

60	0.2009	701.5	1	22.3071	2.49	61	276.1
	0.2005	701.5	2	22.6166	1.95	69	219.7
	0.2000	701.5	3	21.1479	1.98	70	209.9
	0.2000	701.5	4	23.0434	1.65	73	190.4
	0.2002	701.5	5	21.8354	1.59	75	173.5
100	0.1999	708.3	1	24.1445	3.48	41	420.1
	0.2004	708.3	2	24.9277	2.79	51	347.2
	0.2004	708.3	3	22.4710	2.61	59	292.5
	0.2000	708.3	4	23.6520	2.29	62	270.6
	0.2003	708.3	5	24.0330	2.22	62	266.2
200	0.2012	703.5	1	25.1589	2.44	57	305.2
	0.2002	703.5	2	25.4416	2.13	61	271.1
	0.2008	703.5	3	23.7511	2.23	63	263.6
	0.2005	703.5	4	22.6465	2.28	63	257.8
	0.2005	703.5	5	23.6311	2.01	66	237.0

Note: † P stands for pressure, Ms for mass of polymer matrix, C for initial concentration of Wilkinson's catalyst in HNBR matrix, Time for extraction duration, I for ICP results, Ext. for extraction ratio, Residue for the concentration of Wilkinson's catalyst remaining in HNBR matrix after extraction treatment.

From the data listed in Table 3-5, we can see that the duplication of the data collected in two independent groups of operation is good. The sample deviation is 1.4 wt%, calculated based on Equation 3-4. Therefore, there is a good duplication for the experiment, especially at the low pressure range.

$$s = \sqrt{\frac{\sum\left(x_i - \overline{x_i}\right)^2}{49}} \qquad \textbf{Equation 3-4}$$

where *s* stands for the sample deviation, *i* for a certain experimental condition consisting of temperature, pressure and treatment time duration, x_i for the extraction ratios obtained at the experimental condition of *i*. $\overline{x_i}$ for the average extraction ratio of two measurements at an identical experimental condition *i*.

3.4 Summary

In this Chapter, the methodology involved in developing a green separation technique for recovery of organometallic catalysts from polymers is reported, as well as the investigation of several potential factors which were expected to have effects on an extraction process using CXM and PMDETA. The reported procedures include fluorous Wilkinson's catalyst synthesis, catalytic hydrogenation of bulk NBR, extraction sample preparation, extraction using $scCO_2$ or CXLs, sample digestion, and ICP analysis. The procedures used in an extraction process using CXM and PMDETA have been very well stabilized, whereas those involved in an extraction using $scCO_2$ are not so standard and will be indicated with more details in the following Chapter, if necessary.

The operational parameters involved in an extracion process using CXM and PMDETA were carefully studied, including the distribution of Wilkinson's catalyst in HNBR, the effects of drying method for preparation an HNBR film, the effects of sampling method, the effects of digestion solution treatment method, and the matrix effects of solution towards the ICP analysis results. The experiment duplication was also carefully investigated and it was found that the operation and analysis method has a very good duplication with a sample deviation of 1.4 wt%.

Chapter 4
Recovery of Rhodium Catalysts Using Supercritical Carbon Dioxide

Efforts have been made to approach the objective in two ways. One approach was to synthesize new catalyst which is $scCO_2$ soluble and effective in selective hydrogenation of the C=C bond in NBR. The fluorinated analogue of Wilkinson's catalyst was synthesized successfully and illustrated to have limited efficiency in selective hydrogenation of the C=C bond in NBR. However the recovery of the fluorinated analogue of Wilkinson's catalyst could not be achieved using $scCO_2$ and co-solvent methanol. The other approach was to employ $scCO_2$ and $scCO_2$ dissolvable chelating ligand to separate Wilkinson's catalyst from HNBR/NBR. The $scCO_2$ dissolvable chelating ligand TTA was employed to conduct the extraction. TTA was found to be able to extract rhodium from its aqueous solution and crystal but not able to extract rhodium from HNBR/NBR matrix. All the observations obtained pointed out the direction at using the extraction system of CO_2 expanded liquid and chelating ligand. CO_2-expanded water and CO_2-expanded alcohols were tested for their extraction efficiency. All the detailed progress will be expanded in the following sections.

4.1 Fluorinated analogue of Wilkinson's catalyst

$ScCO_2$ as a reaction solvent offers many advantages over conventional organic solvents, including increased reaction rates, higher selectivity, and facile separation of reactants, catalysts, and products after reaction. Moreover, $scCO_2$ is nontoxic, nonflammable, inexpensive, and readily available in large quantities and has a low critical temperature and a moderate critical pressure. With such properties, $scCO_2$ has the potential to replace organic solvents in a number of applications.

However, despite the potential benefits of using $scCO_2$ in homogeneous catalysis, there have been surprisingly few pertinent studies in this area. The application of $scCO_2$ in homogeneous catalysis has been significantly hindered by the limited solubility of effective catalysts in $scCO_2$. For example, the maximum solubility of the homogeneous catalyst dichlorobis (triphenylphosphine) nickel (II) in $scCO_2$ was reported to be mere 0.01 mM at T =55 °C, P=300 bar and ρ =0.83 g/mL [*148*]. Likewise, the solubility of Wilkinson's catalyst in $scCO_2$ at T = 45 °C, P= 273 bar and ρ= 0.88 g/mL was no more than 0.02 mM [*149*]. In contrast, typical catalyst concentrations employed in homogeneous catalysis are on the order of 1.0 mM, showing the need for at least a 100-fold increase in solubility.

If $scCO_2$ is to be favored over organic solvents, catalysts need to be moderately soluble in $scCO_2$ at pressures as low as 100 bar. This requires modification or redesign of conventional organometallic catalysts or some other way to dissolve catalytic amounts of the complexes in $scCO_2$. One way to increase solubility in $scCO_2$ is to utilize CO_2-philic moieties such as fluoroether, fluoroalkyl, fluoroacrylate, siloxane, or phosphazene [*150*]. In our search for a soluble and active catalyst for homogeneous reactions in $scCO_2$, we have synthesized a fluorinated analogue of the well-known Wilkinson's catalyst (see Figure 4-2). The new complex $RhCl(TTFMPP)_3$ was produced by incorporating trifluoromethyl (p-CF_3) groups into the phenyl rings of the phosphine ligands of Wilkinson's catalyst. The synthesis method was based on the method for Wilkinson's catalyst [*26*]. A Bio-Rad FTS 3000MX spectrometer was used for Fourier transform infrared (FT-IR) analysis. The FT-IR spectra of the fluorinated Wilkinson's catalyst and the fluorinated ligand tris(p-trifluoromethylphenyl) phosphine (TTFMPP) are shown in Figure 4-1. The FT-IR spectra of $RhCl(TTFMPP)_3$ and

TTFMPP appear to be almost the same. Taking into account the typical synthesis route used (same as the one used by Wilkinson's catalyst), the FT-IR results basically confirmed that the new complex obtained was $RhCl(TTFMPP)_3$.

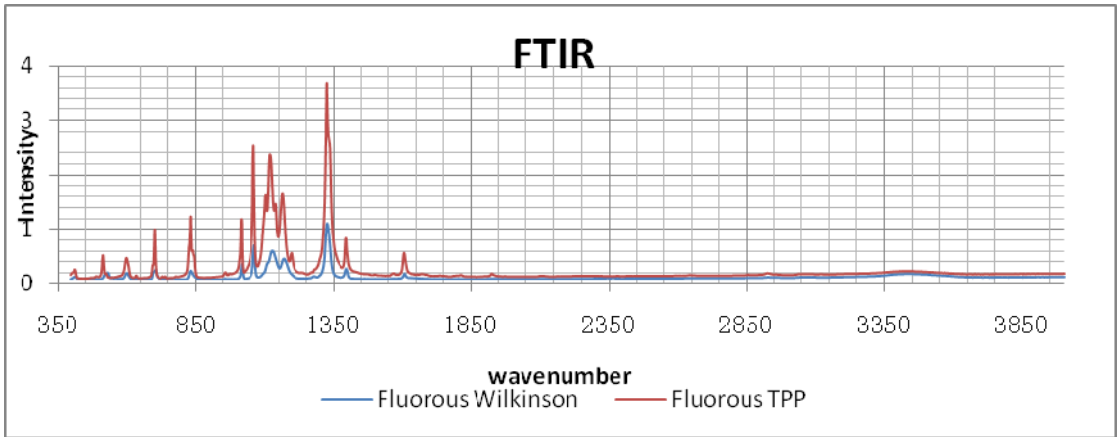

Figure 4-1 FT-IR of $RhCl(TTFMPP)_3$ and TTFMPP

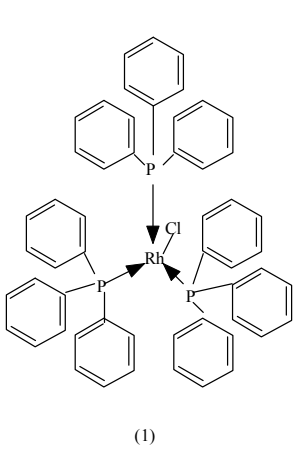

(1)

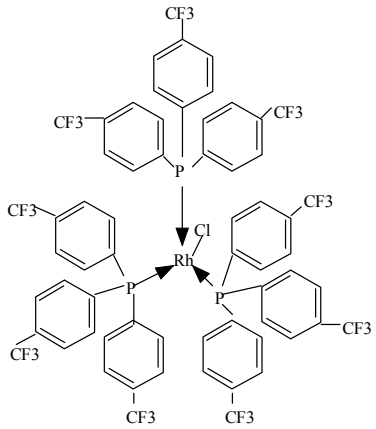

(2)

Figure 4-2 Conventional Wilkinson's Catalyst (1) and Modified Catalyst (2)

4.1.1 Solubility of the fluorinated Wilkinson's catalyst in $scCO_2$

New synthesized fluorinated Wilkinson's catalyst was illustrated to be $scCO_2$ soluble at 70 °C and 270 bar through observation. The solubility observation was carried out in a 150

mL high pressure reactor equipped with visual windows. The 150 mL high pressure reactor was equipped in the supercritical fluid extraction apparatus R100 supplied by the Thar technologies, Inc. The red color was observed to appear when the pressure reached 270 bar at 70 °C. However the systematic solubility measurement of this new catalyst in $scCO_2$ has not been completed because the specific equipment required was unavailable.

4.1.2 NBR bulk hydrogenation with the fluorinated Wilkinson's catalyst

The NBR bulk hydrogenation was conducted in a 300mL Parr 316 Stainless Steel reactor system. The NBR sample was cut into small pieces with dimensions 0.3 mm×1 mm×1 mm and then was mixed with catalyst. The mixture of solid NBR and catalyst was contained in a 20 mL vial before it was set into the 300 mL Parr reactor. By doing this, the sample can be easily collected when the reaction is stopped. The catalyst loading is 600 ppm based on rhodium at reaction temperature 145 °C, H_2 pressure 69 bar and stirring speed 500 rpm. After 6 h reaction, the sample was collected and dissolved in methyl ethyl ketone (MEK) and a polymer film was cast onto a sodium chloride disc for FTIR analysis. Cross linking (gel formation) was judged by checking if the resultant HNBR was totally soluble in MCB or MEK at room temperature by the naked eye. Table 4-1 shows results for a group of bulk hydrogenation experiments. The hydrogenation experiment using the water soluble catalyst RhCl(dpm) [dpm= $Ph_2P(m\text{-}C_6H_4SO_3H)$, i.e. diphenylphosphino-benzene-*m*-sulfonate] was conducted at 140 °C. The other hydrogenation experiments presented in Table 4-1 were carried out at 145 °C.

Table 4-1 Experimental parameters and results obtained for bulk hydrogenation with different catalysts and ligands†

Item	NBR g	Catalyst	M_c g	Ligand	M_L g	Time	HD mol%
Exp 1	0.6147	$RhCl(TTFMPP)_3$	0.0031	TTFMPP	0.031	6	30
Exp 2	0.6291	$RhCl(TTFMPP)_3$	0.0058	TPP	0.0578	6	87
Exp 3	0.6364	$RhCl(TPP)_3$	0.0050	TTFMPP	0.0711	6	0
Exp 4	0.6265	RhCl(dpm)	0.0058	TPP	0.0547	8	0

Note: †M_c stands for the mass weight of the catalyst, M_L for the mass weight of the ligand, HD for the hydrogenation degree.

It can be seen from Table 4-1, the fluorinated Wilkinson's catalyst has certain hydrogenation efficiency, and however the 30% hydrogenation under the specified operation conditions is still far below the 95% which is required as the minimum hydrogenation for an acceptable HNBR product. It is also easy to see that the group of fluorinated Wilkinson's catalyst and TPP ligand works well to reach 87% under the same operational conditions and reaction time as TPP is 10 times more than the catalyst in the reaction mixture and replaces of TTFMPP ligand as the reaction proceeds. The zero hydrogenation of Exp 3 verified the results of Exp 1 that the fluorous Wilkinson's catalyst [$RhCl(TTFMPP)_3$] has very poor or even no activity toward selective hydrogenation of the C=C bonds of NBR, because TTFMPP ligand was used in Exp 3 and the loading of which is 10 folds of that of the fluorous catalyst too. The electron-drawn effect of the fluorine moiety, i.e. CF_3 is supposed to be the factor that caused the reduced reactivity of the new synthesized fluorous Wilkinson's catalyst. The water soluble catalyst RhCl(dpm) did not present any hydrogenation either even

with TPP as an added ligand. One explanation is that the RhCl(dpm) is decomposed under a temperature of more than 90°C.

From an overall appraisement of the results presented in Table 4-1, conventional Wilkinson's catalyst showed the best efficiency in catalyzing selective hydrogenation of the C=C bonds in NBR. The modified Wilkinson's catalysts such as $scCO_2$ soluble $RhCl(TTFMPP)_3$ and water soluble RhCl(dpm) were however found of poor performance. The thermal decomposition of the water soluble catalyst at elevated temperature made it not suitable for application in bulk hydrogenation, whereas the fluorous Wilkinson's catalyst still has space for performance enhancement by optimization of the fluorous chain. Additionally, the experiments reported in Table 4-1 have been conducted only once and more experiments can be conducted to further verify and reveal the reasons when required in the future. In order to obtain a quick idea regarding to the feasibility of this approach via catalyst modification, the recovery experiment of the fluorous Wilkinson's catalyst from HNBR using $scCO_2$ was reported as follows.

4.1.3 Recovery of the fluorous Wilkinson's catalyst using $scCO_2$

The HNBR with catalyst after bulk hydrogenation was re-cut into pieces with dimensions 0.3 mm×0.3 mm×0.3 mm and extracted with $scCO_2$ and 5% (v/v) methanol as co-solvent. The extraction was conducted using the 150 mL reactor equipped in the R100. The temperature and pressure used for the extraction were 70 °C and 270 bar, respectively. The procedure used for the $scCO_2$ extraction was described as following. The HNBR strips were placed in the 150 mL reactor. The reactor was then sealed. CO_2 flowed through a heat exchanger to cool down before it was pumped by the high pressure liquid pump. In the mean time,

methanol was added via another high pressure co-solvent pump. The mixture of CO_2 and methanol was heated up to the pre-set temperature by a heat exchanger and then entered the reactor. When the temperature and pressure in the reactor arrived at their respective pre-set values, the addition of CO_2 and methanol was stopped and the inlet and outlet valves of the reactor were closed. The stirring was kept at 400 rmp for 30 min. The inlet and outlet valves of the reactor were then opened and the pumps of CO_2 and methanol were started with a flow rate of 10 g/min and 0.66 mL/min, respectively. The dynamic extraction with continuous flowing of methanol and CO_2 lasted for 90 min. The whole extraction process comprised 30 min of static extraction and 90 min of dynamic extraction. After the extraction operation, the pumps were stopped and the back pressure regulator was set at 0 to allow the releasing of CO_2. The whole process was controlled by a computer with software "Processsuite" installed. The sample after extraction was digested by HPA-S according to the procedure described in 3.2.4 and the digestion solution was analyzed by ICP to know the rhodium left in the HNBR matrix. The extraction results are presented in the Table 4-2.

From the data presented in Table 4-2, we can conclude that the new synthesized fluorinated Wilkinson's catalyst is difficult to be extracted out from the HNBR matrix with $scCO_2$ and methanol as co-solvent under 270 bar and 70 °C. It was well known that the diffusion of chemical molecules in the matrix of solid polymers is very slow. The diffusion of Wilkinson's complexes is even slower due to the formation of a coordination bond between rhodium (I) and the C≡N group present HNBR. In other words, the solvating power of $scCO_2$ towards the fluorous Wilkinson's catalyst is not strong enough and the coordination

bond between rhodium (I) and the C≡N group presents even more challenges for the separation of the Wilkinson's complexes from the nitrile rubber, i.e. HNBR.

Table 4-2 Experimental parameters and results obtained for the $scCO_2$ extraction of rhodium catalyst from HNBR at 70 °C and 270 bar in 2 h

Item	M_s g	C_0 ppm	M_d g	I ppm	Ext.[3] wt%
Sample1[1]	0.1944	334.72	12.90	3.52	0
Sample2[1]	0.4203	334.72	9.44	12.04	29
Sample3[2]	0.3333	612.90	10.43	25.46	0
Sample4[2]	0.3044	612.90	12.22	9.82	0

Note: † refer to the note of Table 3-1. 1."Sample1" and "Sample2" were from the same bulk hydrogenation sample with $RhCl(TTFMPP)_3$ and TTFMPP as catalyst and ligand, respectively. "Sample1" was never extracted and treated as blank. "Sample2" was extracted with $scCO_2$. 2."Sample3" and "Sample4" were from the same bulk hydrogenation sample with $RhCl(TTFMPP)_3$ and TPP as catalyst and ligand, respectively. "Sample3" was never extracted and treated as blank, "sample4" was extracted with $scCO_2$. 3. The extraction ratio was calculated referring to the Equation 3-1.

4.2 Recovery of rhodium catalysts using $scCO_2$ and chelating ligands

As can be seen from the discussion conducted in Section 4.1, the fluorinated Wilkinson's catalyst presented limited efficiency for catalytic hydrogenation of NBR. Moreover, the hydrogenation efficiency was highly dependent on the type of ligand used. An 87% hydrogenation was achieved with the fluorinated Wilkinson's catalyst $RhCl(P(p\text{-}C_6H_4CF_3)_3)_3$ when the ligand TPP was utilized. The effective catalyst was supposed to be still the conventional Wilkinson's catalyst, i.e. $RhCl(TPP)_3$. Therefore, efforts were made to use a $scCO_2$ dissolvable chelating agent to assist the recovery of Wilkinson's catalyst from HNBR.

TTA was reported to be a good chelating ligand in $scCO_2$ to extract lanthanides from nitric acid aqueous solution and TTA was illustrated to work well on metal ions with +2 and

+3 valence [*151*]. Thus an attempt was made to employ it in $scCO_2$ with methanol as co-solvent to extract rhodium catalysts. A few experiments were carried out on the rhodium recovery with $scCO_2$ and TTA as a chelating ligand from various matrices such as water, NBR and wet crystalline $RhCl_3$ itself.

4.2.1 Extraction of $RhCl_3$ from aqueous solution using $scCO_2$ and TTA

The supercritical CO_2 extraction procedure was described in Section 4.1.3. Only the high pressure vessel used was a 500 mL extraction vessel of R100, not the 150 mL reactor of R100. The operational procedure and pressure varying diagram for the typical extraction of $RhCl_3$ from its water solution are shown in Figure 4-3. About 0.003 g of $RhCl_3$ was dissolved in 20 mL water to make a water solution contained in a 100 mL jar. A certain quantity of TTA was stored in another separate 20 mL vial. Both the jar and vial have a cover with a hole in it to let the $scCO_2$ enter and leave. The system was operated at 60 °C and 150 bar, 5% (v/v) methanol was used as co-solvent to increase the metal ion's solubility in $scCO_2$. Methanol ratio was kept at 5% (v/v) for most of the extraction processes. Only before the end of the extraction, methanol was stopped and thus the leftover methanol in water was kept as low as possible.

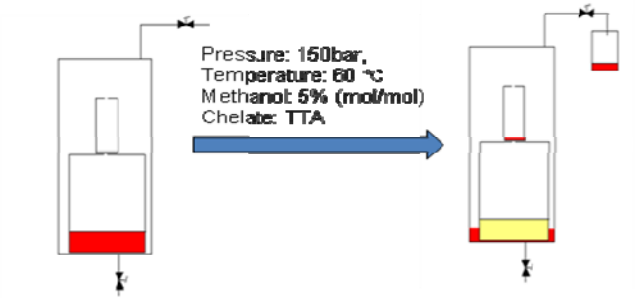

a. Schematic diagram of $RhCl_3$ extraction using $scCO_2$ and TTA

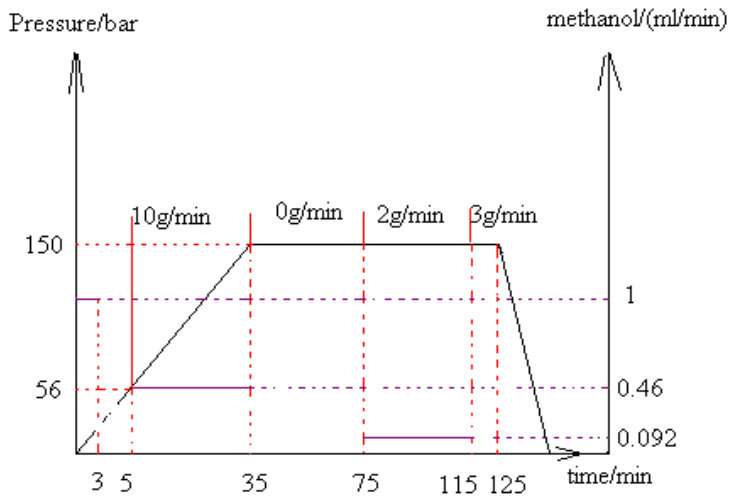

b. CO_2 and methanol flow-rates and system pressure varying procedure

Figure 4-3 Equipment illustration and pressure varying procedure in rhodium extraction

In each run of extraction, the amount of $RhCl_3$ was fixed at 0.003 g, while the amount of TTA applied varied from 0.0025 to 0.04 g. The molar ratio of TTA to rhodium for a TTA amount of 0.0025 and 0.04 g was 1 and 16, respectively. The water solution after extraction was diluted into a 100 mL volumetric flask and analyzed using ICP-OES. All the data are presented in Table 4-3.

As can be seen from Table 4-3 and Figure 4-4, the rhodium extraction ratio increased quickly as the TTA loading increased from 0.0025 to 0.02g. Once the TTA loading reached 0.02 g, the rhodium extraction ratio did not continue to increscent as it did at the low loadings. Since the co-solvent methanol used in the extraction process benefited the complex's solubility in $scCO_2$ and in water, some rhodium complex still remains in the water phase.

Table 4-3 Experimental parameters and results obtained for the extraction of $RhCl_3$ from its aqueous solution under 150 bar at 60 °C†

$RhCl_3$ g	TTA g	T °C	P bar	Time min.	Ext. wt%
0.003	0.0025	60	150	125	12
0.003	0.0050	60	150	125	15
0.003	0.010	60	150	125	38
0.003	0.020	60	150	125	60
0.003	0.040	60	150	125	68

Note: † T stands for temperature, P for pressure, Ext. for extraction ratio in weight.

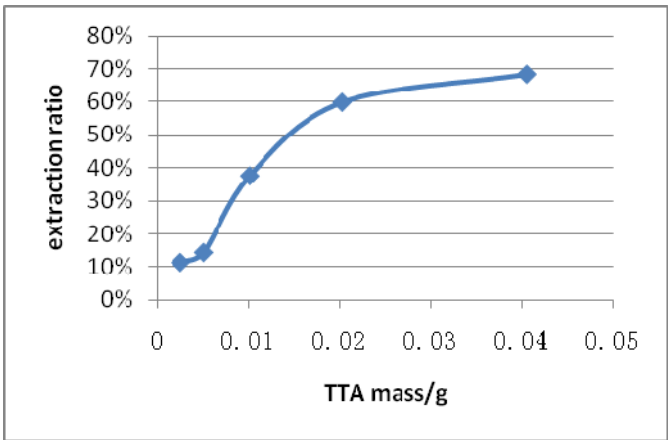

Figure 4-4 Extraction Ratio vs TTA Loading

4.2.2 Extraction of rhodium catalysts from their crystals using $scCO_2$ and TTA

The extraction process applied for extraction of $RhCl_3$ and $RhCl(TPP)_3$ from their solid forms were realized in the 150 mL reactor equipped in the R100. The extraction procedure applied was that given in Section 4.1.3. The wet rhodium compounds were placed in the reactor and the ligand was contained in an independent tube, so that the $scCO_2$ was saturated with TTA before it contacted the rhodium compounds, and avoided surplus TTA from being carried away by the dynamic $scCO_2$ fluid as well. The operational conditions were 60 °C and

150 bar, 5% (v/v) methanol: the same as that applied in the extraction of a $RhCl_3$ aqueous solution. After the experiments were completed, the $scCO_2$ was released slowly, and the residue in the reactor was checked to confirm the extraction efficiency. Both $RhCl_3$ and $RhCl(TPP)_3$ were found to be extracted by $scCO_2$ containing TTA.

4.2.3 Extraction of rhodium catalysts and from a NBR matrix using $scCO_2$ and TTA

The extraction procedure used is given in Section 4.2.2. The flow rates of CO_2 and methanol were 10 g/min and 0.66 mL/min. NBR containing $RhCl_3$ or $RhCl(TPP)_3$ used as the extraction sample. The rhodium concentration in the NBR sample was around 3000 ppm. TTA was found to have a limited function in extracting $RhCl_3$ and $RhCl(TPP)_3$ from NBR. The best extraction obtained under 150 bar and 60 °C was 20-30 wt%. The red color of $RhCl(TPP)_3$ could even be observed after 6 h of flow extraction under 150 bar and 60 °C. Therefore, TTA is not a good chelating ligand for the targeted system. Furthermore, using TTA as chelating ligand introduced a new contaminant of TTA into the matrix, while the extraction efficiency is not satisfactory. Taking into account that fluorine is not environmentally friendly, the high cost of fluorine ligand and the poor efficiency of the extraction, this part of work was not continued.

4.3 Extraction of $RhCl_3$ using CXLs

The extraction system of $scCO_2$ and TTA showed excellent proficiency in recovery of rhodium catalysts from their aqueous solution and their crystals, but failed in showing any efficiency in separation of the rhodium catalyst from a NBR matrix. This extraction system suffered from the limited solvation power of $scCO_2$ and weaker bonding between TTA and

rhodium, compared to the bonding between rhodium and C≡N group of HNBR and NBR. Furthermore, the fluorinated compounds are expensive and environmentally harmful.

CXLs have stronger solvation power than $scCO_2$ for most organic chemicals. Moreover, CXLs have tunable physical properties as well as $scCO_2$. The solvation power of CXLs can be adjusted from the neat organic solvent to $scCO_2$ by controlling the fraction of CO_2 through manipulating the operational pressure and temperature. Instead of $scCO_2$, CXLs were employed to examine their performance in recovery of rhodium catalyst from NBR or HNBR in the following section.

4.3.1 Extraction of $RhCl_3$ using CXW

In this part of work, $RhCl_3$ was used as the targeted catalyst that is required to be separated from polymers. Therefore, the objective of this part of the experiment is to extract $RhCl_3$ with CXW. The sample was prepared according to the method described in Section 3.2.2, except with HNBR, Wilkinson's catalyst, MEK replaced by NBR, $RhCl_3$ and acetone, respectively. The typical operation procedure is provided in Section 3.2.3, however there was no chelating ligand used and 15 mL of methanol was replaced by 40 mL of water in the extraction process. The extraction process was carried out at 50 °C.

The analysis method applied in this part of the experiment is not ICP-OES, but a colormetric UV-Vis method developed by Marczenko etc [*152*]. The NBR/$RhCl_3$ matrix does not need to be digested, instead the water solution of the experiment was collected and dissolved in a 100mL volumetric flask and the solution will enter into the reaction for the UV-vis analysis.

Table 4-4 Experimental parameters and results obtained for the extraction of $RhCl_3$ from NBR using CXW†

Item	M_s	C_0	P	Time	Ext.
	g	ppm	bar	h	wt%
1	2.0456	4186.0	100	2	68
2	2.0110	4380.5	100	4	68
3	1.9025	4515.2	100	1	7
4	2.7539	2922.0	Atm.	2	35
5‡	2.2280	3601.2	150	2	31
			150	2	1
			150	2	1

Note: † C_0 stands for the initial concentration of rhodium in NBR matrix, P for the pressure of CO_2, Ext. for the extraction ratio of rhodium. ‡ Item 5 has been extracted repeatedly for 3 times, each time 2 h.

All the extraction ratio data presented in the Table 4-4 are based on a UV-vis method. The extraction ratio could reach as high as 68 wt% after 2 h operation under 100 bar and 50 °C. No apparent improvement on the extraction ratio occurred when the operation time was extended from 2 to 4 h. However when the operation time was shortened from 2 to 1 h, the extraction ratio dropped from 68 wt% to 7 wt%. The extraction ratio reached a level of 35 wt%, even without addition of CO_2. A sequence of 3 separate extractions on Item 5 under 150 bar and 50 °C was performed. The extraction ratio in the second and third time is very low at 1 wt% and 1 wt%, which are within the error of the analysis method-color reaction-UV-vis. Item5's result showed that increasing the extraction times did not accordingly improve the overall extraction ratio.

With the installation of HPA-S and development of an ICP-OES method, the experimental results of the extraction process using CXW were measured and confirmed. The results are presented in Table 4-5.

Table 4-5 Experimental parameters and results obtained for the extraction of $RhCl_3$ from NBR using CXW, analyzed by ICP†

	M_s g	C_0 ppm	M_d g	I ppm	Ext. wt%
sample1	0.3838	3438.14	11.27	46.52	60
sample2	0.3805	3438.14	16.94	31.80	59
sample3	0.2876	3438.14	10.51	32.06	66
sample5	0.3960	3438.14	13.96	39.65	59
sample6	0.2476	3204.59	9.93	67.98	15
sample7	0.2829	3204.59	10.69	55.52	34

Note: † M_s stands for the mass weight of the sample, M_d for the mass weight of the digestion solution, I for the ICP analysis results, Ext. for the extraction ratio calculated with Equation 3-1.

Compared with the data in Table 4-4 which was based on the analysis of the extraction solution, the extraction ratio calculation in Table 4-5 is based on the matrix digestion and analysis of the rhodium leftover in the matrix. The operation time of all the samples in Table 4-5 is 8 h based on 4 repeats and each time 2 h under 100 bar and 50 °C. ICP-OES with a 0.045 ppm detection limit is much more accurate than the color reaction UV-vis method with 0.1 ppm detection limit and complicated operation steps which give rise to more errors. For sample1-5, NBR was utilized as the matrix, while for sample6-7 HNBR was utilized as the matrix. For the HNBR as matrix samples, i.e. sample6 and sample7, the extraction results are much lower than those of sample1-5. The analysis results for sample 1-5 presented in Table

4-5 are at the same level of the analysis results of similar samples presented in Table 4-4, even though a different sampling method and different analysis method were used.

CXW was found to have certain efficiency in recovery of $RhCl_3$ from NBR. This part of work was ended with around 60 wt% recovery of the water soluble catalyst from NBR with high initial concentration of 3000 ppm rhodium. There is still a residue of around 1200 ppm rhodium in the NBR matrix after extraction using CXW. The part of the $RhCl_3$ which was successfully extracted out was supposed to be the free portion which was most probably distributed on the surface area of the NBR/HNBR and did not bond with the C≡N group of NBR or HNBR. Since the more than 60 wt% recovery took place at the high initial concentration of rhodium, it is also speculated that the diffusion of the rhodium complex in HNBR or NBR matrix is highly concentration dependent, the recovery could not be realized with the rhodium's concentration dropping.

In addition, CXW has much poorer efficiency in recovery of $RhCl_3$ from HNBR than from NBR (see Table 4-5). The difference could be caused firstly by the lower viscosity of NBR than HNBR, secondly by the presence of C=C double bond in NBR which competes rhodium with C≡N group and facilitates the diffusion of $RhCl_3$ in it.

4.3.2 Extraction of $RhCl_3$ using CXLs and chelating ligands

In the previous section, the CXW system was found to recover $RhCl_3$ out of NBR with a recovery ratio of around 60 wt% and rhodium residue of around 1200 ppm. CXW was found unable to further improve the extraction ratio of $RhCl_3$ by the means of extending treatment time or increasing treatment times. The failure of the CXW extraction was explained by the limited diffusion rate of $RhCl_3$ within NBR arising from the coordination bond between

rhodium and the C≡N group present in the matrix. Therefore, chelating ligand was used as a trial to overcome the adverse effect of the C≡N group.

The initial concentrations of the samples used in these experiments were still in the level of 3000 ppm and the matrixes were made of HNBR and $RhCl_3$. The chelating agent of TMEDA was employed to assist the recovery of $RhCl_3$ from HNBR using CXW. CXW is an acidic environment and the pH value of it is highly dependent on the fraction of CO_2 in water. The acidic and mutable environment of CXW limited the options of effective chelating ligands. By contrast, ethanol maintains neutral with dissolution of CO_2 and CXE was expected to provide a neutral and relatively stable solvent environment for formation of rhodium complexes. For comparison, TMEDA was applied in ethanol to conduct the extraction experiment. The extraction routs for different extraction system are presented in Table 4-6 , while the results obtained are presented in Figure 4-5.

Table 4-6 Extraction Routes Description†

Item	M_s	C_0	Extraction Route Description
sample14	0.3250	3204.59	treated with CXW (40 mL H_2O) under 100 bar and 50 °C for 3times, every time 2 h.
sample15	0.1914	3204.59	treated with with CXW (20 mL H_2O) and TMEDA (5 mL) under 100 bar and 40 °C for 2 h, then rinsed with ethanol for 1 h.
sample16	0.2077	3204.59	treated with 20 mL ethanol and 5 mL TMEDA for more than 8 h under atmosphere conditions.

Note: † M_s stands for the mass weight of the HNBR sample, C_0 for the initial concentration of rhodium in HNBR.

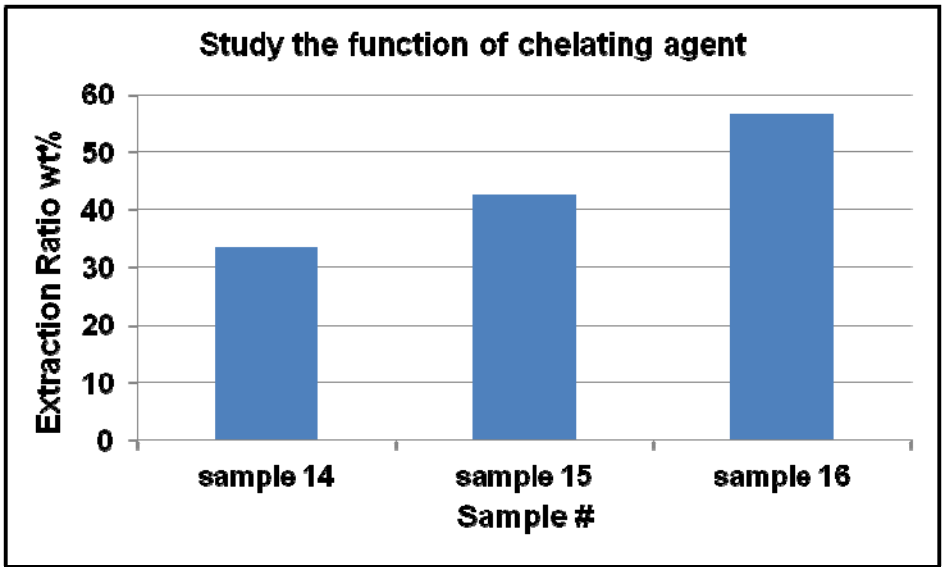

Figure 4-5 Ligand Function Confirmation

As seen from Figure 4-5, using CO_2 expanded water gave the worst extraction result, about 34 wt%. The application of TMEDA as chelating ligand in CXW improved the rhodium recovery from 34 to 43 wt% under the same operation condition. Ligand TMEDA's combination with ethanol showed the best result of 55 wt% even without the addition of $scCO_2$. The comparison result revealed that, firstly, chelating ligand was able to greatly improve the recovery of rhodium; secondly, ethanol is a better extracting solvent than water even without using of CO_2.

The extraction ratio was observed to improve for the HNBR sample when the chelating ligand TMEDA was added into CXW. In addition, improved extraction efficiency was observed when ethanol was used to take the place of water even without addition of CO_2. Taking into account the fact that methanol is cheaper than ethanol, and that PMDETA has one more N chelation site than TMEDA, the decision was made to use the extraction system comprised of methanol and PMDETA to carry out the extraction. Four experiments were

designed to check the efficiency of the PMDETA and CXM system at reduced rhodium initial concentration. The samples used in this group of investigation are still made of $RhCl_3$ and HNBR. Two different initial rhodium concentrations 981.79 and 652.27 ppm were studied. The detailed extraction routes are listed in Table 4-7 and the results are presented in Figure 4-6.

Table 4-7 Extraction Routes Description†

	M_s g	C_0 ppm	Extraction Route Description
sample24	0.2153	981.79	Dealt with 5 mL PMDETA and 20 mL methanol at atmospheric conditions for 14 h in two times.
sample25	0.2495	981.79	Dealt with 5 mL PMDETA and 20 mL CXM under 100 bar at 40 °C for 2h.
sample26	0.1629	652.27	Dealt with 5 mL PMDETA and 20 mL methanol at atmospheric conditions for 14 h in two times.
sample27	0.1717	652.27	Dealt with 5 mL PMDETA and 20 mL CXM under 100bar at 40 °C for 2h.

Note: † see notes in Table 4-6.

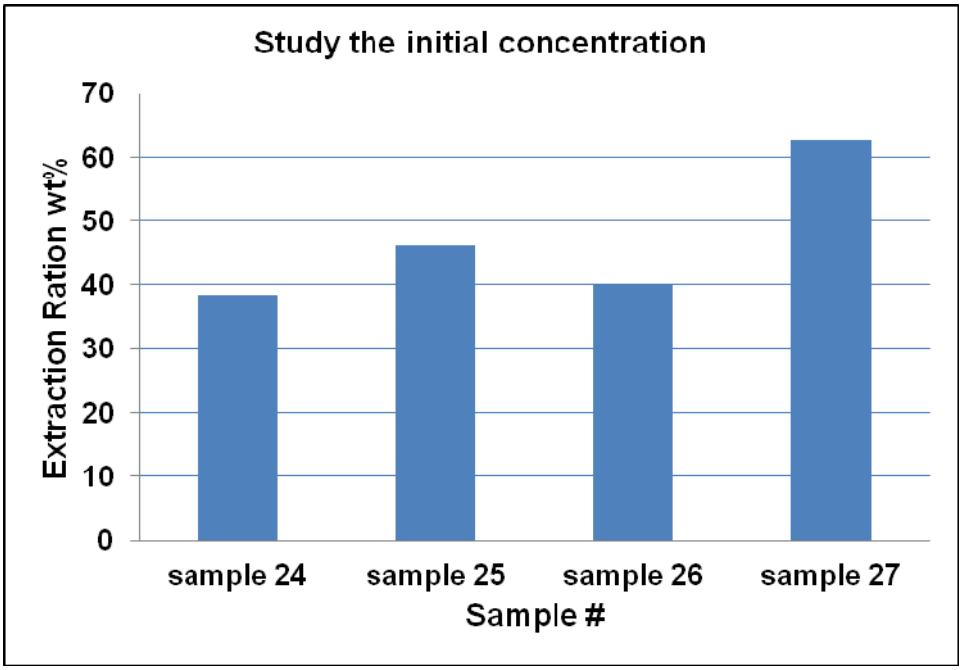

Figure 4-6 Extraction Efficiency of Different Initial Concentration

As seen from Table 4-7 and Figure 4-6 that PMDETA can also assist the recovery of $RhCl_3$ from HNBR via methanol or CXM. In addition, with the initial concentration of rhodium in HNBR reduced from around 3000 to 652 ppm, the efficiency of recovery was observed kept at a similar level, but not dropping as observed at the cases without addition of chelating agent, i.e. PMDETA. Therefore the methanol/PMDETA showed promise in separating rhodium complex from HNBR and will be investigated with respect to their use for recovery of Wilkinson's catalyst from HNBR in the later chapters.

4.4 Summary

All the efforts involved in this Chapter are targeted to develop a green technology in order to recover the rhodium catalysts in from polymers of NBR and HNBR. The journey was started from supercritical carbon dioxide technology and ended with CO_2-expanded liquids

technology. $ScCO_2$ dissolvable Wilkinson's catalyst $RhCl(TTFMPP)_3$ was successfully synthesized and found to have a certain hydrogenation efficiency. However the new synthesized catalyst which was supposed to be soluble in $scCO_2$ could not be extract by $scCO_2$. Later, the $scCO_2$ dissolvable chelating ligand TTA was employed to recover the rhodium catalyst. Although $scCO_2$ can be used to extract rhodium catalyst from their aqueous solutions and wet crystals using the $scCO_2$ dissolvable chelating ligand TTA, TTA can not help recover $RhCl_3$ and $RhCl(TPP)_3$ from the NBR matrix. The absence of efficiency of $scCO_2$ even with assistance of TTA was attributed to its weak solvent power.

CXW showed efficiency in recover $RhCl_3$ from NBR, especially when the initial concentration of rhodium was as high as 3000 ppm. However, this good performance could not be achieved when the initial concentration dropped to 1000 ppm or when the matrix changed from NBR to HNBR. When the attention on chelating ligands was diverted from $scCO_2$ dissolvable to conventional solvents dissolvable, promising observations were obtained on employment of PMDETA and CXM. CXM and PMDETA were able to realize the effective rhodium recovery even when the initial concentration of rhodium drops to around 650 ppm. In the following chapters, investigation of the extraction system consisted of PMDETA and CXM will be reported in the later chapters.

Chapter 5
Recovery of Wilkinson's Catalyst Using CXLs

Based on the discoveries obtained in the previous Chapter, CXLs were employed for separating Wilkinson's catalyst from HNBR, which is considered to be straightforwardly related to the catalytic hydrogenation of NBR in latex and bulk form. In this Chapter, the work done to optimize the recipe and operational conditions is discussed. A more exhaustive investigation on the function of pressure is discussed in a later Chapter.

5.1 CO_2-expanded water

Water is an ideal green solvent. Meanwhile, water is the bulk solvent in NBR latex and the principal solvent in the NBR latex direct hydrogenation catalyzed by Wilkinson's catalyst. Hence water was first employed to generate the CXL for separation of Wilkinson's catalyst from the HNBR matrix. The common water soluble chelating agents including EDTA, EDTA-Na_2, DETA, TMEDA, and PMDETA were applied as chelants in CXW to carry out the extraction experiments. The experimental conditions and results are presented in Table 5-1.

As can be seen from the results listed in Table 5-1, CXW did not show sufficient proficiency in removal of Wilkinson's catalyst from the HNBR matrix with the assistance of any of the investigated chelating agents. The extraction results obtained by using EDTA and EDTA-Na_2 are a little better than those when using DETA, TMEDA and PMDETA, but still far from the performance desired. The possible reasons that caused these results may arise from two aspects. One could be their special chemical properties or limited solubility in water, which in turn results in their slow complexation rate with the rhodium cation [Rh(I)]

of Wilkinson's catalyst. The other one could be the unfavourable physical properties of CXW itself.

Table 5-1 Experimental conditions and performance of various chelating ligands on removal of Wilkinson's catalyst from HNBR using CXW†

Ligand	Ms (g)	C_0 (ppm)	M_L (g - mL)	V (mL)	P (bar)	T (°C)	Time (h)	Ext. (%)
EDTA	0.1999	713.6	0.5	20	60	80	3	15
EDTA-Na_2	0.2005	713.6	1.5	20	60	80	3	26
DETA	0.2000	687.9	2.5	15	60	80	3	0
TMEDA	0.2001	687.9	2.5	15	60	80	3	0
PMDETA	0.2002	687.9	2.5	15	60	80	3	0

Note: † Ligand stands for acronym of the chelating agent, Ms for mass of HNBR matrix, C_0 for initial concentration of rhodium in HNBR, L for application amount of chelating agent (the unit for measuring EDTA and EDTA-Na_2 is gram, and the unite for measuring the other three chelating agents is mililitre), V for the using amount of solvent, P for pressure of CO_2, T for temperature, Time for extraction duration, Ext. for extraction ratio;

The molecular structures of these selected chelating agents are illustrated in Figure 5-1. The applicable physical or chemical properties are summarized in the Table 5-2.

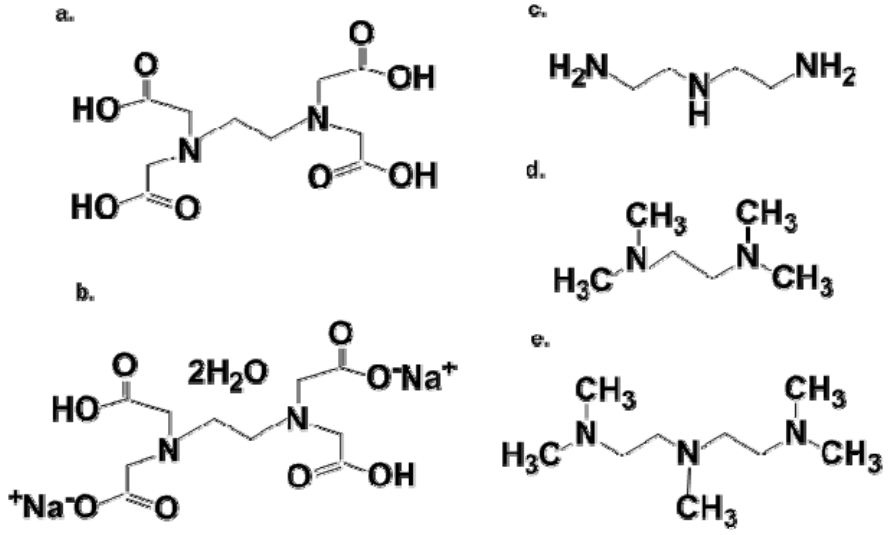

Figure 5-1 Molecular structures of EDTA, EDTA disodium salt dihydrate, DETA, TMEDA and PMDETA in the order of a, b, c, d, and e.

Table 5-2 Applicable physical or chemical properties of the chelating ligands investigated

Acronym	Definition	Molecular formula	Molecular structure	SS †	Reaction with CO_2 ‡	Boiling Point °C
EDTA	Ethylenediaminetetra acetic acid	$C_{10}H_{16}N_2O_8$	Figure 5-1a	Water, methanol, ethanol,	Non-Reactive	N/A
EDTA-Na_2	Ethylenediaminetetra acetic acid disodium salt	$C_{10}H_{14}N_2O_8Na_2 \cdot H_2O$	Figure 5-1b	Water	Non-Reactive	N/A
DETA	Diethylenetriamine	$C_4H_{14}N_3$	Figure 5-1c	Water, methanol, ethanol,	CO_2 capture	206
PMDETA	*N,N,N′,N′,N″*- penta-methyldiethylenetriamine	$C_9H_{23}N_3$	Figure 5-1e	Water, methanol, ethanol,	Non-Reactive	198
TMEDA	*N,N,N′,N′*-tetramethyl-ethanediamine	$C_6H_{16}N_2$	Figure 5-1d	Water, methanol, ethanol,	Non-Reactive	120-122

Note: † SS stands for the solvents can dissolve the indicated chelating ligand. EDTA is sparsely soluble in water, methanol and ethanol; EDTA-Na_2 is soluble in water; DETA is soluble in water, methanol and ethanol, PMDETA and TMEDA is slightly soluble in water, but soluble in methanol and ethanol.

Ethylenediaminetetraacetic acid, abbreviated as EDTA, is a polyamino carboxylic acid, which is widely used to capture or sequester metal ions in industry, medicine and laboratory applications. In these applications, EDTA functions as a hexadentate (two nitrogen and four carboxyl oxygen atoms) chelating ligand to form stable complexes with most of the metals in the Periodic Table. EDTA is sparsely soluble in water, ether and common organic solvents but soluble in ammonia and sodium hydroxide solution [*153*].

Diethylenetriamine, abbreviated as DETA, is one of the polyethylene amines. DETA is a weak base and its aqueous solution is alkaline. In coordination chemistry, DETA functions as a tridentate chelating ligand to form two five-membered chelate rings. DETA is soluble in water and polar organic solvents, but not in simple hydrocarbons [*154*].

N,N,N',N',N''-pentamethyldiethylenetriamine, abbreviated as PMDETA, is a basic, bulky, and flexible, tridentate ligand. PMDETA is derived from DETA by replacement of the five N-H groups with five N-methyl groups. With the replacement of N-H groups by N-methyl groups, all three amines in PMDETA become tertiary. PMDETA can form two five-membered chelate rings as well. PMDETA is slightly soluble in water and soluble in methanol, ethanol, ethers and alkanes [*155*].

Tetramethylethylenediamine, abbreviated as TMEDA, is another common chelating ligand having similar molecular structure with PMDETA but with one less N-donor. In coordination chemistry, TMEDA behaves analogously to PMDETA, but attaches less strongly to metal ions since it is merely bidentate. TMEDA has comparable dissolution properties as PMDETA in water and the other organic solvents [*156*].

These chelating agents were chosen as chelating candidates due to their ready availability, small molecular size and solubility in water. EDTA is the most common ligand in the polyamino carboxylic acid family of ligands [*157*]. EDTA is a hexadentate chelating ligand and can form stable chelates with almost all transition metal ions. In the Wilkinson's catalyst extraction process utilizing EDTA, EDTA is expected to substitute the chloro ligand and one or two of the TPP ligands of Wilkinson's catalyst so as to produce a hopefully water soluble complex $Rh(EDTA)(TPP)_n (n \leq 2)$. However, EDTA has very limited solubility in water, thereby it is very likely that $Rh(EDTA)(TPP)_n$ has even lower solubility in water owing to the TPP ligand. Additionally, the dissolution of CO_2 in water decreased the pH of the aqueous solution of EDTA and EDTA-Na_2, which adversely affected the chelating power of EDTA and EDTA-Na_2. This may explain why less than 20 wt% of Wilkinson's catalyst was removed from HNBR after 3 h of extraction using EDTA as the chelating agent. Although EDTA-Na_2 is more soluble in water than EDTA and showed superiority over EDTA in separating Wilkinson's catalyst from HNBR, the advantage is limited in the presence of CO_2. Unlike EDTA and EDTA-Na_2, DETA, PMDETA, and TMEDA are non-ionic chelating agents and can only replace the TPP ligands of Wilkinson's catalyst excluding the chloro ligand [*155, 156, 158*]. As can be seen from their molecular structures presented in Figure 1, both DETA and PMDETA are tridentate ligands that form two five-membered chelate rings. TMEDA has one less amine group and serves as a bidentate ligand for sequestering metal ions. DETA, PMDETA and TMEDA are all slightly soluble in water and were found to be capable of sequestering the Rh(I) of Wilkinson's catalyst and to form soluble complexes without the addition of any other solvent. The extraction efficiency of

these three chelating agents in CXW can be explained by the common feature of them. These three chelating agents can only replace the TPP ligands of Wilkinson's catalyst which are insoluble in water. Thus, the substitution of TPP by them hardly occurs to any extent, as most of the chelation requires a suitable solvent in which both the chelating agent and the metal to be chelated are soluble.

In other words, the utilization of water as the solvent for the extraction restricts the chelating agents to the range of water soluble anion chelating agents. The chelation of Wilkinson's catalyst in water is supposed to be initiated by substituting the water soluble chloro and followed by replacing the hydrophobic TPP ligand. Taking into account that the oxidation number of rhodium in Wilkinson's catalyst is +1 with only one chloro ligand, the chelation rate of Wilkinson's catalyst in water is considered to be very low. On the other hand, restricted by the insufficient solvation power towards CO_2, CXW is not significantly expanded and its properties, except for acidity, are essentially unchanged compared to pure water. The increase of the acidity of water by dissolution of CO_2 will impair the reactions even further which prefer basic conditions.

5.2 CO_2- expanded alcohols

Alcohols such as methanol and ethanol are very common organic solvents. Meanwhile, methanol and ethanol are relatively benign to the environment and have no solvation power towards HNBR, and thus, their recovery after extraction is feasible and convenient. CXM and CXE were employed to separate Wilkinson's catalyst from the HNBR matrix with assistance of various chelating agents. The chelating agents applied are the non-ionic

chelating agents previously used in CXW, i.e. DETA, TMEDA, and PMDETA. The experimental conditions and results are shown in Table 5-3.

Table 5-3 Experimental conditions and performance of various chelating ligands on removal of Wilkinson's catalyst from HNBR using CXM and CXE†

Ligand	Ms (g)	C_0 (ppm)	L (g - mL)	V (mL)	P (bar)	T (°C)	Time (h)	Ext. (%)
				CXM				
DETA	0.2000	684.0	2.5	15	60	80	3	39
TMEDA	0.2000	687.9	2.5	15	60	80	3	60
PMDETA	0.2007	701.5	2.5	15	60	80	3	64
				CXE				
DETA	0.2000	684.0	2.5	15	60	80	3	42
TMEDA	0.2000	687.9	2.5	15	60	80	3	58
PMDETA	0.2002	701.5	2.5	15	60	80	3	61

Note: † refer to note of Table 5-1.

It can be seen from the results presented in Table 5-2 that CXM and CXE have quite similar performance for all the investigated chelating agents for the removal of Wilkinson's catalyst from HNBR at 80 °C and 60 bar. Both CXM and CXE are potentially promising extraction solvents for removal of Wilkinson's catalyst from HNBR with the assistance of a suitable chelating agent. As mentioned in the previous section, these three chelating agents can even complex the Rh(I) of Wilkinson's catalyst without the presence of any solvent. Methanol and ethanol are good solvents for these three chelants and TPP as well. TPP's solubility in methanol and ethanol increases extensively with an increase in

temperature. Although Wilkinson's catalyst is sparsely soluble in methanol or ethanol, the solubility of the ligand TPP in methanol and ethanol improves the concentration of Wilkinson's catalyst at the interface of HNBR and CXM, and is favourable for the reaction between the chelants and the catalyst. Compared to water, methanol and ethanol are more miscible with CO_2, and can dissolve large amounts of CO_2, and consequently undergo significant changes in virtually every physical property. The physical properties of CXM and CXE can be continuously tuned from pure methanol or ethanol to $scCO_2$ by changing the operational pressure of CO_2. Besides, methanol and ethanol provide greater solubilization for HNBR than water, and thus can strengthen the plasticization of HNBR induced by dissolution of CO_2.

From the results presented in Table 5-2, it is also apparent that PMDETA has superior performance over DETA and however slightly better performance than TMEDA. Although DETA has stronger chelating power than PMDETA, since the σ-donating properties of the amino groups of DETA are greater than those of PMDTA [*158*], DETA was found to have poorer performance than PMDETA in the extraction of Wilkinson's catalyst using CXM or CXE. A viscous precipitate was observed at the bottom of the extraction jar when the extraction experiment was performed using DETA as the chelant. This is probably owing to the high interaction of DETA with CO_2 and the carbonate of DETA is generated by the interaction of them. The formation of carbonate reduced the concentration of DETA in methanol, which thereby hampered the extraction performance. In addition, the formation of carbonate forms an ionic liquid and increases the viscosity of the extraction phase, which adversely affected the extraction efficiency using DETA and CXLs. TMEDA has a similar

molecular structure to PMDETA except that it has one less N-donor, as shown in Figure 5-1. PMDETA has three N-donors and can substitute all three TPP ligands co-ordinated to Wilkinson's catalyst, which greatly facilitates the extraction of Wilkinson's catalyst from HNBR to CXM and CXE. However, TMEDA can only replace two of the TPP ligands and the complex formed with TMEDA is expected to have a lower solubility and diffusivity than that formed with PMDETA. This may impair the extraction performance of TMEDA. In addition, as it will be discussed later, high temperature is important for the extraction process. The boiling point of TMEDA is lower than that of PMDETA, which will cause more loss of TMEDA by evaporation during the operation and raises environmental concerns [*155, 156*].

Based on the above discussion, PMDETA is the optimal chelating ligand for extraction of Wilkinson's catalyst. CXM and CXE have similar performance, but CXM was selected over CXE as the extraction solvent, taking into account that methanol is a common laboratory and industrial material and furthermore is cheaper than ethanol. PMDETA and CXM were employed as the chelating agent and the extracting solvent, respectively, to conduct consecutive investigation and optimization on the other experimental conditions such as the thickness of the sample, the operational temperature and pressure.

5.3 Characterization of the complex of Wilkinson's catalyst and PMDETA

The molecular structure of Wilkinson's catalyst is shown in Figure 5-2A. The TPP ligands attached to the rhodium are very labile and easy to dissociate by 2 or 3 in the catalytic reaction process. The physical and chemical properties of the Wilkinson's catalyst are listed in the Table 5-4.

PMDETA is a basic, bulky, and flexible, tridentate ligand, which often forms two five-membered chelate rings as illustrated in the Figure 5-2 B. The physical and chemical properties of PMDETA are listed in the Table 5-4.

Table 5-4 Physical and chemical properties of Wilkinson's catalyst and PMDETA†

MF	M (g/mol)	ρ (g/mL)	MP (°C)	BP (°C)	Color	SS
Wilkinson's catalyst						
$C_{54}H_{45}ClP_3Rh$	925.22	1.379	245-250	N/A	Red solid	Benzene, MEK, MCB, etc.
PMDETA						
$C_9H_{23}N_3$	173.3	0.83	24.9179	198	Yellow liquid	Water, methanol, ethanol, acetone, ethers, etc.

Note: † MF stands for molecular formula, M for molar mass, ρ for density at 25 °C, MP for melting point, BP for boiling point, SS for the solvents dissolve the discussed chemicals.

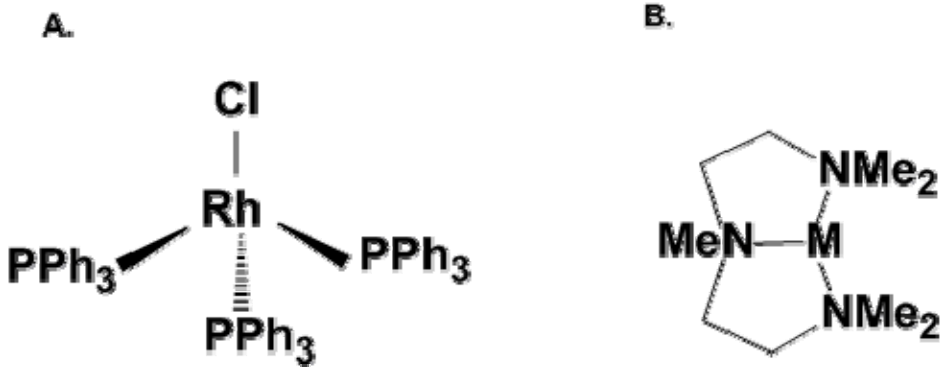

Figure 5-2 A. draw of the molecular structure of the Wilkinson's catalyst; B. draw of the molecular structure of the coordination complex formed by PMDETA and most of the metals.

As discussed above, the Wilkinson's catalyst is labile to loss of one or two triphenylphosiphine ligands, which facilitates the coordination between PMDETA and rhodium. One experiment is designed to examine the possible molecular fomula of the

complex formed between PMDETA and $RhCl(TPP)_x$. 1 mL PMDETA (around 0.005 mol) and 0.02 g Wilkinson's catalyst (approximately 0.00002 mol) were added into 15 mL methanol. It took around 6 h for the Wilkinson's catalyst to completely dissolve into the methanol and PMDETA. After the clear yellow solution was achieved. 3 mL of a solution of methanol/PMDETA/RhClPMDETA in which around 0.001 mol of residual PMDETA was topped with 2 mL of methanol and 0.08 g of Wilkinson's catalyst (approximately 0.00008). The complete dissolution of the Wilkinson's catalyst did not happen within 4 days until an additional 10 mL of methanol was added into the solution. 3 mL of the solution of methanol/PMDETA/RhClPMDETA in which around 0.0002 mol PMDETA was refilled with 12 mL methanol and 0.1 g Wilkinson's catalyst (approximately 0.0001). This time, it took 15 days for the Wilkinson's catalyst to be homogeneously dissolved into the methanol/PMDETA. The color of the solution was orange. Some crystals were observed on the wall of the vial which were suspected as being triphenylphosphine which was replaced by the PMDETA. 12 mL of the solution was decanted and dried to produce a powder. 3 mL of the solution (0.00004 mol PMDETA) was topped with 12 mL methanol and 0.03 g Wilkinson's catalyst (0.00003 mol). For comparison, the reaction was carried out at 50 °C. It took 4 h for the Wilkinson's catalyst to vanish in the methanol. The whole process is summarized in Table 5-5.

From the work described above, it can be discovered: firstly, the chelating reaction between PMDETA and Wilkinson's catalyst can be stimulated by increasing temperature; secondly, PMDETA is a superior chelating reagent for the Wilkinson's catalyst, which can form a stable complex with Wilkinson's catalyst at molar ratio of approximate 1:1; thirdly,

the application amount of methanol is critical for the extraction of Wilkinson's catalyst, which indicates the solubility of the complex from the PMDETA and the Wilkinson's catalyst is limited in methanol.

Table 5-5 Titration of PMDETA with Wilkinson's catalyst†

PMDETA (mol)	$RhCl(TPP)_3$ (mol)	Methanol (mL)	T (°C)	t (h)	Color-L	Color-S
0.005	0.00002	15	23	6	Yellow	Yellow
0.001	0.00008	5	23	96	N/A	N/A
0.001	0.00008	15	23	24	Orange	Yellow and Orange
0.0002	0.0001	15	23	360	Orange	Dark orange
0.00004	0.00003	15	50	4	Orange	Dark orange

Note: † T stands for reaction temperature, t for time required for the Wilkinson's catalyst to be dissolved totally in methanol/PMDETA, Color-L for the color of the clear solution achieved when the Wilkinson's catalyst vanished in the methanol/PMDETA completely. Color-S for the color of the solid obtained when the clear solution was dried.

5.4 Study on the usage of PMDETA

A group of experiments have been designed to optimize the loadings of PMDETA under the conditions in which the extraction efficiency is not reduced. The sample collection method applied to conduct this part of the experiment is referred to as a time saving sample collection method (refer to the method A of Section 3.2.3). The experimental conditions and results are presented in Table 5-6 and Figure 5-3.

Table 5-6 Experimental parameters and extraction results obtained at 40 °C and 100 bar with different loadings of PMDETA †

V_L mL	Ms (g)	C_0 (ppm)	Time (h)	M_d (g)	I (ppm)	Ext. (%)	Residue (ppm)
1	0.2070	663.1	3	22.6021	5.1108	16	558.0
	0.2021	663.1	4	19.1536	5.5630	20	527.2

2.5	0.2078	663.1	5	18.0549	5.6876	25	494.2
	0.2108	663.1	1	14.0089	6.4679	35	429.8
	0.2005	663.1	2	13.1939	6.0971	39	401.2
	0.2019	663.1	3	17.4142	3.9378	49	339.6
	0.2004	663.1	4	12.423	5.4240	49	336.2
	0.2024	663.1	5	20.2507	3.2751	51	327.7
5	0.2228	653.9	1	11.51142	9.8027	22	506.5
	0.1945	653.9	2	15.50395	5.9068	28	470.8
	0.2236	653.9	3	11.72453	8.7396	30	458.3
	0.1973	653.9	4	15.1348	5.8941	31	452.1
	0.2194	653.9	5	10.96646	8.9353	32	446.6

Note: † refer to the note of Table 3-1, V_L stands for the usage of chelating ligand.

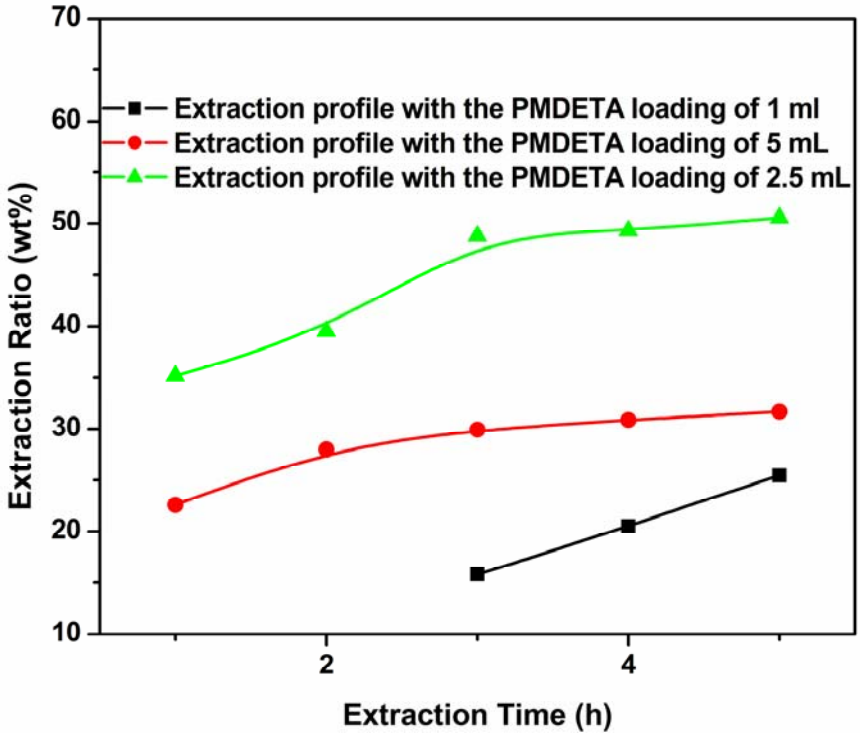

Figure 5-3 Static extraction profiles of CXM and different loadings of PMDETA on HNBR/Wilkinson's catalyst films at 40 °C and 100 bar

It can be seen from Figure 5-3 that the extraction profiles of different loadings of PMDETA are distributed from the top to bottom in the order of 2.5, 5 and 1mL. It reveals that 2.5 mL is the most efficient amount of PMDETA over all three. The rhodium contained in the HNBR matrix was 1.29×10^{-6} mol, and PMDETA applied was equivalent to 0.024, 0.012 and 0.0058 mol for the case of 5, 2.5 and 1mL, respectively. PMDETA is able to form stable and a methanol dissolvable complex with Wilkinson's catalyst based on rhodium with a molar ratio of 1:1 from the study conducted in Section 5.3. The molar amount of PMDETA was 3700 fold of that of rhodium even in the case of 1 mL PMDETA. That means the amount of PMDETA was far more than the quantity required forming a stable complex with rhodium in all three investigated cases.

Sufficient PMDETA is crucial to the extraction process for principally two reasons: first, the equilibrium concentration of PMDETA on the surfaces of the HNBR film grows with the concentration of it in methanol under certain conditions; second, the formation rate and stability of the complex of rhodium and PMDETA increases with the concentrations of PMDETA in both methanol and HNBR. The poor performance of 5 mL was possibly caused by two sources: one is the increase of viscosity of the extraction solvent mixture; the other one is the mass transfer resistance from the newly generated liquid film of PMDETA, which could precipitate from methanol because of super saturation. Furthermore, the excessive use of PMDETA is considered to be a burden of environment and suppresses the greenness of the whole process. Therefore, the dosage of 2.5 mL was finally picked for PMDETA to conduct the later investigations of the function of temperature and pressure on the extraction process with respect to the environmental issues.

5.5 Study on the application of the amount of methanol in each run

The amount of methanol applied in each run for static extraction is also worthy of study in the light of the phenomena observed in Section 3.2.3. Different amounts of methanol, i.e. 10, 15 and 20 mL, have been utilized to conduct the extraction with PMDETA and CO_2. All the comparisons took place at 80 °C and 60 bar (CO_2 pressure). The experimental parameters and results are presented in Table 5-7.

Table 5-7 Experimental parameters and extraction results obtained with different usages of methanol at 80 °C and 60 bar †

V_s mL	M_s (g)	C_0 (ppm)	Time (h)	M_d (g)	I (ppm)	Ext. (%)	Residue (ppm)
10	0.2000	684.0	3	25.5860	2.11	60	270.4
15	0.2007	701.5	3	23.0607	2.17	64	249.8
20	0.2002	684.0	3	24.4032	1.93	65	235.7

As can be seen from Table 5-7, the extraction ratio in 3 h under 60 bar at 80 °C grows with the usage of methanol. The increments are 4 wt% when the usage of methanol increases from 10 to 15 mL, and 1 wt% when the usage of methanol increases from 15 to 20 mL, respectively. Under conditions of the same amount of addition of methanol, the growth of the extraction ratio with the second 5 mL of methanol addition is limited. Taking into account this limited growth of extraction ratio at the expense of enlarged consumption of methanol, the usage of 15 mL methanol was selected for further study.

5.6 Investigation of the thickness of the HNBR film

The thickness of the HNBR film was thought to be an important parameter that can affect the extraction efficiency of the investigated extraction system. In order to explore the effects of the thickness of the HNBR film on the extraction efficiency, HNBR films with thickness of

0.6 and 0.3 mm were prepared using the same preparation procedure to carry out the extraction experiments. In each extraction experiment, the loading amounts of HNBR, PMDETA and methanol were 0.2 g, 2.5 mL, and 15 mL, respectively. The operational temperature was fixed at 80 °C, while the operational pressure was varied from 20 to 200 bar. The extraction results are presented in Figure 5-4.

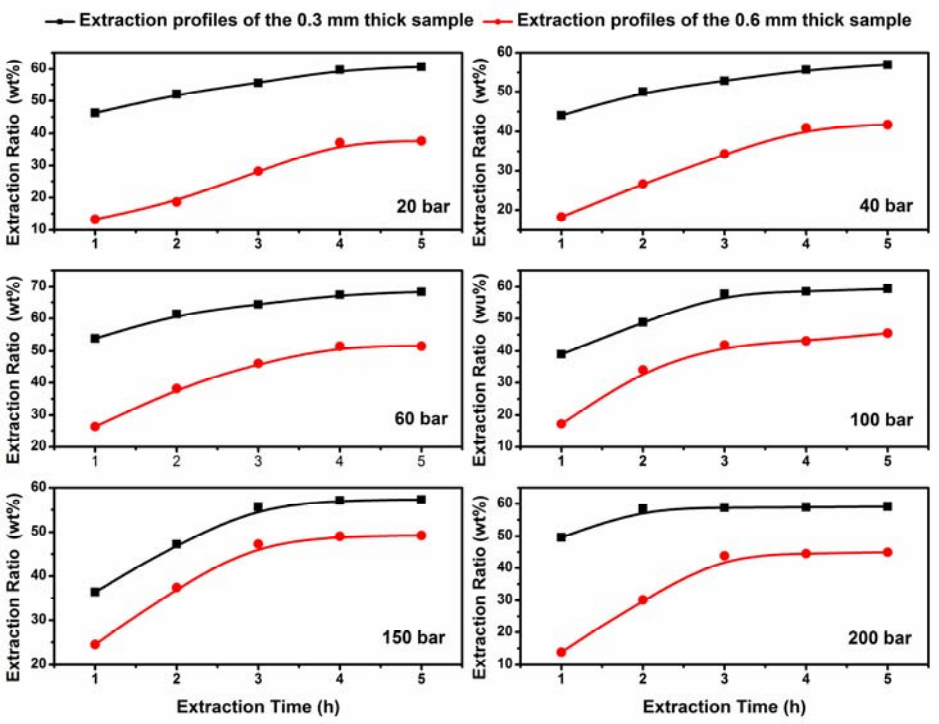

Figure 5-4 Static extraction profiles of CXM and PMDETA on HNBR films with thickness of 0.3 or 0.6 mm under various pressures (20, 40, 60, 100, 150 and 200 bar) at 80 °C

As can be seen from the extraction results presented in Figure 5-4, the thickness of the HNBR film has a significant effect on the extraction efficiency. Over the entire investigated pressure range varying from 20 to 200 bar, the extraction ratios achieved for a HNBR sample with a thickness of 0.3 mm were much higher than those achieved for a HNBR sample with thickness of 0.6 mm for the same duration of extraction treatment. As the mass weight of the

HNBR sample in each run of extraction is the same, around 0.2 g, the interfacial area of the HNBR sample and the CXM is inversely proportionally to the thickness of the HNBR film. Large interfacial area benefits the extraction process in two ways: one is to increase the contacting area between methanol and HNBR, which speeds up the absorption, reaction, and desorption of chemicals at the interface of methanol and HNBR; the other one is the correspondingly shortened mass transfer pathway reduces the mass transfer resistance in the HNBR matrix. As also can be seen from the Figure 5-4, the gap between the extraction profiles for the 0.3 and 0.6 mm thick samples under various CO_2 pressures is reduced with an increment of pressure. With increasing pressure, more CO_2 is dissolved into the HNBR and the physical properties of HNBR, e.g. free volume and permeability, are greatly improved, which in turn promotes the mass transfer within the HNBR and to some extent offsets the advantages of the sample with a thickness of 0.3 mm.

In light of the above discussion, the thinner the HNBR film prepared, the better the extraction efficiency to be achieved. The HNBR samples employed in order to investigate the other parameters, e.g. temperature and pressure, have a thickness of 0.3 mm. This developed technology is expected to be applied in recovery of Wilkinson's catalyst from HNBR particles coagulated from its latex which has a diameter less than 70 nanometer, being much smaller than 0.3 mm. Therefore this investigation will be instructive for future applications of the technique.

5.7 Investigate of the function of CO_2

The addition of CO_2 into the extraction system under a certain pressure was expected to improve the physical properties of both the HNBR and methanol to enhance the mass transfer

taking place in the system. A group of experiments were designed to examine the unique function of CO_2 in the extraction system by elimination of CO_2 or replacing CO_2 with N_2 and running the extractions using the same procedure. The extraction experiments with N_2 replacing CO_2 were carried out at 20 and 60 bar at 80 °C, while the extraction experiments without addition of CO_2 were conducted at 80 °C as well. The comparison between the extraction profiles collected with N_2 as expanding gas and with CO_2 as expanding gas is presented in Figure 5-5.

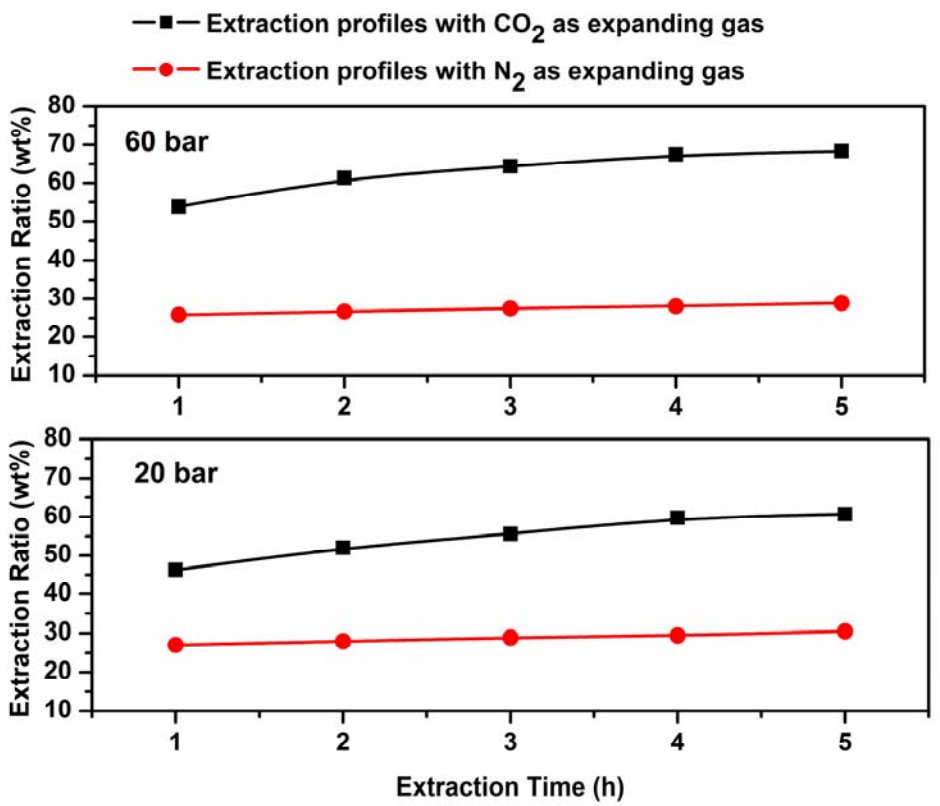

Figure 5-5 Static extraction profiles of methanol, PMDETA and compressed CO_2 or N_2 on HNBR films under different pressure of 20 and 60 bar at 80 °C

As can be seen from Figure 5-5, the extraction profiles obtained using CO_2 as the expanding gas are on top of the extraction profiles obtained using N_2 as the expanding gas under both 20 and 60 bar. On comparison of the results under 60 bar as an example, the

extraction profile using CO_2 as the expanding gas grows from 54 to 68 wt% as the extraction time increases from 1 to 5 h, while the extraction profile using N_2 as the expanding gas varies from 26 to 29 wt % as the extraction time extends from 1 to 5 h. Unlike CO_2, N_2 does not have high solubility in either HNBR or methanol and therefore N_2 is not able to modulate the physical properties of HNBR and methanol by dissolution into them. The pressure produced by N_2 reduces the free volume of the polymer chains of HNBR and restricts the diffusion of small molecules inside HNBR. The gap between the extraction profiles collected using CO_2 and using N_2 expanded methanol increased upon pressure increasing. In the extraction system using CO_2, the plasticization of HNBR by dissolution of CO_2 grows with the pressure of CO_2 and the extraction ratio obtained under 60 bar is higher than the extraction ratio obtained under 20 bar. In contrast, the free volume of the HNBR chains is reduced when the applied pressure of N_2 and the extraction ratio achieved under 60 bar is lower than the extraction ratio achieved under 20 bar when N_2 takes the place of CO_2.

Therefore, CO_2 is crucial to realize the effective recovery of rhodium by using the investigated extraction system. The inert gas N_2 cannot replace CO_2 to carry out the extraction successfully. In addition, CO_2 is common and environmental benign, the addition of CO_2 into the system dramatically reduced the consumption of methanol as well, which makes the technology a “greener” extraction technique.

5.8 Summary

This Chapter reported the research work of using CXLs and chelating agent for recovery of Wilkinson’s catalyst from HNBR. Four factors including the extraction solvent, the chelating

ligand, the expanding gas, and the thickness of HNBR have been investigated and summarized as follows.

CXW is not a good extracting solvent for removing of Wilkinson's catalyst from HNNR, as the low oxidization number of rhodium and the three bulky and hydrophobic TPP ligands of Wilkinson's catalyst increase the difficulties to find an effective ion chelant that can complex Wilkinson's catalyst in CXW. Besides, CXW suffers from narrow tunability and variable acidity. CXM was evaluated as a better extraction solvent over CXE taking into account that CXM and CXE showed similar performance and methanol is cheaper than ethanol.

PMDET showed the best performance in CXM among all the investigated three chelating agents, DETA, PMDETA and TMEDA. Moreover, PMDETA was praised as a favorable chelant for chelating the Rh(I) of Wilkinson's catalyst with respect to its tridentate structure and higher boiling point than TMEDA.

The usage of methanol and PMDETA in each run of extraction was optimized at 15 and 2.5 ML, respectively. The thickness of HNBR film was demonstrated to have a significant effect on the extraction efficiency. The thinner the HNBR film is, the better the extraction efficiency that can be achieved. 0.3 mm was decided to be the thickness of the HNBR films for the subsequent study. N_2 was used as an alternative of CO_2, but showed much poorer efficiency than CO_2, which was considered as verification of the distinctive function of compressed CO_2 in the extraction system.

Chapter 6
Tunability of the Process via Changing Temperature and Pressure

The extraction system employed to conduct the recovery of rhodium is a complicated working system comprised of extraction solvent, chelating ligand, expanding gas and HNBR film. In the previous Chapter, work was reported about the application of basically two classes of CXLs for separation of Wilkinson's catalyst from HNBR matrix with the assistance of a variety of chelating agents. The investigated CXLs include the Class I CXL CXW and the Class II CXL CXE and CXM, while the investigated chelating agents involved EDTA, EDTA-Na_2, DETA, TMEDA and PMDETA. The results of this part of work indicated that the properties of the extraction solvent have great effects on the chelation reaction between Wilkinson's catalyst and chelating agents. Methanol and ethanol were found to be good solvents for the chelation reaction between the catalyst and the chelating agents dissolvable in them. As one of the most crucial components in the extraction system, the application conditions of CO_2 have not been investigated in the previous Chapter. The presence of CO_2 provides great tunability of the extraction system including the volume and the polarity of the extraction phase, which can be regulated by changing the operational temperature and pressure. Therefore, in this Chapter the investigation of the functions of temperature and pressure will be reported in detail. In the mean time, the interpretation of the functions of operational temperature and pressures are carried out by integration the phase equilibrium data of a mixture of CO_2 and methanol reported by previous researchers [*159-162*] and the phase equilibrium data of a mixture of HNBR and CO_2 simulated using the Perturbed Chain Statistical Associating Fluid Theory (PC-SAFT) equation of state and the

parameters reported by Solms [*163*]. Based on a comprehensive understanding of the extraction data, two extraction mechanisms were proposed to explain the extraction process and some suggestions were put forward to enhance the recovery of rhodium from HNBR.

6.1 Experimental data collection

The extraction efficiency of this working system is considered to be strongly dependent upon various factors characterized by the temperature, pressure, and pressure varying pattern applied in the extraction process. The extraction process can be controlled by modulating the physical properties of the extraction system through adjusting the operational temperature and pressure of CO_2. Apart from this, the extraction process can be regulated via the pressure applying pattern as well. In this Chapter, attention will be focused on discussing the effects of temperature and pressure. The investigation on the effect of a pressure applying pattern will be reported in the following Chapter.

The samples used in the extraction experiments have a thickness of 0.3 mm and an initial rhodium concentration of about 700 ppm. The extraction process is regarded as a static extraction taking place under constant temperature and pressure (referring to Section3.2.3). The pressure range investigated was 0, 20, 40, 60, 100 and 200 bar, while the effect temperature was investigated at 40, 50, 60, 70, 80, 90 and 100 °C. Under any fixed pressure and temperature, the static extraction experiments were carried out with different durations of treatment varying from 1 to 5 h, with 1 h addition for each sample. The experimental data are collected and processed referring to Equation 3-2. The extraction profiles describing how the extraction ratio trends with extraction time under various pressures and temperatures are

illustrated in Figures for a straightforward interpretation of the function of temperature and pressure.

6.2 Function of temperature

6.2.1 Experimental results

Based on the discussion conducted in the previous chapters the reaction of PMDETA and Wilkinson's catalyst is seen to greatly dependent on temperature. High temperature hastens the replacing of the ligand TPP on Wilkinson's catalyst by PMDETA, which could further accelerate the extraction of Wilkinson's catalyst using PMDETA as a chelating ligand. Apart from this, temperature can affect the physical properties of HNBR, higher temperature lead to lower viscosity due to the dramatic movement of the polymer chains. High temperature is also able to decrease the viscosity of methanol and increase the solubility and diffusion of chemicals in it. In order to explore the effect of temperature on the extraction results, the extraction profiles at different temperatures are illustrated in Figure 6-1 and Figure 6-2.

The effect of temperature on the extraction process was initially investigated under atmospheric pressure, i.e. in the absence of CO_2 at 40, 50, 60 and 80 °C, and a comparison of the extraction profiles at different temperatures is illustrated in Figure 6-1. As shown in Figure 6-1, the extraction rate shows variation with the operational temperature and duration time. The average extraction rate over any given time span is found to increase notably with an increment of temperature, as seen from the extraction profiles collected at different temperatures. The extraction rate at a fixed temperature slows down as the extraction proceeds, as seen from examining the trend of one extraction profile with time. The extraction ratio obtained at 5 h is considered to be in the vicinity of the equilibrium recovery

and used for comparison of the equilibrium extraction ratios at different temperatures. Therefore, a preliminary conclusion can be drawn referring to Figure 6-1 that increasing temperature improves the extraction performance by two aspects: the enhanced extraction rate and the equilibrium extraction ratio.

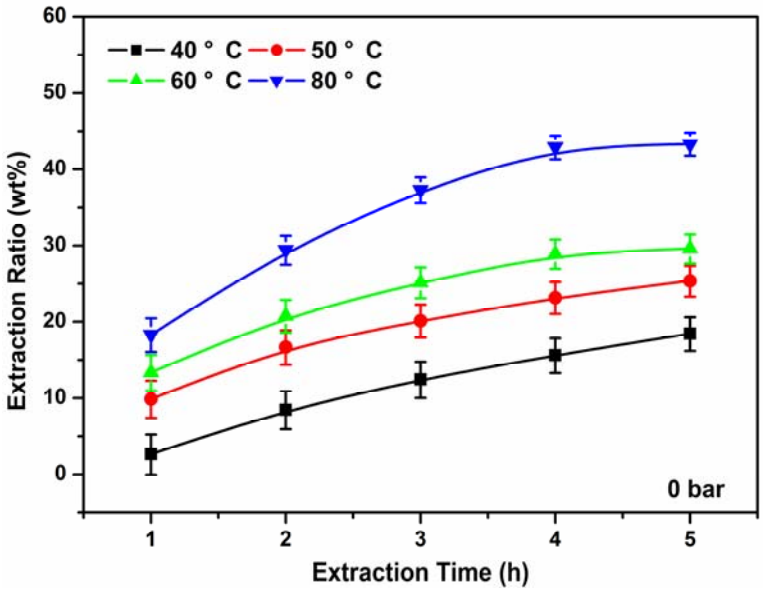

Figure 6-1 Static extraction profiles of Wilkinson's catalyst using CXM and PMDETA from HNBR films at different temperatures of 40, 50, 60, and 80 °C at atmospheric pressure.

Moreover, the effect of temperature on the extraction results was investigated under the conditions of CO_2 presence. The investigated temperatures were extended from 80 to 100 °C, while the investigated pressures varied among 20, 40, 60, 100 and 200 bar. Under each fixed pressure of CO_2, the static extraction profiles over 5 h at various temperatures were collected and presented in one figure to reveal the influence of temperature. The figures under pressures of 20, 40, 60, 100 and 200 bar are presented in the sub-figures a, b, c, d, e of Figure 6-2.

With the introduction of an additional parameter, CO_2 pressure, the beneficial effect of temperature on the extraction rate was not as distinctive as under the atmospheric conditions. As can be seen from Figure 6-2, under all the investigated pressures from 20 to 200 bar, the extraction ratios obtained within the same extraction durations were found to increase with an increase in temperature over all the investigated extraction durations, when the temperature was varied from 40 to 80 °C. Thus, one can draw the same conclusion that with under atmospheric pressure that increasing temperature can greatly improve the extraction efficiency, when the temperature is below 80 °C. However, when the temperature is increased to above 80 °C, the notable effect of temperature on the extraction efficiency is reduced and not as distinct as what is observed at the temperatures below 80 °C. The extraction profiles at 90 and 100 °C are almost overlapped under 20 and 40 bar, as seen in sub-figure 'a' and 'b' in Figure 6-2. Besides, the order of the extraction profiles at temperatures above 80 °C became pressure dependent. Under the low pressures of 20 and 40 bar, the extraction profiles at high temperatures still sit on top of those at lower temperatures and with slightly superior (see a, b in Figure 6-2). Under 60 bar, the extraction profile at 90 °C stands on top of the one at 80 °C, the extraction profile at 100 °C sits however below the one at 80 °C with minor discrepancy (see c in Figure 6-2). Under 100 bar, the extraction profile at 100 °C starts higher than the one at 90 °C, but tends to slightly below it after the second hour of extraction, whereas the extraction profile at 80 °C sits below both over all the investigated extraction durations (see d in Figure 6-2). Under 200 bar, the extraction profile at 90 °C sits above the one at 80 °C, whereas the extraction profile at 100 °C sits slightly below the one at 80 °C (see e in Figure 6-2).

In line with the above, increasing temperature has a beneficial effect on the extraction process. This favorable function of temperature dominates in the low temperature range from 40 to 80 °C, but became relatively weak when the temperature rose above 80 °C. The disparities among the extraction profiles at 80, 90 and 100 °C became not as noticeable as among the temperatures below 80 °C. The improvement in the extraction efficiency through increasing temperature became marginal. The gap of extraction efficiency between different temperatures above 80 °C is expected to be modulated via an alteration of CO_2 pressure. Pressure can influence the dissolution of CO_2 in both HNBR and MeOH, thereby influencing their physical properties and the extraction results, which will be discussed in detail in Section 6.3.

a.

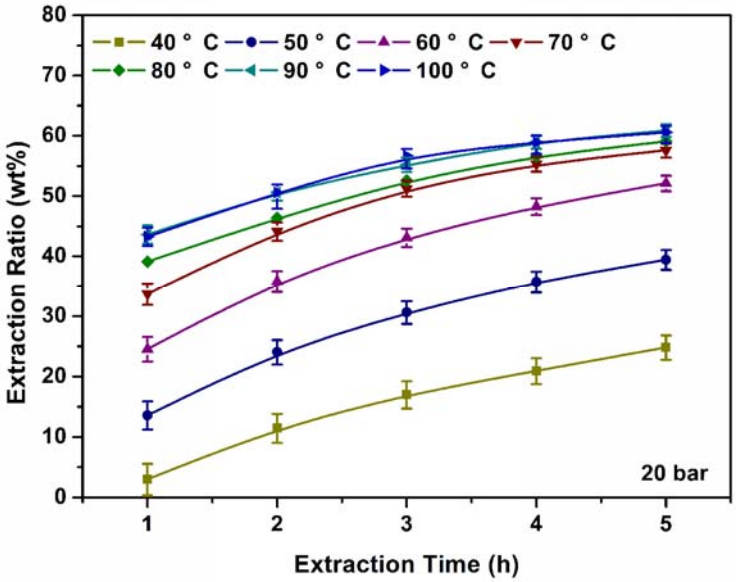

b.

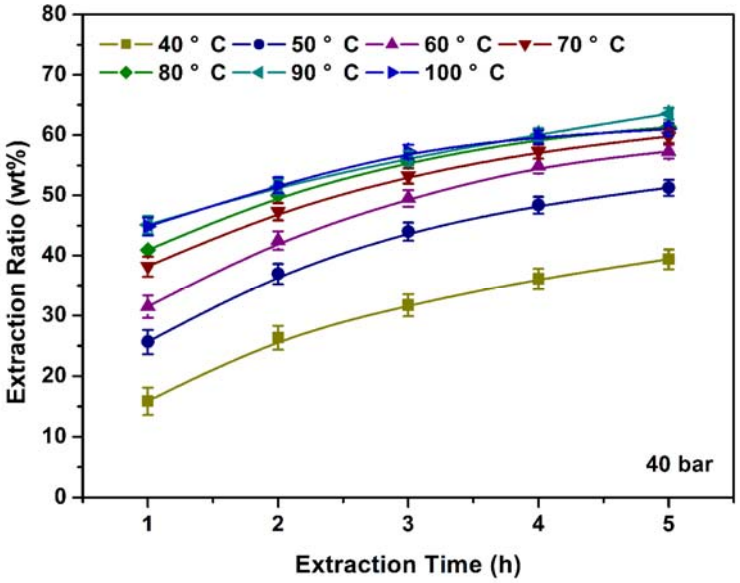
40 ° C
50 ° C
60 ° C
70 ° C
80 ° C
90 ° C
100 ° C
Extraction Ratio (wt%)
Extraction Time (h)
40 bar

c.

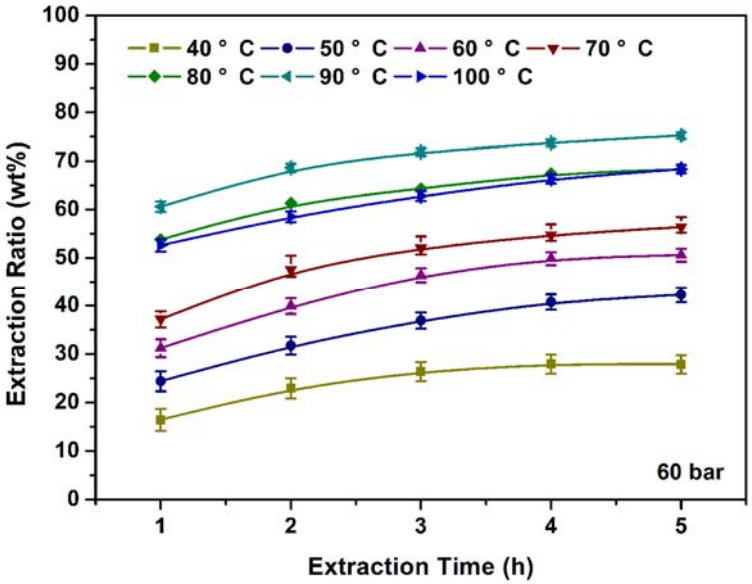
40 ° C
50 ° C
60 ° C
70 ° C
80 ° C
90 ° C
100 ° C
Extraction Ratio (wt%)
Extraction Time (h)
60 bar

d.

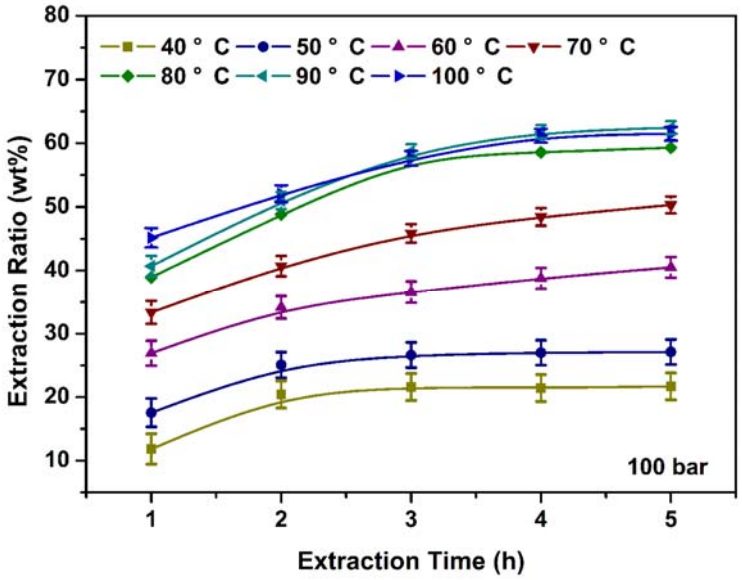

e.

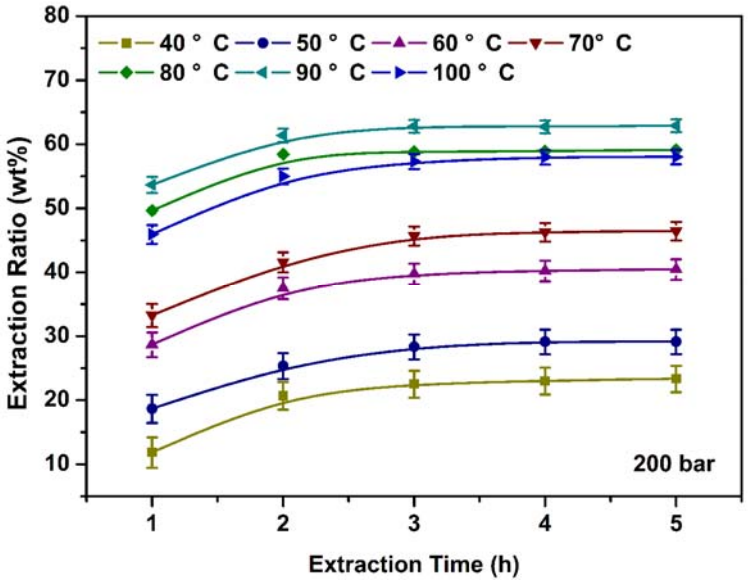

Figure 6-2 Static extraction profiles of Wilkinson's catalyst from HNBR films using CXM and PMDETA at different temperatures of 40, 50, 60, 70, 80, 90, 100 °C under a fixed pressure: a. 20 bar, b. 40 bar, c. 60 bar, d. 100 bar, e. 200 bar.

6.2.2 Analysis of the effects of temperature

The effect of the temperature on the extraction efficiency can be appreciated from three aspects as follows

Firstly, temperature can influence the chelation reaction rate between Wilkinson's catalyst and PMDETA. The stability of the ligand TPP attached on Wilkinson's catalyst. Osborn and Wilkinson et. al. reported that one of the TPP ligand attached to Wilkinson's catalyst is labile and easy to dissociate from the 16-electron catalyst and form the 14-electron complex $RhCl(TPP)_2$ [*26*]. The formally three co-ordinate species $RhCl(TPP)_2$ has vacant co-ordination sites which can be occupied either by weakly bound solvents molecules or by other ligand atoms. Mohammadi [*164*] and Parent [*146, 165*] reported that the six coordinate dihydride of Wilkinson's catalyst ($RhClH_2(TPP)_3$) can undergo loss of TPP ligand at elevated temperature, which is not appreciable at room temperature. Raising temperature encourages the dissociation of TPP, and even cause further TPP dissociation to generate a 12-electron complex RhCl(TPP). Therefore, it becomes obvious that the extraction rate was observed to increase greatly with an increment of temperature, taking into account that more rhodium complexes with vacant co-ordination sites were produced in a short time and that the co-ordination rate between PMDETA and these complexes ($RhCl(TPP)_2$ or RhCl(TPP)) was increased.

Secondly, temperature can impact the solubility of chemicals in the extraction phase of CXM. The solubility of TPP and RhClPMDETA in CXM increases with an increase of temperature, which accelerates the transfer or desorption of TPP and RhClPMDETA from the surfaces of HNBR to CXM. The increased desorption rate of RhClPMDETA from HNBR

to CXM does great favor to the extraction rate, while the enhanced desorption rate of TPP affects the extraction process adversely. As the extraction proceeded, more and more TPP ligand detached from Wilkinson's catalyst and the free TPP ligand in HNBR will dissolve into methanol along with the new formed complex of RhClPMDETA. The existence of TPP in HNBR is known to be crucial to ensure the free movement of Wilkinson's catalyst in HNBR [*4*]. As stated before, the vacant co-ordination sites on the 14-electron and 12-electron complexes of Wilkinson's catalyst can be easily occupied by solvent molecules or other ligand atoms, such as the CN and C=C residue in HNBR. Thus, it is almost impossible for $RhCl(TPP)_2$ and RhCl(TPP) to move freely inside the HNBR without excess TPP ligand. The continuous decrease of TPP in HNBR impaired the amount of free Wilkinson's catalyst diffusing from the internal part of HNBR to its surfaces, and it further slowed down the extraction rate and caused the extraction to end. Therefore, increasing temperature will accelerate the end of an effective separation of the catalyst due to the rapid loss of TPP ligand. In conclusion, although a good extraction rate was observed at a high temperature, e.g., 80 °C at the beginning of the extraction, the increment observed was very limited by extending the extraction time from 1 to 5 h. No matter how far away the extraction ratio is from the 100 wt%, an increase in the extraction ratio with time has to stop when no effective amount of TPP is left in HNBR.

Thirdly, temperature can influence the physical properties of HNBR and CXM. Increasing temperature reduces the viscosity of HNBR and CXM, and enhances the diffusivity of solutes within HNBR and CXM. Hence, the extraction process benefits from increasing temperature.

At low temperature, i.e., 40 °C, the detachment of TPP from Wilkinson's catalyst was only a little, and thus the chelation reaction rate was low. The transferring rate of free TPP ligand from HNBR to methanol was even slower, and thereby the free TPP ligand was mostly retained in the HNBR. Therefore, the extraction ratio was observed to continuously and slowly increase with an extension of extraction time. When temperature was elevated, both the detachment rate of TPP from Wilkinson's catalyst and the diffusivity of Wilkinson's catalyst inside of HNBR were increased, the extraction rate was hence greatly improved. On the other hand, the transferring of TPP from HNBR to methanol was accelerated by elevated temperature. Therefore, the extraction profile flattened out gradually and limited any further increase in the extraction ratio was obtained by extending the extraction time. Higher temperature resulted in a shorter time being required for observing the flattening of the extraction profile.

In conclusion, increasing temperature greatly favored the extraction process, especially over the relatively lower temperature range. In the meantime, the benefit on the extraction process via increasing temperature became marginal when temperature was further increased above 80 °C. Moreover, increasing temperature accelerated the loss of TPP from HNBR to methanol and caused the recovery of Wilkinson's catalyst to come to an end. In order to retain more TPP inside of HNBR, the operational temperature is better at a low value, i.e., 50 °C, but its extraction rate is too slow and therefore is not desirable. Therefore, the operational temperature has to be high, e.g., 80 or 90 °C, while some other effective method is employed to diminish the loss of TPP in the process of extraction. This is expected to be solved by addition of CO_2 under suitable pressure.

6.3 Effect of CO_2 pressure

6.3.1 Experimental results

The extraction profiles at different pressures at various temperatures of 40, 50, 60, 70, 80, 90 and 100 °C are illustrated in the order of a, b, c, d, e, f and g in Figure 6-3. In each sub-figure of Figure 6-3, the temperature applied is the same for all the extraction profiles, but the pressures are different (0, 20, 40, 60, 100 or 200 bar).

a.

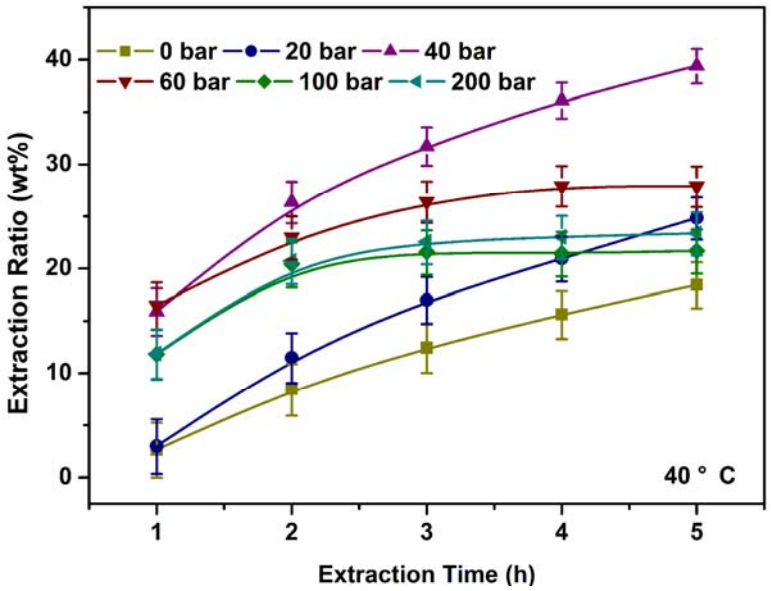

b.

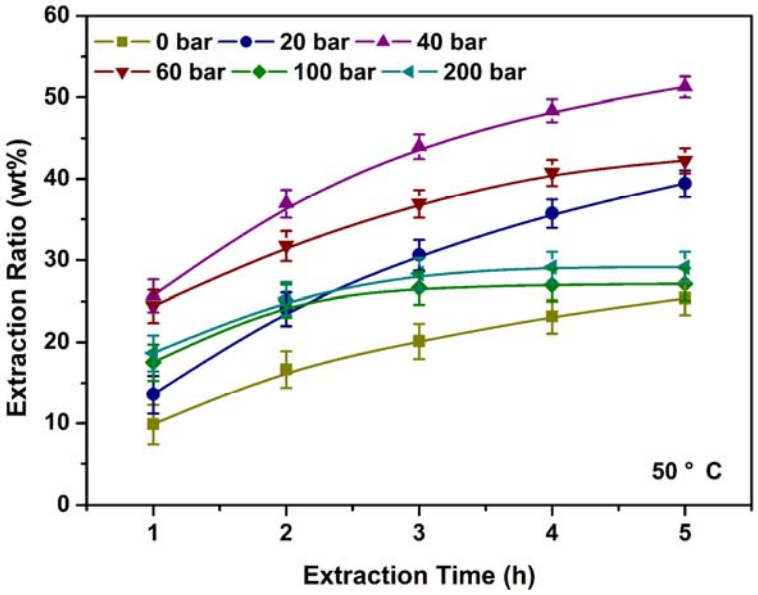
0 bar
20 bar
40 bar
60 bar
100 bar
200 bar
Extraction Ratio (wt%)
Extraction Time (h)
50 ° C

c.

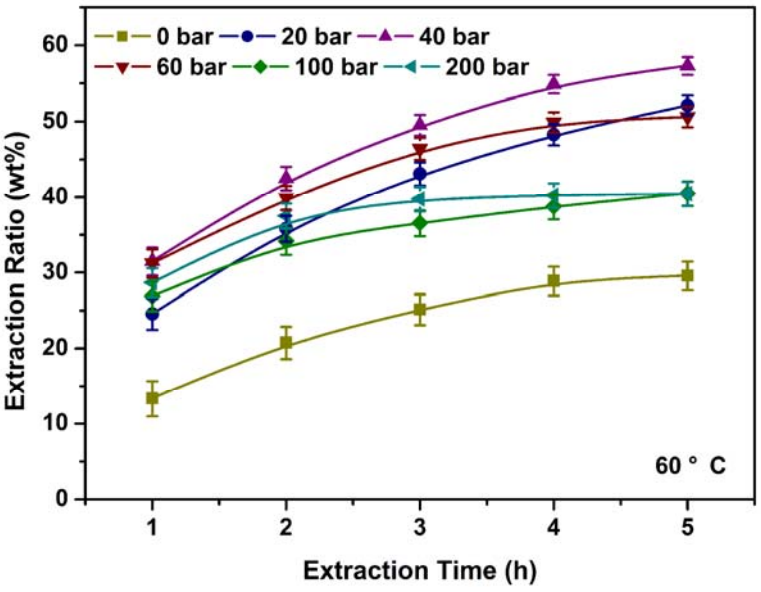
0 bar
20 bar
40 bar
60 bar
100 bar
200 bar
Extraction Ratio (wt%)
Extraction Time (h)
60 ° C

d.

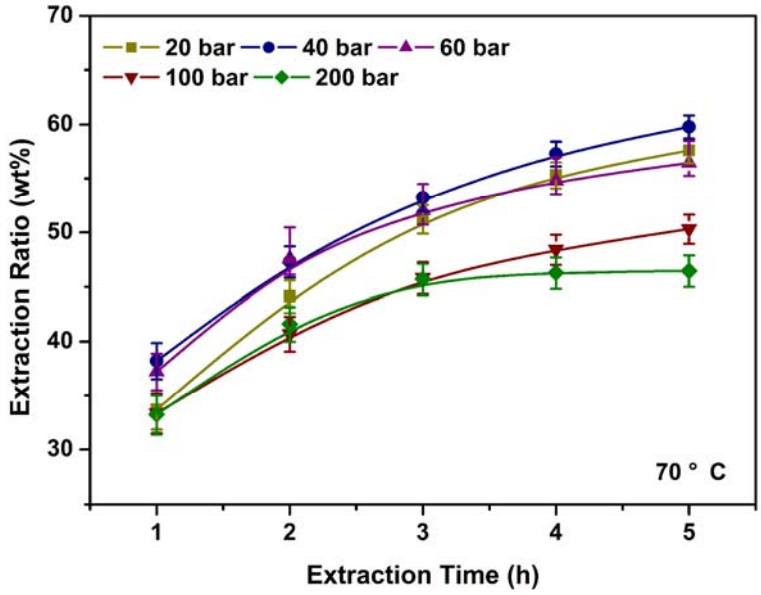
20 bar
40 bar
60 bar
100 bar
200 bar
70 ° C
Extraction Ratio (wt%)
Extraction Time (h)

e.

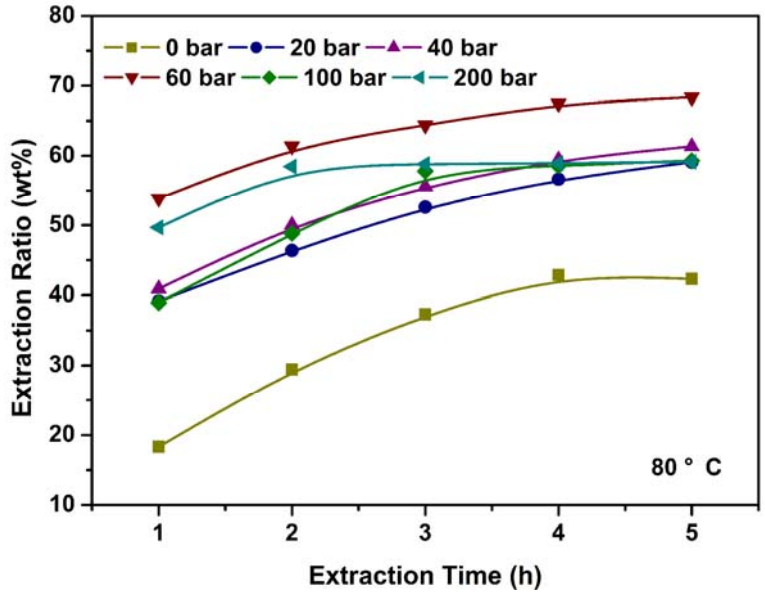
0 bar
20 bar
40 bar
60 bar
100 bar
200 bar
80 ° C
Extraction Ratio (wt%)
Extraction Time (h)

f.

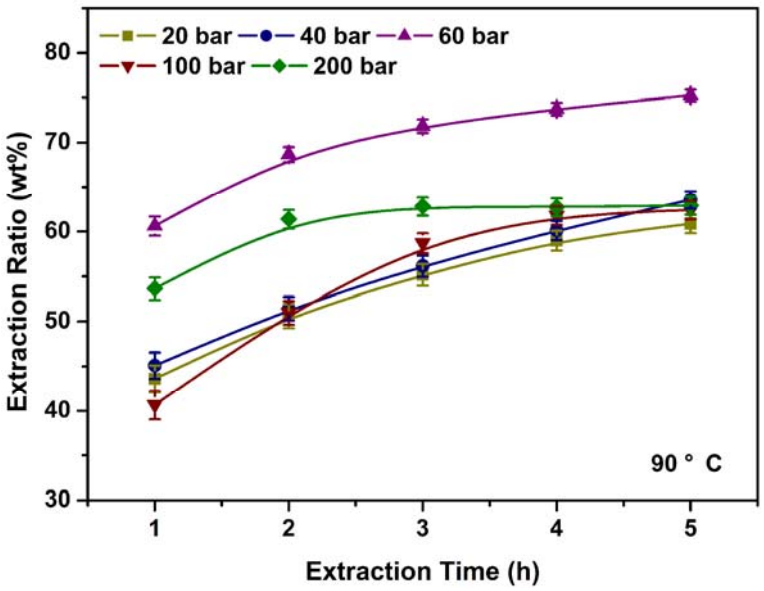

g.

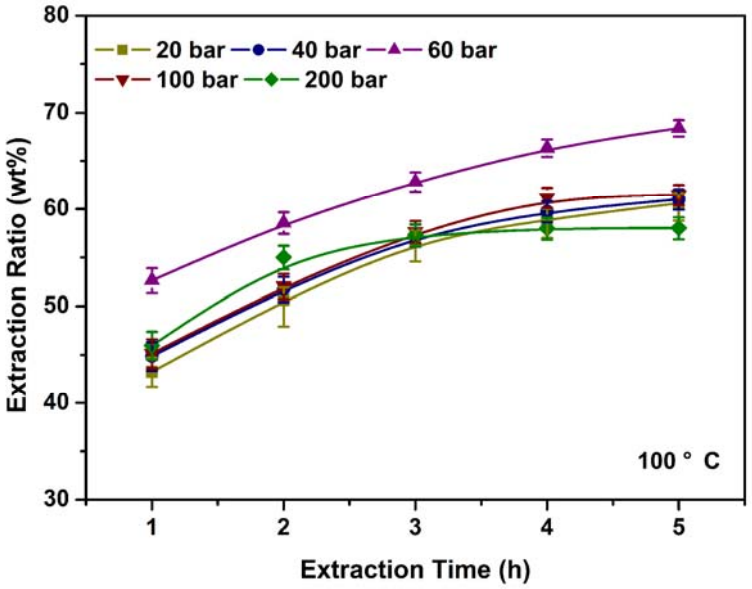

Figure 6-3 Static extraction profiles of Wilkinson's catalyst from HNBR films using CXM and PMDETA under different pressures of 20, 40, 60, 100 and 200 bar at a fixed temperature: a. 40 °C, b. 50 °C, c. 60 °C, d. 70 °C, e. 80 °C, f. 90 °C, g. 100 °C.

It can be seen from the figures at 40, 50, 60 and 80 °C (see a, b, c, e of Figure 6-3) that the presence of CO_2 in the extraction process is crucial to ensure the efficiency of this reported extraction technology. The extraction without CO_2 significantly underperformed all of the extraction processes using CO_2, as shown in the sub-figures a, b, c, e of Figure 6-3. Given addition of a small amount of CO_2 at 20 bar, the superior performance was distinctively observed across all the extraction durations at 40, 50, 60 and 80 °C in Figure 6-3.

In addition, the extraction performance at the same temperature, but under different CO_2 pressures is found to vary with pressure as well. As it is apparently revealed in Figure 6-3, pressure does not have a monotonic effect on the extraction performance, but there exists an optimal operational pressure over the investigated pressure range for each temperature. The extraction performance at a fixed temperature increases with increasing pressure firstly, and declining as the pressure is further increased above the optimal pressure. The optimal operational conditions are theoretically defined as under which the maximum equilibrium extraction ratio can be gained using a reasonably short treatment time. Under a high pressure of 100 or 200 bar, the equilibrium extraction ratios at different temperatures can be directly read in Figure 6-3, at which the extraction profiles flatten out with the treatment time. It can also be seen that the extraction profiles under high pressures of 100 and 200 bar can always flatten out in 2 to 4 h. Under a lower pressure of 20, 40, or 60 bar, the equilibrium extraction ratio can be appraised by the extraction ratio achieved in 5 h. At a high temperature above 80 °C, the increment in the extraction ratio via extending the treatment time from 1 to 5 h is very limited. Therefore, it is easy to claim that the equilibrium extraction ratio is approximately the extraction ratio in 5 h. Although the recovery at low temperature was

found to continuously increase with the operation time, and the equilibrium extraction ratio is found to be higher than that achieved in 5 h; the extraction performance is evaluated by the 5 h recovery but not the equilibrium extraction ratio due to the slow recovery rate. In conclusion, the performance is evaluated by the recovery in 5 h. Among the investigated pressures of 20, 40, 60, 100 and 200 bar, 40 bar was found to provide the best extraction ratio at 40, 50, 60 and 70 °C, while 60 bar showed superior performance at 80, 90 and 100 °C. At a fixed operational temperature, the pressure of CO_2 is expected to influence the extraction process through modulating the physical properties of both HNBR and methanol via its dissolution in both of them. CO_2's dissolutions in both HNBR and methanol are expected to be dependent on the operational temperature and pressure. Therefore, the optimal operational pressure is theoretically different at different temperatures. However, because the investigated operational pressures of CO_2 have been restricted among 20, 40, 60, 100 and 200 bar, the optimal operational pressures are not able to be completely determined, and the best operational pressures illustrated in Figure 6-3 at different temperatures only indicate the approximate optimal pressure at each temperature.

6.3.2 Phase behavior of HNBR/CO_2 and methanol/CO_2

The present working system is a complicated mixture of HNBR, CO_2, methanol, PMDETA, and Wilkinson's catalyst, in which CXM acts as the extraction reagent; HNBR, plasticized by CO_2 and methanol, are regarded as the matrix; Wilkinson's catalyst is the extraction target; and PMDETA plays the role of a chelating reagent. The physical properties of CXM and CO_2 plasticized HNBR at a certain temperature are steeply dependent on the concentration of dissolved CO_2, which can be manipulated by adjusting the temperature and pressure of CO_2.

Therefore the investigated extraction system is divided mainly into two independent thermodynamic systems: HNBR/CO_2 and MeOH/CO_2. The dissolution behavior of CO_2 in both HNBR and methanol were exhaustively investigated and reported as below.

6.3.2.1 Solubility of CO_2 in HNBR

von Solms et al. reported some of the solubility data of CO_2 in HNBR under the pressure varying from 11 to 54 bar at temperatures of 20, 60 and 80 °C [*163*]. From what is reported by von Solms et al, it can be revealed that the absorption of CO_2 in HNBR increases with increasing pressure and decreases with increasing temperature. Apart from these results, von Solms simulated the solubility data by the simplified Perturbed-Chain Statistical Associating Fluid Theory (PC-SAFT) equation of state.

As special equipment for measuring the solubility of CO_2 in HNBR was not available in our lab, the PC-SAFT EoS implemented in Aspen Plus was employed to simulate the solubility of CO_2 at 40, 50, 60, 70, 80, 90 and 100 °C under pressures varying from 0 to 200 bar. The simulation was initiated by an exhaustive understanding of the work of von Solms and the development of PC-SAFT.

In the PC-SAFT equation of state [*166*], the molecules are conceived to be chains composed of spherical segments in which the pair potential for the segment of a chain is given by a modified square-well potential. When the molecules exhibit various attractive interactions, the whole equation of state is given as the sum of the ideal-gas contribution (id), a hard-chain term (hc) connecting the spherical segments, a contribution for the dispersive attraction (disp), a term for associating interactions (assoc), and contributions due to polar interactions. Non-associating pure components are characterized by three molecular

parameters: the (temperature-independent) segment diameter σ, the depth of the potential ε, and the number of segments per chain m. For associating components [*167*], two additional association parameters are required for their characterization: the association energy ε^{AB} and volume κ^{AB} for each site-site interaction. For mixtures, the parameter k_{ij} is introduced for the binary interaction between molecule '*i*' and '*j*'.

The investigated system of HNBR/CO_2 consisted of the polymer HNBR and the small molecule CO_2. A simplified PC-SAFT EoS was proposed [*168*] and used by von Solms to conduct the simulation. Compared to the full version of PC-SAFT EoS developed by Sadowski and coworkers [*169-172*], the simplified PC-SAFT EoS assumes that all of the segments in the mixture have the same diameter, with the constraint that the mixture volume fraction calculated using this new diameter gives the same volume fraction as the actual mixture. By using this assumption, the new 'average' diameter can be defined and the computing times involved in the simulation process are significantly reduced but with limited accuracy reduction. Von Solms et al. used a novel method proposed by his group to estimate the parameters for polymers [*173*]. The essential principles involved in this method are that there exist linear relationships between the number of segments per chain m and molecular weight, and the depth of the potential over Boltzmann's constant ε/k, which can be respectively expressed in Equation 6-1and Equation 6-2. A_m and A_ε can be determined by the molecular weight of a monomer and its m and ε/k. The m and ε/k of any monomer can be regressed by fitting its pure-component data with PC-SAFT. The pure-component data used for parameters regression include the vapor pressure, liquid molar volume and additional PVT data [*169*]. Therefore the selection of the monomer becomes crucial in estimation of the

parameters for polymers, especially for the copolymers. Von Solms employed valeronitrile as the monomer of HNBR to estimate HNBR's parameters. The parameters von Solms and co-workers used to simulate the solubility of CO_2 in HNBR are as follows, the size parameter σ (Å) = 4.0217, the energy parameter over Boltzmann's constant ε/k (K) = 249.5, the segment ratio m=0.0263, and the binary interaction parameter k_{ij} = 0.04.

$$m = A_m \mathrm{MW} + 0.9081 \qquad \textbf{Equation 6-1}$$

$$m\varepsilon / k = A_\varepsilon \mathrm{MW} + 127.3 \qquad \textbf{Equation 6-2}$$

The PC-SAFT EoS implemented in Aspen Plus is based on the full version of PC-SAFT developed by Gross and Sadowski [*167, 169, 170, 172, 174, 175*]. The simulation work in this project was all carried out with this PC-SAFT EoS implemented in Aspen Plus. The parameters of HNBR reported by von Solms [*163*] were applied to carry out the simulation via the full version PC-SAFT EoS. Since von Solms et al. did not reveal what parameters they used for CO_2 in their simulation via the simplified PC-SAFT, the parameters for pure CO_2 that we used are from Gross and Sadowski [*169*]. The parameters for HNBR and pure CO_2 and MeOH are listed in Table 6-1. Two more parameters ε^{AB} and κ^{AB} are needed for MeOH as an associating material. The experimental data for CO_2's solubility in HNBR measured by vol Solms [*163*] were used to regress the binary interaction parameters between CO_2 and HNBR via the full version of PC-SAFT implanted in Aspen Plus. The binary interaction parameter k_{ij} allows complex temperature independence as expressed in Equation 6-3 and Equation 6-4.

$$k_{ij} = k_{ij}^0 + k_{ij}^1 / T_r + k_{ij}^2 \ln T_r + k_{ij}^3 T_r + k_{ij}^4 T_r^2 \qquad \textbf{Equation 6-3}$$

$$T_r = T / T_{\text{ref}}$$ **Equation 6-4**

k_{ij}^0 to k_{ij}^4 are the cofactors of the dependence of k_{ij} on temperature. Their values are listed in Table 6-2. T_{ref} is a reference temperature number and the default value is 298.15K.

The simulation results of CO_2 dissolution in HNBR (measured by mass ratio of CO_2 to HNBR) as a function of the pressure over the range of 0 to 200 bar at various temperatures of 40, 50, 60, 70, 80, 90 and 100 °C are plotted in Figure 6-4. In order to illustrate the verification of the binary interactions we used, the solubility measured by von Solms et al. under different pressures and temperatures are plotted in Figure 6-4 as well.

Table 6-1 Pure-component parameters of the PC-SAFT equation of state for HNBR, MeOH and CO_2

Component *i*	Parameters					
	M_i [g/mol]	m_i [-]	σ_i [Å]	ε_i/k [K]	κ^{AiBi} [-]	ε^{AiBi}/k [K]
HNBR[a]	100000	0.0263	4.0217	249.5	0	0
MeOH [*167*]	32.042	1.5255	3.2300	188.90	0.035176	2899.5
CO_2 [*169*]	44.01	2.0729	2.7852	169.21	0	0

Note: a. for polymers, m should be read as m/MW, i.e. multiply this value by the molecular weight of the polymer to find m. The molecular weight used here for HNBR is 100 000 [*163*].

Table 6-2 Interaction parameters to correct cross-dispersive interactions for CO_2 (*i*) + HNBR (*j*) or MeOH (*j*) systems

j	k_{ij}^0	k_{ij}^1	k_{ij}^2	k_{ij}^3	k_{ij}^4
HNBR[a]	-0.3840	0.5263	0.6120	0	0
MeOH [*176*]	0.0354	-5.8339	0	0	0

Note: a. the parameters to correct cross-dispersive interactions for CO_2 (i) and HNBR (j) system were obtained via simulating the solubility of CO_2 in HNBR using the software of ASPEN

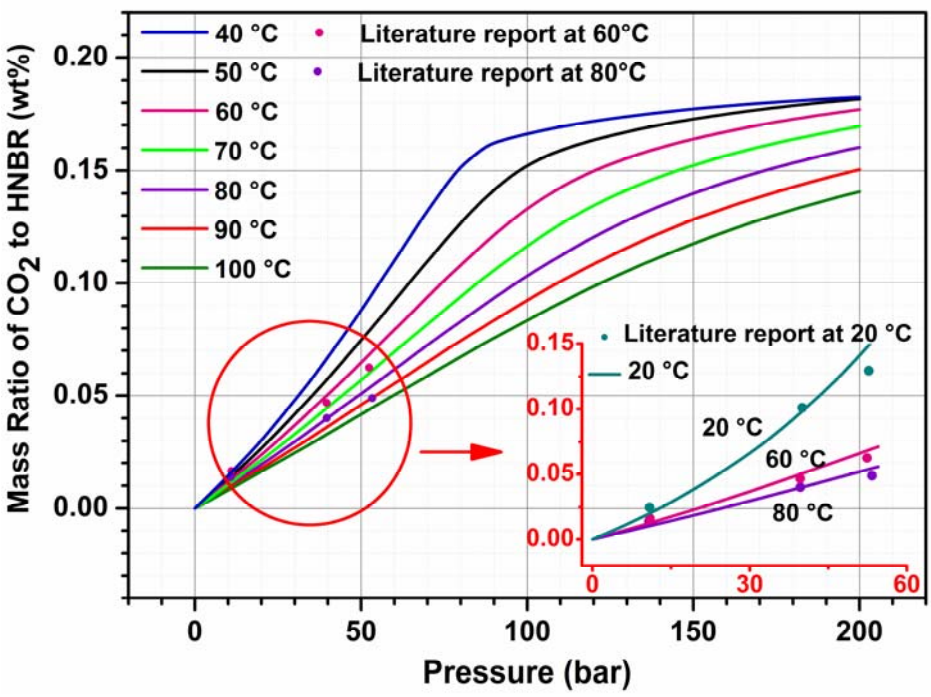

Figure 6-4 Saturation mass ratios of CO_2 to HNBR as a function of pressure at different temperatures of 40, 50, 60, 70, 80, 90, and 100 °C, simulated using the PC-SAFT equation of state and parameters (M_w=100,000, m=0.0263, σ(Å)=4.0217, ε/k(K)=249.5, k_{ij}^0= -0.3840, k_{ij}^1= 0.5263, and k_{ij}^2= 0.6120) based on von solms' report [*163*]

From the enlarged diagram located in the lower right corner of Figure 6-4, it can be seen that the simulation curves using the temperature dependent k_{ij} produce accurate predictions of the experimental data reported by von Solms et al. From the simulation results under our experimental conditions, as shown in Figure 6-4, the concentration of CO_2 in HNBR increases with increasing pressure over all the investigated temperatures, and thus the mass transfer inside of the HNBR matrix increases with an increase in pressure. At a fixed temperature, the fraction of CO_2 in HNBR increases steeply with an increase of pressure over a low pressure range, and then increases very litter after a certain pressure. Taking the trend at 50 °C for example; the trend of the varying curve of the fraction of CO_2 in HNBR with

pressure becomes flat after a pressure of around 100 bar. In addition, the fraction of CO_2 in HNBR at a fixed pressure decreases with increasing temperature and the variation of the concentration of CO_2 with temperature is upon the effects of pressure. The gaps between the concentrations of CO_2 at different temperatures expands with an increase of pressure firstly and yet narrows down with further increasing pressure (see Figure 6-4)

6.3.2.2 Solubility of CO_2 in methanol

The phase behavior of the binary mixture of CO_2 and methanol has been measured and reported by previous researchers at different temperatures. The phase equilibrium data and their respective resources are listed in Table 6-3. The isothermal phase equilibria of the binary system of methanol and CO_2 at various temperatures of 40, 50, 60, 70, 80, 90 and 100 °C were simulated by the PC-SAFT equation of state using the parameters listed in Table 6-1, as reported by Romάn-Ramírez et al [*176*]. The simulation results are presented in the subfigure of Figure 6-5a. In order to verify the simulation results, the isothermal equilibrium data of methanol and CO_2 reported by the other researchers [*160, 177, 178*] at 40, 80 and 100 °C are presented in the Figure 6-5b. It can be seen from the results presented in Figure 6-5 that the simulation results have good predictions under the pressure range below the critical point of the mixture, while the predictions in the near critical region are relatively poor. In fact, the failure in accurate prediction of the phase equilibrium of the near critical region is a common problem of most equations of state. The critical points of the binary system of methanol and CO_2 from different sources are listed in Table 6-4. The critical pressures and mole fractions of CO_2 in CXM at 62, 69.79, 87.5 °C were used for 60, 70 and 90 °C due to the absence of these data [*160, 177-179*].

Table 6-3 Published phase equilibrium data for the binary system of MeOH+CO_2

System	T/°C	refs
MeOH+CO_2	40	[*177, 180-182*]
	50, 80, 120 and 200	[*160*]
	25, 50, 100, 150 and 200	[*178*]
	60, 70, 80, 90, 100, 110 and 120	[*179*]

Table 6-4 Critical points of the binary system of MeOH+CO_2 at different temperatures

T °C	P_c bar	x or y mol/mol	refs
40	82.1	0.968	[*177*]
50	95	0.85	[*160*]
62	115.56	0.775	[*161*]
69.79	127.07	0.721	[*161*]
80	140.3	0.75	[*159-161*]
87.5	145.33	0.654	[*161*]
100	154.2	0.6735	[*178*]

a.

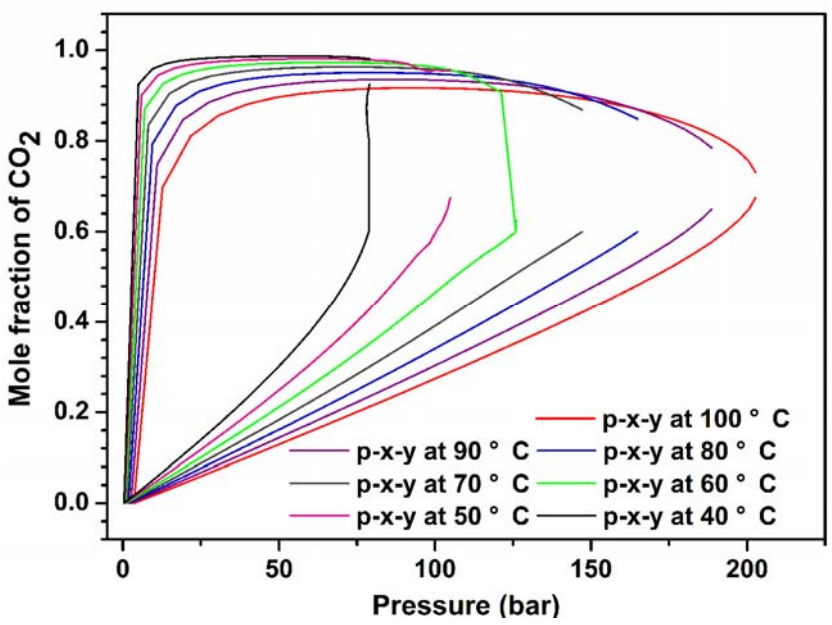

b.

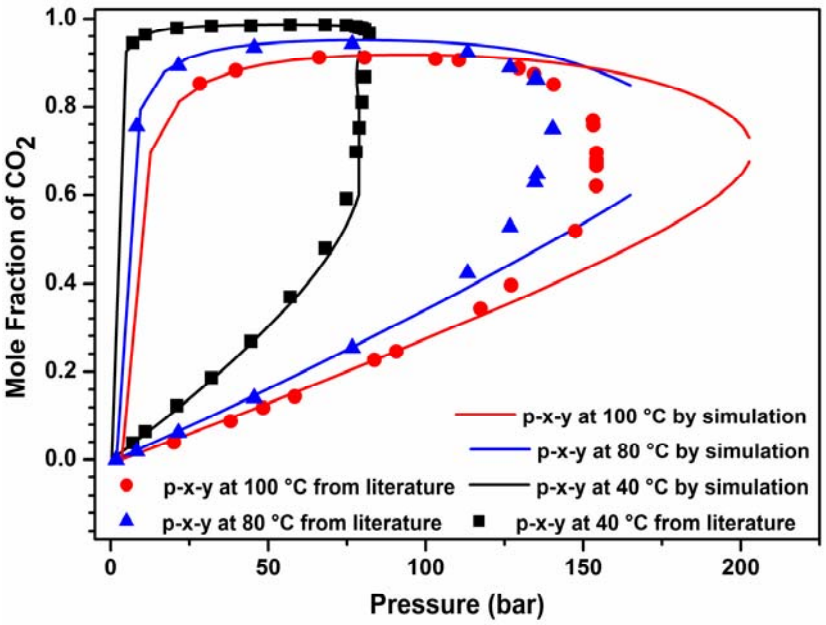

Figure 6-5 Isothermal phase equilibrium for binary system of MeOH+CO_2 simulated by PC-SAFT using the parameters (m=1.5255, σ=3.2300, ε/k=188.9, κ^{AB}=0.035176, ε^{AB}/k=2899.5, k_{ij}^{0}=0.0354, k_{ij}^{1}=-5.8339): a. simulation results for temperatures from 40 to 100 °C, b. comparion of the simulation results and the literature reports at temperatures of 40, 80 and 100 °C.

6.3.3 Identification of the extraction phase

In the investigated extraction process, Wilkinson's catalyst was considered to be extracted by CXM with assistance of the chelating agent PMDETA from the polymer matrix, in which CXM was considered as the extraction phase. However, the extraction phase of CXM could transform to the supercritical mixture of CO_2 and methanol when the extraction was carried out at an extremely high CO_2 pressure above the critical pressure. For studying the variation of the extraction phase, isothermal vapor-liquid equilibrium (VLE) data at temperatures from 40 to 100 °C obtained by PC-SAFT Eos simulation are presented in Figure 6-6a to Figure 6-6g, as well as the loading compositions based on CO_2 and methanol at different operational pressures at the same temperature. The loading amount of CO_2 in each run of the extraction was estimated from its density and volume. The density of CO_2 was calculated based on the operational temperature and pressure using EOS-SCx version 0.2w free software from http://hp.vector.co.jp/authors/VA030090/. The volume of CO_2 was approximated as 485 mL taking into account 500 mL as the total volume of the extraction vessel, in which 15 mL was occupied by methanol. The usage of methanol was constant, i.e. 0.37 mol at all the operational conditions.

a.

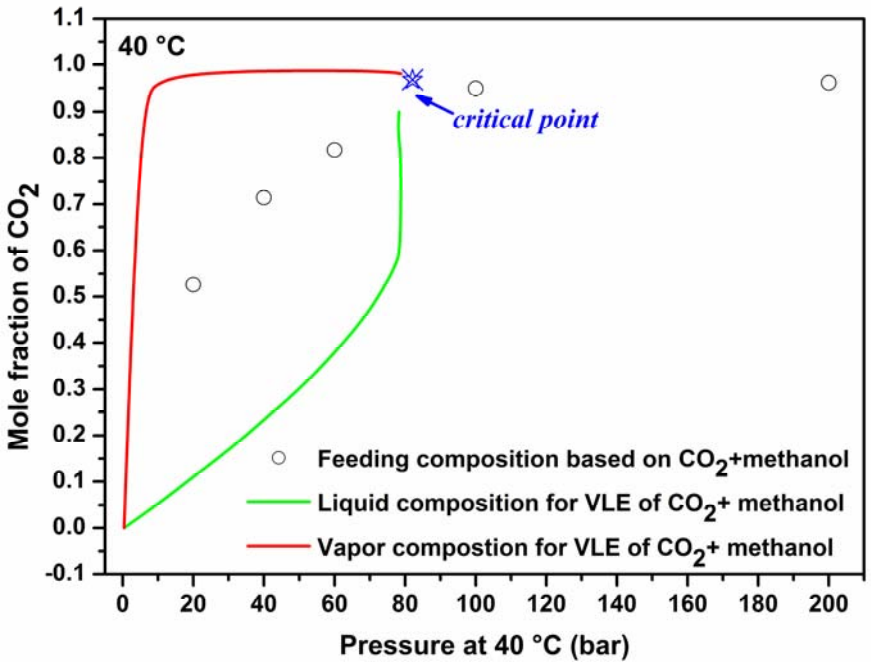
40 °C
critical point
Mole fraction of CO_2
Pressure at 40 °C (bar)
Feeding composition based on CO_2+methanol
Liquid composition for VLE of CO_2+ methanol
Vapor compostion for VLE of CO_2+ methanol

b.

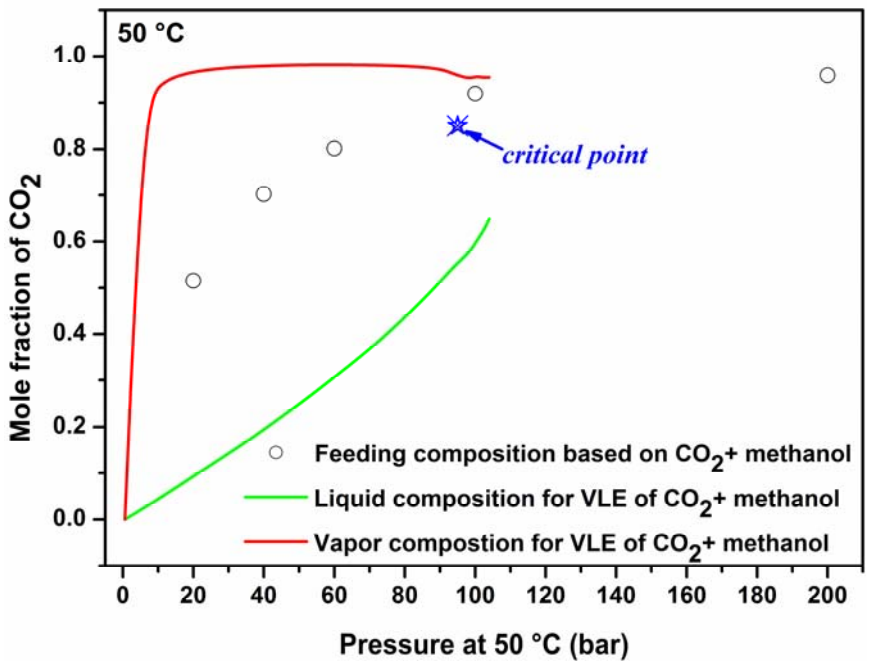
50 °C
critical point
Mole fraction of CO_2
Pressure at 50 °C (bar)
Feeding composition based on CO_2+ methanol
Liquid composition for VLE of CO_2+ methanol
Vapor compostion for VLE of CO_2+ methanol

c.

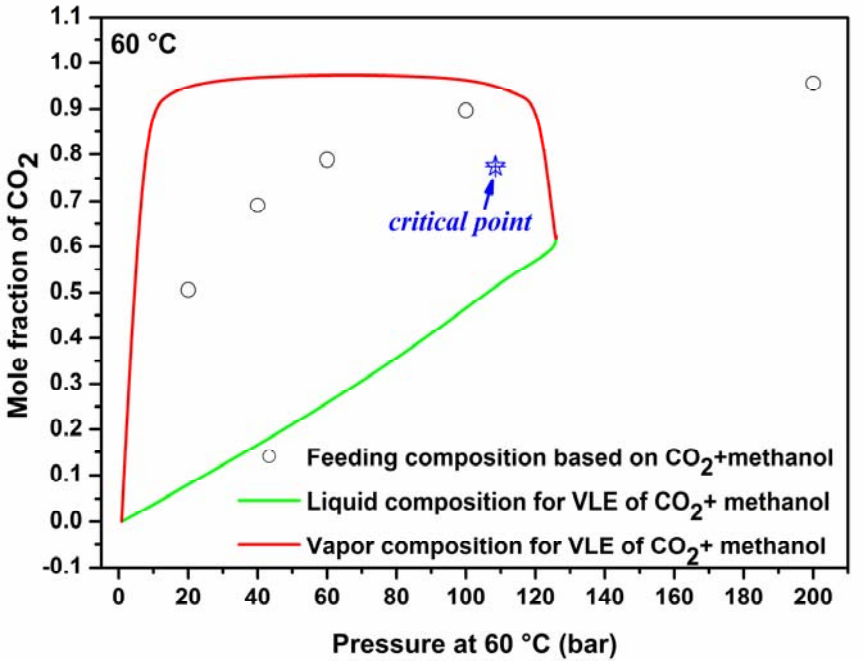
60 °C
Mole fraction of CO_2
Pressure at 60 °C (bar)
critical point
Feeding composition based on CO_2+methanol
Liquid composition for VLE of CO_2+ methanol
Vapor composition for VLE of CO_2+ methanol

d.

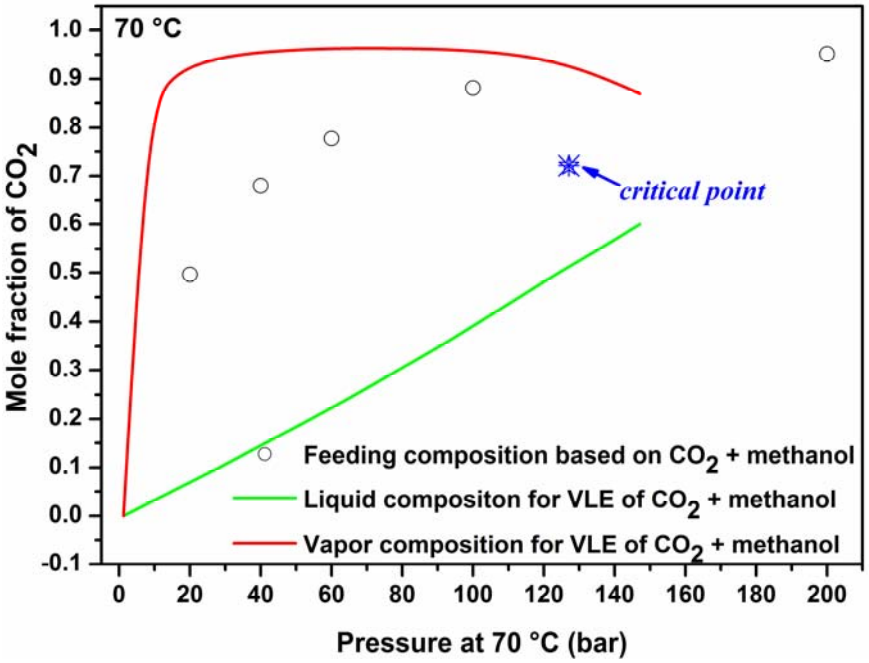
70 °C
Mole fraction of CO_2
Pressure at 70 °C (bar)
critical point
Feeding composition based on CO_2 + methanol
Liquid compositon for VLE of CO_2 + methanol
Vapor composition for VLE of CO_2 + methanol

e.

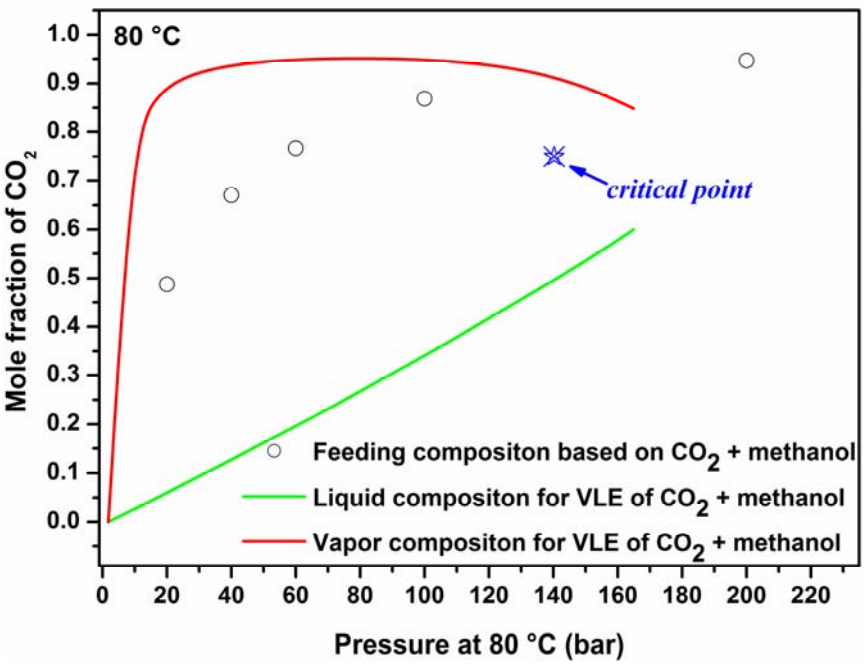
80 °C
Mole fraction of CO_2
Pressure at 80 °C (bar)
critical point
Feeding compositon based on CO_2 + methanol
Liquid compositon for VLE of CO_2 + methanol
Vapor compositon for VLE of CO_2 + methanol

f.

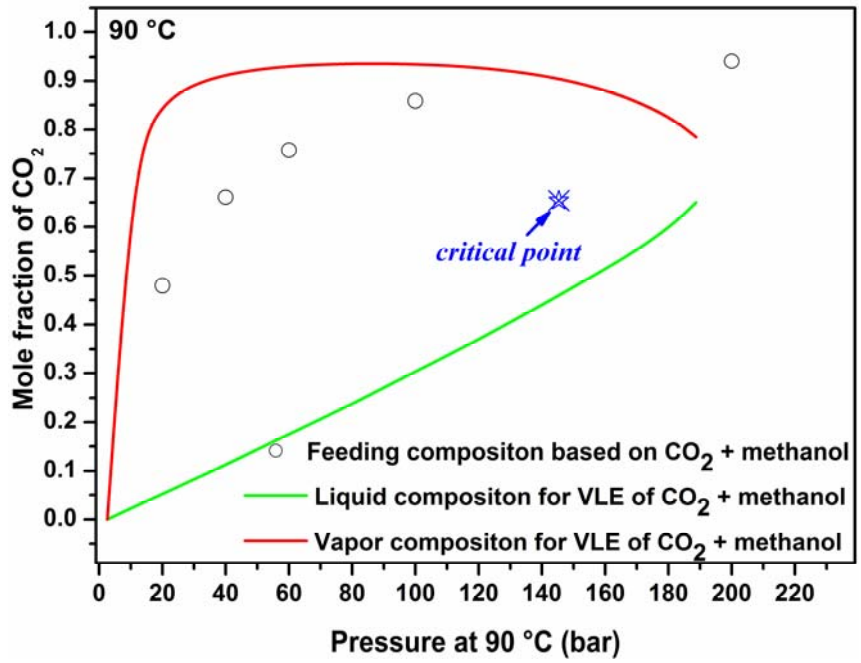
90 °C
Mole fraction of CO_2
Pressure at 90 °C (bar)
critical point
Feeding compositon based on CO_2 + methanol
Liquid compositon for VLE of CO_2 + methanol
Vapor compositon for VLE of CO_2 + methanol

g.

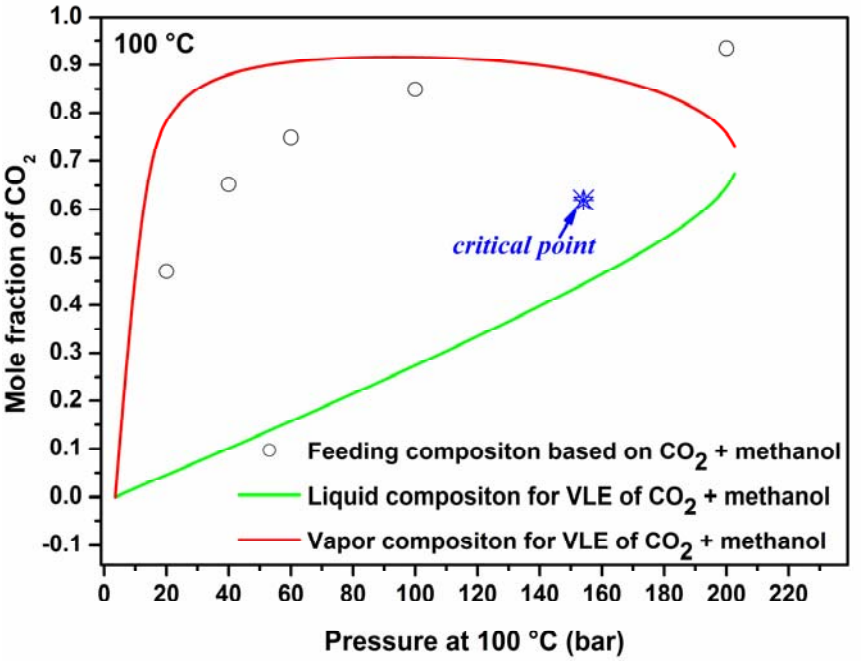

Figure 6-6 Isothermal vapor and liquid equilibrium (VLE) phase compositions of CO_2 and methanol at different temperatures of 40, 50, 60, 70, 80, 90, and 100 °C and the feeding mole fraction of CO_2 based on CO_2 and methanol under various experimental pressures at the respective same temperature.

It can be seen from Figure 6-6 that at a certain temperature, the feeding compositions of those pressures below the critical pressure were found to be in between the vapor and liquid equilibrium compositions. Thereby the extraction phase at pressures below the critical pressure was CXM. In addition, the extraction phase i.e. CXM composition represented by the mole fraction of CO_2 was equal to the liquid composition at VLE of CO_2 and methanol at the respective pressure and temperature. According the critical pressures of the mixture of CO_2 and methanol as listed in Table 6-4, the critical pressures of 40 and 50 °C are lower than 100 bar, whereas those at temperatures from 60 to 100 °C are above 100 bar but below 200 bar. Therefore the extraction phase at 100 and 200 bar at 40 and 50 °C is considered to be a supercritical mixture of CO_2 and methanol, as well as that at 200 bar at 60 to 100 °C. At

these conditions, the mole fraction of CO_2 in the extraction phase is equal to the CO_2 mole fraction for the total loading amount of CO_2 and methanol.

6.3.4 Variation of the extraction phase polarity

The expansion degree of methanol from dissolution of CO_2 increases upon CO_2 pressure increasing at a pressure range below the critical value. However, the polarity of CXM decreases with an increase in the pressure. In order to observe the variation of the extraction phase polarity, the mole fractions of CO_2 in the extraction phase at different operational conditions are presented in Figure 6-7 along with the π^* value of CXM over the mole fraction of CO_2 at 40 °C [*138*]. The π^* value is a measure of the ability of a solvent to stabilize a charge or dipole and is commonly regarded as a crucial parameter for evaluating the solvent polarity in the studied system, which is found to be greatly dependent on the mole fraction of CO_2 dissolved in CXM and less dependent on temperature [*138*]. As seenfrom Figure 6-7 the mole fractions of CO_2 in the extraction phase increase with pressure increasing from 20 to 200 bar at all investigated temperatures, while the π^* value decreases with an increase of the CO_2 mole fraction in methanol [*138*]. This illustrates that increasing the operational pressure results in more CO_2 being dissolved in CXM and the solvent polarity of CXM characterized by its π^* value will be impaired. As for the extraction phase of a supercritical mixture of CO_2 and methanol, its solvent power has been reported to increase upon an increase in density or pressure [*117*]. It can be seen from Figure 6-7 that there is a continuous drop of solvent polarity of the CXM upon an increase in the mole fraction of CO_2. It is reasonable to say that there is turning point in the vicinity of the critical pressure, after which the solvent polarity of the extraction phase increases with increasing pressure.

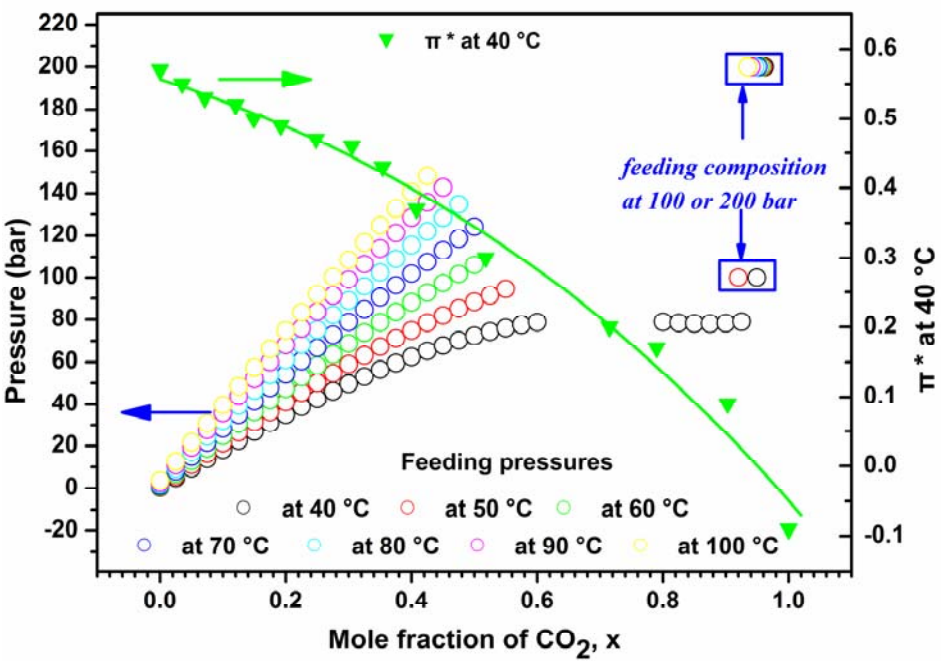

Figure 6-7 Mole fractions of CO_2 (denoted by x) in the extraction phase as a function of the feeding pressure at various temperatures, and the solvent polarity of CXM (characterized by π*) as a function of the mole fraction of CO_2 at 40 °C from the literature [*138*].

6.4 Interpretation of the tunability

The dissolution of CO_2 in HNBR works as a plasticizer to reduce the viscosity of the HNBR and increase the free volume of the HNBR polymer chains, which can facilitate the solution-diffusion process of the small molecules in the polymer matrix. At the same time, the favorable effect on the HNBR matrix induced by the dissolution of CO_2 is considered to strengthen with an increase in the concentration of dissolved CO_2 in HNBR. It can be seen from Figure 6-4 that the concentration of CO_2 in HNBR increases upon increasing pressure over the whole investigated temperature range. The negative effect of increasing viscosity resulted by increasing hydraulic pressure need not be taken into account over the investigated pressure range, i.e. below 200 bar. Hence it is reasonable to generalize that increasing the

pressure of CO_2 is advantageous to the extraction process with respect to swelling the polymer matrix which stimulates the diffusion rate of solutes in it.

On the other hand, the dissolution of CO_2 into methanol provides CXM as a solvent between neat methanol and neat $scCO_2$ and several of its physical properties such as volume, polarity, viscosity, and solute diffusivity become strongly dependent on the concentration of the dissolved CO_2. Among these physical properties, the effects of the changes in the viscosity and solute diffusivity on the extraction rate are negligible, as the diffusivity of chemicals in pure methanol is fast enough and the enhancement of solute diffusivity by dissolved CO_2 offers no more benefit on the extraction rate. However, the change of CXM volume affects the concentration of PMDETA so that it influences the complex reaction rate of Wilkinson's catalyst and PMDETA. As CO_2 pressure increases, the concentration of PMDETA in CXM decreases accordingly. This impairs the recovery rate of Wilkinson's catalyst from the polymer matrix. The variation of the polarity of CXM can influence the chelating reaction rate on the interfaces of HNBR/CXM and affect the solubility of solutes of TPP and RhClPMDETA in CXM. Pure methanol is a favorable solvent for RhClPMDETA and TPP. With the decreasing solvent polarity of CXM as a result of CO_2 dissolution, the dissociation of RhClPMDETA and TPP in CXM will be adversely affected, which in turn depresses the formation and desorption rate of RhClPMDETA from the surfaces of HNBR.

Under low pressures, the CXM is still a good solvent for RhClPMDETA with limited polarity degradation. Although the concentration of PMDETA in CXM decreases with the methanol phase expanded by CO_2, it is still above the concentration required for coordinating the Rh(I) on the HNBR surfaces. Hence, by increasing the pressure from 0 to a certain

pressure of 40 or 60 bar, the extraction rates were found to be improved (see Figure 6-3). As the pressure was further increased from 40 or 60 bar to 100 bar, the concentration of PMDETA in CXM becomes less and is not sufficient for coordinating the Rh(I) on the surfaces of HNBR. The concentration of Rh(I) on the surfaces of HNBR is expected to be even higher under higher pressure as the diffusion of Wilkinson's catalyst in HNBR is stimulated by increasing pressure. Additionally, the formation and desorbing rate of RhClPMDETA from the HNBR surfaces could also be impaired by the poor polarity of CXM. In short, the combination of the above effects led to the observation that there was an optimal pressure over the investigated pressure range.

However, another increase of the extraction rate was observed over the high pressure range, especially for pressure range above the critical pressure, as seen in Figure 6-3. This is proposed to be attributable to the transformation of CXM to a supercritical mixture of CO_2 and methanol. The solvent power of $scCO_2$ is known to increase with increasing density or pressure. Furthermore, the diffusion and reaction rate of chemicals in $scCO_2$ are generally reported to be faster than that in a conventional solvent. PMDETA was reported to be dissolvable in $scCO_2$ with an effective concentration for atom transfer radical polymerization (ATRP) under a CO_2 pressure above 300 bar at 110 °C (density of CO_2 = 0.622 g/mL) [*183*]. PMDETA is soluble in cyclohexane, which is generally used as an indicator of substances' solubility in $scCO_2$. PMDETA can form a very stable complex with Rh(I) based on the discussion conducted previously, hence, it does not undergo dissociation of its ligand like Wilkinson's catalyst does. In summary, it is reasonable to believe that PMDETA and RhClPMDETA were dissolved in the supercritical mixture of CO_2 and methanol and the

advantages of the supercritical fluid leads to the observation of another extraction rate increasing with an increase of pressure at the high pressure range.

6.4.1 Optimal Pressure of CO_2

Limited by the number of the pressures investigated in the experiments, the best operational pressures at 40, 50, 60 and 70 °C were all found to occur at 40 bar, and the best operational pressure at 80, 90 and 100 °C was 60 bar. But the best operational pressure observed for each temperature is not necessarily their exact optimal operational pressure. The advantages shown by the best operational pressure at different temperatures is believed to vary as temperature changes. Although the optimal pressures have not been precisely determined, these findings oriented the location of the optimal pressure at various temperatures. The optimal pressures at temperatures varying from 40 to 70 °C are expected to be around 40 bar and increase with increasing temperature. Nevertheless, the optimal pressure at temperatures varying from 80 to 100 °C are expected to be around 60 bar and increase with increasing temperature.

As a trial to search the optimal operational pressure, an additional pressure of 80 bar was investigated at 100 °C. The extraction profile collected under 80 bar at 100 °C is presented in the Figure 6-8 together with the profiles collected under 20, 40, 60, 100 and 200 bar. In Figure 6-8, the extraction profile collected under 80 bar pressure is shown on top of all the extraction profiles collected under the other investigated pressures at 100 °C.

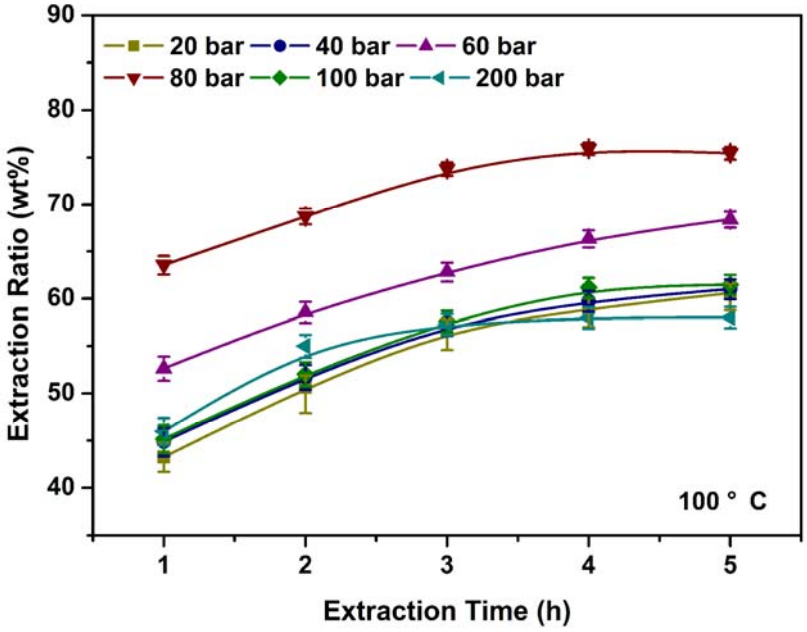

Figure 6-8 Static extraction profiles of Wilkinson's catalyst from HNBR films using CXM and PMDETA under different pressures of 20, 40, 60, 80, 100 and 200 bar at 100 °C.

In addition, it is known the properties of $scCO_2$ at different temperatures and pressures can be generalized through one single variable-density of CO_2. Therefore, density is expected as an intermediate that can be used to determine the optimal pressure. In order to obtain this density, the densities of CO_2 under the investigated experimental conditions of temperature and pressure are presented in . Based on a comprehensive analysis of the best operational pressures observed at different temperatures, 0.14 g/cm^3 is expected to be the optimal CO_2 density, which can be used for determining the optimal pressure at a certain temperature, particularly at temperatures above 80 °C.

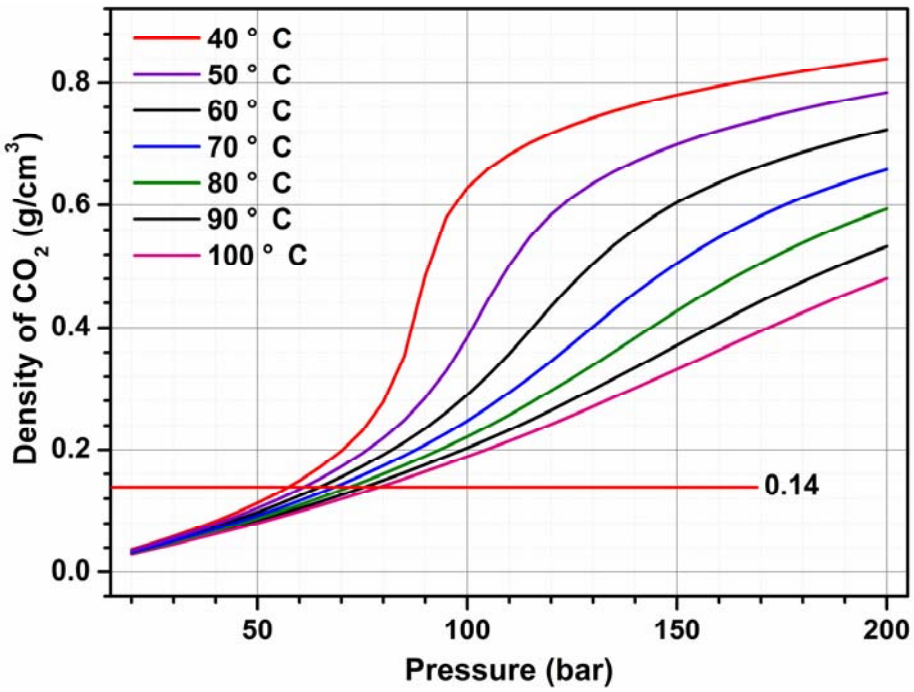

Figure 6-9 Density of CO_2 at different temperatures of 40, 50, 60, 70, 80, 90, and 100 °C and pressure range from 0 to 200 bar.

Compared to temperature, which imposes both chemical and physical effects on the extraction process, pressure of CO_2 only impacts the physical properties of the extraction system. Regarding one of the important physical properties, density of CO_2, pressure has a more profound effect than temperature, especially over the low pressure range. Thus temperature has weak regulation on the plasticizing of HNBR and expanding of methanol via the dissolution of CO_2. Increasing temperature over the low temperature range effectively promotes the extraction rate by increasing the formation rate of RhClPMDETA. However, the benefits acquired by raising operational temperature vanished gradually when the temperature was higher than 80 °C.

In contrast, pressure has a much wider and greater effect on the dissolution of CO_2 in HNBR and methanol. Therefore, pressure has a stronger regulation on the efficiency of the

extraction process via adjusting the concentration of CO_2 in HNBR and methanol. Increasing pressure can significantly enhance the solubility of CO_2 in both HNBR and methanol, and thus improve the plasticizing of HNBR and reduce the solvent power of CXM simultaneously. Although at extreme high pressure, the properties of supercritical fluid can be exploited to benefit the process, it leads to more energy and economic concerns. Pressure is preferred to be optimized over the low pressure range. The optimal pressure can only be speculated, but can not be precisely determined due to the limited number of pressures that were investigated. For the investigated system of HNBR/Wilkinson's catalyst, the optimal operational conditions are thought to be 80 °C and 60 bar.

6.5 Extraction mechanisms

Based on the above discussions focusing on the extraction profiles collected under various operational pressures at 80 °C, an extraction mechanism is proposed for the interpretation of this extraction process. The events in this extraction process are proposed to occur in the following order: (1) PMDETA reacts with Wilkinson's catalyst distributed on the surfaces of the polymer to form RhClPMDETA; (2) the newly generated RhClPMDETA dissolves in CXM from the surfaces of the polymer; (3) Wilkinson's catalyst diffuses towards the interfaces of the polymer and CXM; (4) TPP ligand dissociates from Wilkinson's catalyst; (5) TPP diffuses from the interior of the polymer to its surfaces, and then dissolves in CXM. Event (1) is highly temperature dependent, as the replacement of TPP by PMDETA is initiated by the dissociation of the TPP ligand from Wilkinson's catalyst, which is not appreciable at room temperature, and can be greatly stimulated by elevating temperature. Thus the recovery of Wilkinson's catalyst with this investigated technology has to be carried

out at elevated temperature, such as 80 °C. At a constant temperature, Event (3) is the extraction rate determining step under relatively low pressure conditions, whereas the extraction rates are determined by the diffusion rate of Wilkinson's catalyst within the polymer. Under a high pressure, e.g., 100 or 200 bar at 80 °C, Events (1) and (2) become the extraction rate determining steps, wherein the diffusion rate of Wilkinson's catalyst in the polymer is greatly enhanced and the formation and desorbing rates of RhClPMDETA are however impaired and become the extraction rate determining steps. Event (4) and (5) take place accompanying all the other three events and gradually bring the extraction to an end, which is thought to be greatly dependent on the operational temperature and relatively less dependent on the CO_2 pressure. After the extraction, a small amount of Wilkinson's catalyst is retained in the polymer matrix as a result of the formation of the coordination bond between the 14- or 12- electron complex of Wilkinson's catalyst and the functionalities of the polymer. Measures to retain a sufficient amount of TPP in the polymer matrix are assumed capable of releasing a 14- or 12- electron complexes of Wilkinson's catalyst from the functionalities of the polymer and further improving the recovery of Wilkinson's catalyst. A schematic explanation of this extraction process is illustrated in Figure 6-10.

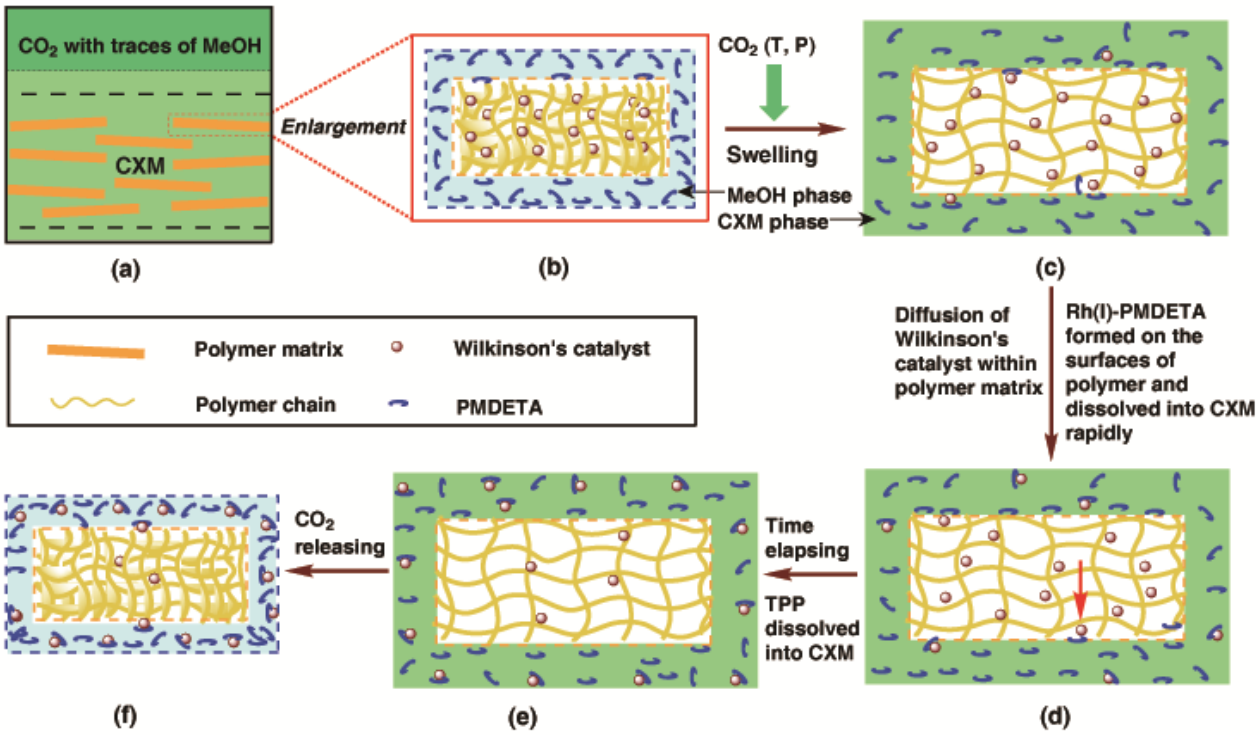

Figure 6-10 Schematic diagram illustrating the extraction process: (a) extraction vessel; (b) one single polymer strip selected for the mass transfer investigation; (c) methanol (MeOH) expanded by CO_2; polymer plasticized by CO_2; PMDETA absorbs on the surfaces of the polymer and reacts with Wilkinson's catalyst distributed on the polymer surfaces; (d) Wilkinson's catalyst diffusing from the interior of the polymer towards its surfaces; (e) Wilkinson's catalyst coordinates with the functional groups of the polymer and is retained in the polymer matrix; (f) separation of Wilkinson's catalyst terminated and the volume of polymer recovered after the CO_2 release.

As mentioned previously, the extraction profiles under 20, 40 and 60 bar with a gradually decreasing extraction rate as the extraction durations is extended from 1 to 5 h (Figure 6-3e). Although no obvious extraction equilibria are observed under these pressures, the increments of these extraction profiles after 5 h are expected to be very close to a final state and their final extraction ratios will be in the same order as that shown by their initial extraction rates. In contrast, the extraction equilibrium under 100 and 200 bar are clearly observed in Figure 6-3 with similar equilibrium extraction ratios. One possible explanation

could be as follows. Usually the equilibrium extraction ratio is determined by the saturation concentration of the targeted extract in the extraction phase (or the solvation power of the extraction phase), yet the situation in this investigated extraction system is more complicated and the equilibrium extraction ratio can not be solely determined by the solvating power of the extraction phase. The TPP ligand of Wilkinson's catalyst is labile and easy to dissociate from the catalyst at high temperature e.g., 80 °C. The solubility of TPP in methanol increases with increasing temperature. In the present system, the samples were prepared with no TPP added into the HNBR except Wilkinson's catalyst. Hence, at the high temperature of 80 °C, TPP continuously dissociates from the catalyst and dissolves into CXM or $scCO_2$ as the extraction is being carried out, which in turn results in an end of the catalyst separation even with a high residue of Rh(I), since the existence of excessive TPP has been reported to be crucial in ensuring the free movement of Wilkinson's catalyst inside HNBR [*4*]. Ascribed to the small molecular size of TPP, the diffusion of TPP in HNBR is expected to be less dependent on the concentration of CO_2 dissolved in HNBR than that coming from Wilkinson's catalyst, which implies the diffusion of TPP in HNBR under 2, 4 and 6 bar could be very similar. In the beginning of the extraction process, enough TPP was present in the HNBR matrix to ensure the free diffusion of Wilkinson's catalyst within HNBR. Under this presupposition of the free diffusion of Wilkinson's catalyst, the diffusion rate of the catalyst within HNBR increased with increasing CO_2 pressure. Therefore, the initial extraction rate represented by the average extraction rate in the first hour was observed to increase with an increase of pressure at 20, 40, and 60 bar. As the extraction proceeds, the extraction rate slowed down gradually due to a decrease in the TPP remaining in HNBR; the reduction in

rate which was similar at the pressures of 20, 40, and 60 bar. Thus, the extraction profiles at 20, 40, and 60 bar are analogous to each other and their equilibrium extraction ratios are in the same order as shown by the initial extraction rate. However, the extraction profiles under 100 and 200 bar with apparent plateaus observed at 2 to 3 h are attributed to one or both of the following aspects. One is the further enhanced diffusion of TPP which results in its loss from HNBR and brings the extraction to an end quickly. The other one is that the dissolving ability of CXM on RhClPMDETA is extensively impaired with a further pressure increase to 100 and 200 bar, and the concentration of RhClPMDETA in the CXM or $scCO_2$ reach their respective saturation values at their respective plateau.

6.6 Reactions and Challenges

The investigated extraction system is a little more complicated than the general extraction system attributed to the fact that some reactions are involved in the extraction process. Apart from the reaction between Wilkinson's catalyst and PMDETA, reaction also occurs between Wilkinson's catalyst and HNBR. The optimized extraction system originally consisted of methanol, CO_2, HNBR, Wilkinson's catalyst and PMDETA. As the extraction proceeds, more species are produced. They are the TPP ligand, RhCl(TPP)n ($n \leq 2$), and RhClPMDETA. The TPP ligands of Wilkinson's catalyst are labile and undergo dissociation from the Rh(I) complex in the presence of solvent at high temperature [*17*]. In this process, free TPP is released from Wilkinson's catalyst and new complexes of $RhCl(TPP)_n$ are formed. When the above described reactions takes place on the surfaces of HNBR, the vacant co-ordination sites of $RhCl(TPP)_n$ resulting from dissociation of TPP ligands will be occupied by PMDETA and the chelating complex RhClPMDETA is thereby produced and dissolved into

CXM. Otherwise, when the above described reactions happen within HNBR, the vacant co-ordinate sites of $RhCl(TPP)_n$ will be occupied by the solvent, i.e. methanol and CO_2 in HNBR and forms $RhCl(TPP)_n$(solvent) or by functionalities, i.e. C≡N and C=C present within HNBR. CO_2 and methanol have poorer coordinating power with Rh(I) compared with the C≡N group and the residual C=C of HNBR. Hence, the solvent on $RhCl(TPP)_n$(solvent) will be replaced easily by these functionalities [*17*]. The coordination of $RhCl(TPP)_n$ with the functionalities of HNBR seriously impedes the free diffusion of Wilkinson's catalyst in HNBR and becomes the principal obstacle in the extraction process. The existence of the chelant within HNBR is expected to be helpful for improving the diffusion of Wilkinson's catalyst within HNBR, since they can compete for $RhCl(TPP)_n$ with the C≡N and C=C groups and help release the Rh(I) from HNBR. The free TPP ligand is assumed to be one of the most promising candidates that can compete for $RhCl(TPP)_n$ with the C≡N and C=C. In the typical NBR latex and bulk hydrogenation processes catalyzed by Wilkinson's catalyst, always an excess of the TPP ligand was added as an additive to maintain the activity of Wilkinson's catalyst and facilitate the diffusion of the catalyst within the HNBR particles as well [*4, 85*]. The PMDETA dissolved in HNBR may not have the ability to compete for $RhCl(TPP)_n$ with the C≡N and C=C of HNBR, taking into account that PMDETA is a tridentate chelating agent and its complexation reaction with the metal ions has more stringent requirements on the solvent environment and steric feasibility. Although the dissolution of CO_2 and methanol in HNBR greatly enhances the free volume of HNBR, it still does not meet the solvent conditions for the complexation reaction involving PMDETA to occur. However, TPP is soluable in methanol and $scCO_2$, and thus is soluble in CXM. As

the extraction proceeds, more and more TPP ligands are detached from Wilkinson's catalyst and transferred from HNBR to CXM. The extraction is brought to an end when the TPP in HNBR is insufficient to compete for $RhCl(TPP)_n$ with the C≡N and C=C functionalities within HNBR. In the light of the above discussion, TPP plays an important role in facilitating the free diffusion of Wilkinson's catalyst within HNBR. The reactions involved in the extraction process are briefly illustrated in Figure 6-11. Wilkinson's catalyst could lose one or more of its TPP ligands to produce the intermediates $RhCl(TPP)_n$, where n could be 0, 1, or 2. All these intermediates are expected to have the same fate. In Figure 6-11, $RhCl(TPP)_2$ was employed as the model intermediate to illustrate the reactions within HNBR.

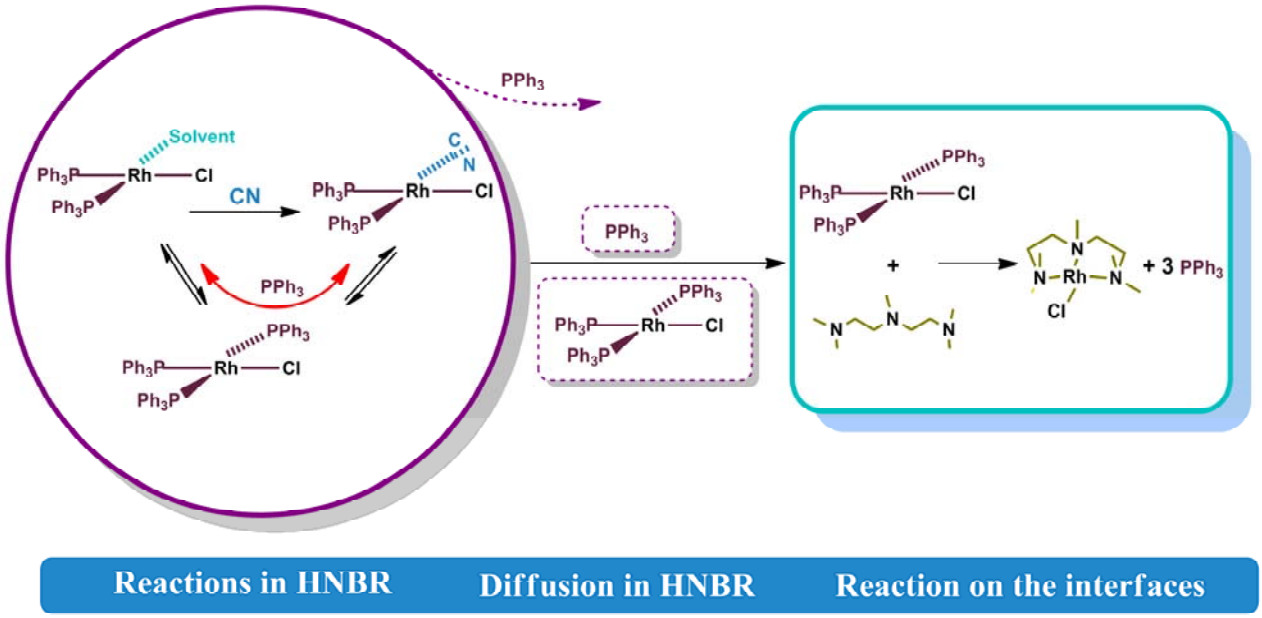

Figure 6-11 Schematic diagram illustrating the events taking place in the extraction process: (a) reactions within HNBR; (b) diffusion of Wilkinson's catalyst and PPh_3 in HNBR; (c) PMDETA complexation of Wilkinson's catalyst on the interfaces of HNBR and CXM

As mentioned before, an excess of the TPP ligand was added to the NBR latex and bulk hydrogenation processes catalyzed by Wilkinson's catalyst to maintain the activity of

Wilkinson's catalyst. This will also favour the recovery of Wilkinson's catalyst from the HNBR produced via latex and bulk hydrogenation processes. In the extraction experiments for investigation of the operational conditions, the HNBR extraction samples were prepared by merely adding Wilkinson's catalyst due to the fact that no concrete information about the concentration of TPP contained within the HNBR particles produced by latex hydrogenation and bulk hydrogenation was available.

6.7 Summary

In this Chapter, the tunability of the extraction system via changing temperature and pressure are extensively discussed. Raising temperature significantly stimulates the extraction rate, which is attributed to the enhanced diffusivity of Wilkinson's catalyst in HNBR and the increased formation rate of the RhClPMDETA complex with an increase in temperature. However, the benefits in improving the extraction rate by increasing temperature diminish when the temperature reaches above 80 °C. The changing in the extraction phase composition upon changing the CO_2 pressure is carefully studied by employing VLE data for the binary system of CO_2 and methanol. It is found that the extraction phase below the critical pressure is CXM, which has a concentration of CO_2 equal to that of the liquid composition at the VLE of CO_2/methanol. The extraction phase above the critical pressure is a supercritical mixture of CO_2 and methanol. Besides, the regulation from CO_2 pressure is analyzed from the polarity variation of the extraction phase. Compared to temperature, CO_2 has a more complex regulation effect on the extraction process and there is an optimal operational pressure over the low pressure rang, at which the extraction rate is the highest. This optimal operational pressure varies with changing temperature, which is expected to be

determined by the CO_2 density of 0.14 g/mL and temperature. Moreover, an extraction mechanism was illustrated to explain the events involved in a typical extraction process. Finally, based on the interpretation of the experimental data, the reactions and challenges existing in this special system of HNBR/Wilkinson's catalyst are identified and illustrated.

Chapter 7
Two Special Operational Procedures

According to the results and discussions conducted in Chapter 6, a varying pressure was considered as a possible way to improve the extraction rate. A sequential operation with replacing of fresh extraction solvent and chelating ligand was proposed as an alternative to further improve the extraction rate as well. Finally, the extraction technique was tested by applying it to HNBR particles coagulated from the HNBR latex. A detail discussion is conducted as follows.

7.1 Varying pressure procedure

As discussed in previous sections, the extractions under low and high pressures of CO_2 have their respective advantages and disadvantages. The low pressure of CO_2 improves the diffusivity of additives within HNBR, and greatly improves the formation rate of RhClPMDETA and its desorption rate from the HNBR surfaces. By comparison, the high pressure of CO_2 significantly promotes the diffusion of small molecules in HNBR, and suppresses the formation rate of RhClPMDETA and its desorbing rate from the HNBR surfaces to a great extent. Another feature under high pressure is that the releasing of CO_2 can foam HNBR and thereby cause numerous micro-cavities in it, which is able to extensively improve the subsequent diffusion rate in HNBR. To take advantage of the benefits realized under both high and low pressures, a varying pressure procedure was employed as a trial to improve the extraction performance. In this procedure, the initial pressure is set as high as 100 bar and maintained for half an hour, and then decreased rapidly to 50 bar and maintained for another half an hour. This two-level pressure operation is repeated over the extended extraction duration.

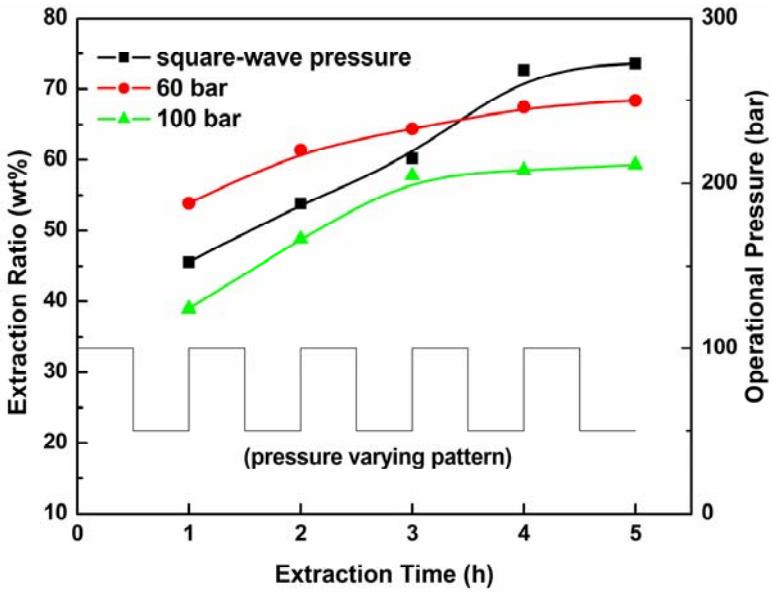

Figure 7-1 Extraction profiles collected under the square-wave pressure varying between 50 and 100 bar, or under a constant pressure of 60 or 100 bar at 80 °C.

Figure 7-1 shows the static extraction profile obtained under varying pressure along with the extraction profiles collected under constant pressures of 60 and 100 bar. After 4 h extraction at 80 °C, the varying pressure procedure results in higher extraction ratios than those obtained under either 60 or 100 bar. After 5 h operation, the recovery of Wilkinson's catalyst reaches 74 wt%, and the concentration of rhodium in HNBR drops from 700 to 196 ppm. These results suggest that the varying pressure in a square-wave manner is a promising method to effectively recover Rh(I) from the HNBR matrix, which can be exploited and optimized in the future to maximize the recovery of the Rh(I) from the HNBR matrix.

7.2 Sequential Extraction

Sequential extraction is a potential process to improve the extraction ratio. A sequential extraction is defined as repetitively running static extraction operations several times over. In this study, the sequential extraction was carried out at 60 bar and 80 °C, and each batch run

lasted 3 h. Fresh methanol and chelating ligand were recharged when the sample was placed back for the next extraction run. Furthermore, before each new extraction run, CO_2 was released and re-pumped into the extraction vessel.

Figure 7-2 shows the extraction ratio obtained as a function of sequential extraction runs. As shown in Figure 7-2, the extraction ratio attained by 1 run of 3 h extraction is as high as 64 wt%. However, the extraction ratio obtained by a sequential operation of 2 and 3 runs is only 67 and 66 wt%, respectively, showing a very minor increment compared with the extraction ratio obtained using a single run extraction. Increasing the runs of a sequential extraction to 2 and 3 with extraction time extending to 6 and 9 h, respectively, did not show notable effectiveness in improving the extraction ratio. For comparison, the static extraction profile collected at different extraction intervals from 1 to 5 h at 60 bar and 80 °C is presented in Figure 7-2 as well. The extraction ratio obtained after a continuous 4 h static operation is 67 wt%, even higher than that obtained with the sequential operation of 3 runs, i.e. 9 h.

The above results indicate that the improvement of extraction ratio by means of sequential extraction is very marginal on the lab-prepared HNBR sample. Furthermore, the failure to improve the extraction ratio on the lab-prepared HNBR sample via sequential operation is consistent with the discussion presented before in that the existence of excessive free TPP ligand is crucial for the free diffusion of Wilkinson's catalyst in HNBR. The extraction will determine if not enough free TPP ligand is present in the HNBR, no matter how much Rh(I) complex remains in the HNBR. From the results presented in Figure 7-2, it can be revealed that the TPP ligand dissociated from Wilkinson's catalyst was mostly

transferred from HNBR to CXM in 3 h at 80 °C and 60 bar. In the static continuous extraction, the concentration of TPP in the CXM starts at 0 and increases on extending the extraction time. On extending the treatment time in the static extraction process from 3 to 4 or 5 h, the free TPP ligand may transfer back and forth between CXM and HNBR, as its concentration in CXM reaches a high level or even the saturation concentration. This is beneficial to the extraction process and explains that an increment of the extraction ratio was observed via extending the static operation time. In the sequential extraction process, with the replacement of a fresh mixture of methanol and PMDETA before each run, the concentration of RhClPMDETA in CXM is reset to 0 as well as that of TPP. This operation was supposed to benefit the extraction process, but accelerates the loss of TPP from HNBR and speeds up the end of the extraction ratio increment.

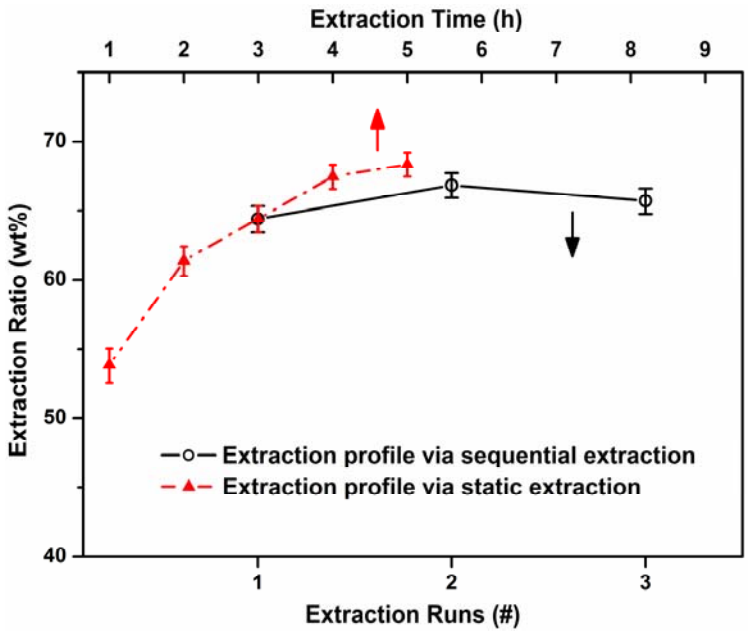

Figure 7-2 Extraction profiles obtained at 80 °C and 60 bar by static operation and sequential operation (Runs 0, 1, 2 and 3 represent 0, 3, 6 and 9 h extraction, respectively)

7.3 Application on the HNBR particles coagulated from the HNBR latex

This developed technique was examined for the removal of Wilkinson's catalyst from the HNBR particles coagulated from the HNBR latex. The HNBR latex was produced by direct catalytic hydrogenation of commercial NBR latex via Wilkinson's catalyst according to the procedure reported in the literature [*4*]. The HNBR particles coagulated from the same HNBR latex were divided into two groups. One group was treated with a static extraction of 3 h at 80 °C and 60 bar. The other one was treated by a sequential extraction of 3 runs, i.e. totally 9 h at the same temperature and pressure, i.e. 80 °C and 60 bar. The extraction results obtained are presented in Figure 7-3.

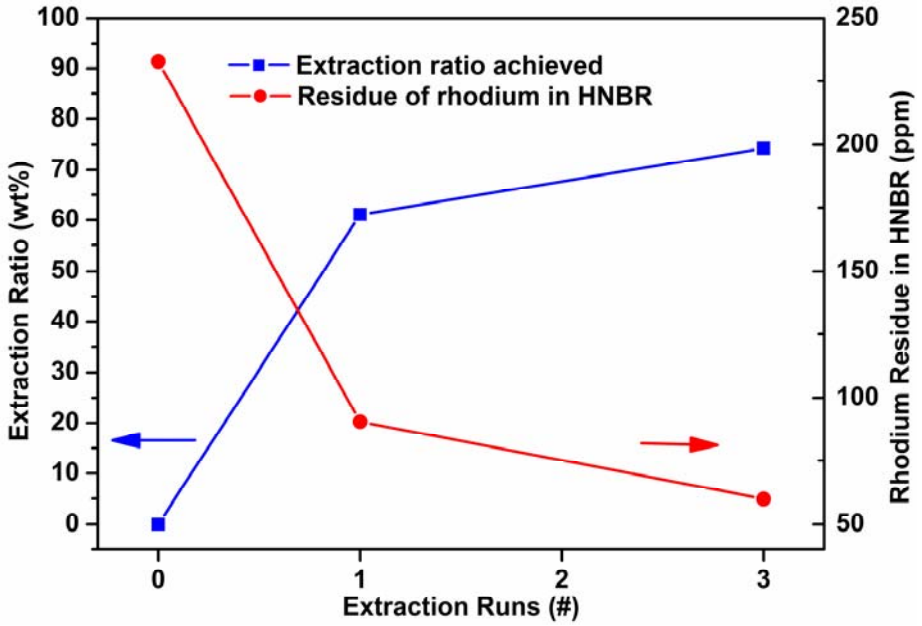

Figure 7-3 Sequential extraction results on the HNBR particles coagulated from its latex at 80 °C and 60 bar (Runs 0, 1, 2, and 3 represent 0, 3, 6, and 9 h extraction, respectively)

As illustrated in Figure 7-3 the same sequential operation that could not improve the extraction ratio by increasing the number of runs on the lab-prepared HNBR sample is

however effective in enhancing the extraction ratio on the coagulated HNBR particles via an addition of runs. With the addition of the extraction run number in a sequential extraction by two, i.e. extending the operation time from 3 to 9 h, the extraction ratio obtained increased from 60 to 75 wt% and the residue of rhodium in HNBR was reduced from 100 to 59 ppm. Compared to the lab-prepared HNBR sample, wherein no free TPP ligand was added, a large amount of free TPP ligand was present in the coagulated HNBR particles as a result of the 10 fold excess of TPP ligand based on the catalyst, which is required to be added into the reaction system in a typical catalytic latex or bulk hydrogenation of NBR in the presence of Wilkinson's catalyst. Furthermore, as low as 59 ppm rhodium residue was achieved in the coagulated HNBR particles which demonstrated that this developed extraction technique of using CXM and PMDETA is effective for the recovery of Wilkinson's catalyst from the latex and bulk hydrogenation processes.

7.4 Summary

A pressure varying procedure showed a superior extraction performance. This is considered to be due to the enhanced surface area of HNBR as a result of the HNBR matrix internal structure change induced by the pressure alternation and the weak reduction of CXM polarity under low pressure. Sequential operation showed no efficiency in improving the extraction rate of a lab-prepared HNBR sample. However, it showed advantages in enhancing the extraction rate of a sample consisting of HNBR particles coagulated from HNBR latex. A residue of 59 ppm rhodium was obtained for the coagulated HNBR particles using CXM and PMDETA at 80 °C and 60 bar. Therefore, the separation technique incorporating CXM and PMDETA is quite effective

Chapter 8
Conclusions and Recommendations for Future Research

8.1 Conclusions

An effective green separation technique using CXM and chelant PMDETA was developed for separation of Wilkinson's catalyst from HNBR. The tunability of the working system was carefully investigated based on the regulation of CO_2 on HNBR and the extraction phase of CXM. The major challenges involved in successful separating Wilkinson's catalyst from HNBR were determined as guidance for future work. The conclusions drawn for each part of work are presented as follows.

8.1.1 Recovery of rhodium catalysts using $scCO_2$

The development of a green separation technique was started by using $scCO_2$ and some $scCO_2$ soluble chelating agents. The following conclusions are drawn regarding this part of work.

- Although a $scCO_2$ dissolvable Wilkinson's catalyst $RhCl(TTFMPP)_3$ was successfully synthesized and found to have certain hydrogenation efficiency, it could not be extracted from the HNBR matrix by $scCO_2$.

- Although $scCO_2$ can extract rhodium catalysts from their aqueous solutions and wet crystals via the $scCO_2$ dissolvable chelating agent TTA, TTA is not able to assist in recovering the rhodium catalyst from the HNBR/NBR matrix.

- The weak solvating power of $scCO_2$ made it not a good solvent for extracting the rhodium catalysts from the polymer matrix of NBR/HNBR, as they have strong matrix effect on the rhodium catalysts dissolved in them.

8.1.2 Recovery of Wilkinson's catalyst using CXLs and chelating agents

CXW, CXM and CXE were investigated in respect to their proficiency for recovery of Wilkinson's catalyst from HNBR with assistance of various chelating agents. The conclusions drawn are presented as follows.

- CXW is not a good extracting solvent for removing of Wilkinson's catalyst from HNNR, since the substitution of any of the ligand of Wilkinson's catalyst can hardly happen in the medium of water.
- CXM was evaluated as a better extraction solvent over CXE, as methanol is cheaper than ethanol.
- PMDET showed the best performance in CXM among all the investigated three chelating agents of DETA, PMDETA and TMEDA.
- Thinner HNBR film has better the extraction efficiency.

8.1.3 Function of temperature and pressure

The effects of $scCO_2$ on the extraction process via changing temperature and pressure were carefully investigated. The following conclusions are made regarding this part of work.

- Raising temperature significantly stimulates the extraction rate as a result of the enhanced diffusivity of Wilkinson's catalyst and the increased formation rate of the

RhClPMDETA complex. The effects induced by temperature become less important when temperature reaches above 80 °C.

- Increasing pressure from 0 to 60 bar at 80 °C effectively improves the extraction rate as a result of the increased plasticization of HNBR. Increasing pressure from 60 to 100 bar at 80 °C however suppresses the extraction rate due to the extensive decrease of the CXM polarity and PMDETA concentration.

- The operation at an extreme high CO_2 pressure of 200 bar at 80 °C was found to have faster extraction rate than that of 100 bar for the initial 1 to 2 h extraction. The superiority of 200 bar was considered to be caused by the advantageous properties of supercritical fluid, because 200 bar is above the critical pressure, i.e. 140.3 bar of the mixture of CO_2 and methanol at 80 °C.

- There exists an optimal operation pressure at a certain temperature, which is proposed to be determined by the CO_2 density of 0.14 g/mL and temperature

- Varying pressure procedure was found of superiority over the constant pressure procedure.

8.1.4 Extraction mechanism involved

An extraction mechanism is illustrated for the interpretation of this extraction process. The following events are expected to take place in order in an extraction process.

- PMDETA reacts with Wilkinson's catalyst distributed on the surfaces of the polymer to form RhClPMDETA;

- The newly generated RhClPMDETA dissolves in CXM from the surfaces of the polymer;

- Wilkinson's catalyst diffuses towards the interfaces of the polymer and CXM;

- TPP ligand dissociates from Wilkinson's catalyst;

- TPP diffuses from the interior of the polymer to its surfaces, and then dissolves in CXM.

8.1.5 Identification of the major obstacle

Based on a comprehensive interpretation of the results observed, the major obstacles were identified by illustrating the reactions occurring within HNBR during the extraction process. The following statements are summarized.

- The coordination of $RhCl(TPP)_n$ with the functionalities of HNBR seriously impedes the free diffusion of Wilkinson's catalyst in HNBR and becomes the principal obstacle in the extraction process.

- The existence of the chelating agent within HNBR is expected to be helpful for improving the diffusion of Wilkinson's catalyst within HNBR, since they can compete for $RhCl(TPP)_n$ with the C≡N and C=C groups and help release the Rh(I) from HNBR. The free TPP ligand is assumed to be one of the most promising candidates that can compete for $RhCl(TPP)_n$ with the C≡N and C=C moieties.

- The ability to retain TPP in the HNBR matrix is expected to favorably enhance the equilibrium extraction ratio

8.1.6 Milestones and contributions

Several achievements are highlighted as important progress for achieving the final objective. They are listed as below.

- The first milestone is using PMDETA and methanol as chelating agent and extraction solvent, respectively, to realize the separation of Wilkinson's catalyst from HNBR with the assistance of $scCO_2$.

- The second contribution is building up a complete experimental and analysis procedure for tracking the experimental results precisely.

- The third contribution is providing a careful interpretation of the data collected. Based on this interpretation, a clear and solid knowledge was obtained regarding the regulation patterns that $scCO_2$ imposed on the extraction process. Besides, a percipient extraction mechanism was proposed for tracking the events involved in an extraction process.

- The fourth important contribution as a milestone is identification of the major challenges involved in separation of Wilkinson's catalyst from the HNBR matrix system. The dissociation of the TPP ligand from Wilkinson's catalyst and the coordination of the Wilkinson's complex with the C≡N group and C=C residue in HNBR significantly restrict the free diffusion of any rhodium complex. Moreover,

excess TPP in HNBR was pointed out as a crucial factor for enabling the free diffusion of the rhodium complex within HNBR.

- The fifth contribution is that this technique comprised of CXM and PMDETA was verified with a residue of 59 ppm rhodium by application on the HNBR particles coagulated from real HNBR latex.

8.2 Recommendations for future research

8.2.1 Further investigation on the $scCO_2$ system

Despite all these discouraging results obtained in respect to using $scCO_2$ as a green media for reaction and recycling of Wilkinson's catalyst in a polymer homogeneous hydrogenation process, there are still some improvements that can be tried to facilitate its application.

First, some alternative fluorine ligands can be investigated as substitutions of TPP in terms of their catalytic hydrogenation reactivity and solubility in $scCO_2$. Some measures have been reported for the fluorinated analogues to preserve the catalytic reactivity of the original catalyst such as to add a spacer group, e.g. aryl or alkyl group between the phosphorus and the fluorine tail [*95, 96*]. The fluorous ligand $P(p\text{-}C_6H_4OCH_2C_7F_{15})_3$ was reported to exhibit high activity and stability in catalytic hydrogenation of alkenes in a fluorous biphasic system [*100*], which deserves consideration for application in the $scCO_2$ system. In such a system, $scCO_2$ is used to stimulate the mass transfer during a reaction and to recover the catalyst after reaction.

Second, higher temperature, i.e. above 100 °C is recommended for future exploitation of $scCO_2$ for recovering fluorous Wilkinson's catalyst from HNBR. There are two reasons

for increasing the extraction temperature. Firstly, the NBR bulk hydrogenation temperature is as high as 145 °C [*5*]. Second, the main mass transfer resistance during the separation of the catalyst is from inside the HNBR polymer matrix. Increasing temperature enhances the free volume of the HNBR polymer chains and hence increases their permeability.

8.2.2 Further investigation of CXM system

In the thesis work, a lot of systematic investigations have concentrated on the CXM system. However, there are still some investigations that can be conducted to improve its performance such as the selection of a good chelating agent.

As revealed in Chapter 6 the chelating reaction between PMDETA and Wilkinson's complex actually only occurs at the interface of HNBR and CXM instead of inside the HNBR matrix. The major factor that explains this phenomenon is that the solvent environment within HNBR is not able to provide the space configuration required for the chelating reaction involving a tri-dentate chelating agent i.e. PMDETA. Hence, some mono-dentate chelating agents such as the P-donor ligands are strongly recommended for the further improvement of the performance of the CXL system. Besides, mono-dentate chelating agents with small molecular size are preferred so that they can form chelating complex with the Wilkinson's complexes within the HNBR.

A further investigation of the pressure varying procedure is also strongly recommended. The pressure varying procedure is promising in further enhancing extraction ration by optimizing the variables involved such as the options of high and low pressure, the combination pattern, and the operation time.

Besides, a modification of the extraction equipment is also recommended. The extraction experiment can be operated in a high pressure vessel with reduced volume so as to lessen the loss of methanol to CO_2 phase. The extraction apparatus can also be simplified by adding dry ice at low temperature so as to eliminate the need for a high pressure pump in order to introduce CO_2. Agitator is also suggested to be mounted in the future when the loading amount of extraction sample is increased.

8.2.3 Recovery of the catalyst in a latex system

As stated in Section 8.2.2 the P-donor ligand is probably a good candidate as a chelating agent for stimulating the free diffusion of Wilkinson's complex within the HNBR matrix. The TPP-the ligand of Wilkinson's catalyst is a P-donor ligand and has a relatively low melting point of 80 °C. TPP liquid droplets can be formed and dispersed in water by agitation at elevated temperature above 80 °C. These small droplets of TPP liquid can serve as reservoirs of Wilkinson's catalyst. Moreover, excess TPP has been found to play a crucial role in promoting the free diffusion of Wilkinson's catalyst within the HNBR particles during the process of direct hydrogenation NBR in the latex form [*4*].

Therefore, in the future research on TPP alone can be utilized in the HNBR latex for extraction of Wilkinson's catalyst from the HNBR particles to TPP liquid droplets at elevated temperature, e.g. 110 °C. In this process, TPP serves two functions, namely as a ligand and an extraction solvent at the same time. With decreasing temperature, the liquefied TPP precipitates from the water phase, thereby the catalyst is separated.

Nomenclature

ε/k	the depth of the potential over Boltzmann's constant , [K]
ε^{AB}/k	the association energy over Boltzmann's constant, [K]
ρ	density, [g/mL]
ρ_c	critical density, [g/mL]
σ	the (temperature-independent) segment diameter, [Å]
θ	thickness of the extraction sample, [mm]
BARF	tetrakis-(3,5-bis-trifluoroimethylphenyl)borate
BINAP	2,2'-bis(diphenylphosphino)-1,1'-binaphthyl
BMIM	1-butyl-3-methylimidazolium
BP	boiling point, [°C] or [K]
C_0	original concentration of rhodium in an extraction sample, [ppm]
CXE	CO_2-expanded ethanol
CXL	CO_2-expanded liquids
CXM	CO_2-expanded methanol
CXW	CO_2-expanded water
DETA	diethylenetriamine
DMF	N,N-dimethyl formamide
DMSO	dimethylsulfoxide
dpm	diphenylphosphinobenzen-m-sulphonate
EDTA	ethylenediaminetetraacetic acid

EDTA-Na_2	ethylenediaminetetraacetic acid disodium salt
EoS	equation of state
Ext.	extraction ratio in, [wt%]
FTIR	fourier transform infrared
H_2O_2	hydrogen peroxide
HD	hydrogenation degree, [mol%]
HNBR	hydrogenatd nitrile butadiene rubber
I	ICP detection for a regular sample, [ppm]
Ia	adjusted ICP detection through dividing it by the factor of 84%, [ppm]
ICP-OES	inductively coupled plasma-optical emission spectrometry
ILs	ionic liquids
Is	ICP detection for a spiked sample, [ppm]
k	Boltzmann's constant, 1.38×10-23 [J/K]
KBr	potassium bromide
k_{ij}	binary interaction between molecule ‘i’ and ‘j’, [-]
L	loss of rhodium caluculated based on the ICP detection, i.e. I, [wt%]
L_a	loss of rhodium caluclated based on the adjusted ICP detection, i.e. I_a, [wt%]
M	molecular weight, [g/mol]
m	and the number of segments per chain, [-]

M_c	weight of catalyst in one run of NBR bulk hydrogenation, [g]
MCB	monochlorobenzene
M_d	weight of the digestion solution, [g]
MEK	methyl ethyl ketone
MF	molecular fomula
M_i	molecular weight of component ‘i’, [g/mol]
M_L	weight of ligand in one run of NBR bulk hydrogenation, [g]
Mn	number average based molecular weight, [g/mol]
MP	melting point, [°C] or [K]
M_s	weight of the extraction sample, [g]
NBR	nitrile butadienerubber
P	pressure, [bar]
P_c	critical pressure, [bar]
PC-SAFT	perturbed chain statistical associating fluid theory
PFDMCH	perfluoro-1,3-dimethylcyclohexane
PFMC	perfluoro(methylcyclohexane)
PMDETA	N,N,N',N',N''-pentamethyldiethylenetriamine
PPh_3	triphenylphosphine
(R)-tolBINAP	(R)-(+)-2,2'-Bis(di-p-tolylphosphino)-1,1'-binaphthyl
$RhCl(PPh_3)_3$	tris(triphenylphosphine) chloro rhodium(I)
$RhCl(TPP)_3$	tris(triphenylphosphine) chloro rhodium(I)

$RhCl_3$	rhodium trichloride
$scCO_2$	supercritical carbon dioxide
SCF	supercritical fluid
ρ	density
SS	solvent that can dissolve it
T	temperture, [°C] or [K]
t	time, [h]
T_c	critical temperature, [°C] or [K]
T_g	glass transition temperature, [°C] or [K]
TMEDA	N,N,N',N'-tetramethylethylenediamine
TPP	triphenylphosphine
TPPTS	tris(sodium-m-sulfonatophenyl)phosphine
T_{ref}	reference temperature, [K]
TTA	thenoyltrifluoroacetone
TTFMPP	tris(*p*-trifluoromethylphenyl)phosphine
V_L	volume of the ligand, [mL]
VOC	volatile organic chemical
V_s	volume of the solvent, [mL]
x	mole fraction of CO_2

Appendix A
Original Experimental Data

Table A-1 Experimental parameters and extraction results obtained under 20 and 60 bar at 80 °C with N_2 added into the system†

Gas	P (bar)	M_s (g)	C (ppm)	Time (h)	M_d (g)	I (ppm)	Ext. (wt%)	Residue (ppm)
N_2	20	0.2000	705.4	1	23.2200	4.43	27	514.5
		0.1999	705.4	2	24.2347	4.19	28	508.0
		0.2005	705.4	3	24.2656	4.14	29	501.4
		0.2001	705.4	4	24.9910	3.98	29	497.7
		0.2005	705.4	5	24.0311	4.09	30	490.3
	60	0.2005	698.2	1	21.4501	4.84	26	517.8
		0.2002	698.2	2	24.2629	4.22	27	511.7
		0.2003	698.2	3	24.3462	4.16	27	506.2
		0.2004	698.2	4	24.3207	4.14	28	502.1
		0.2001	698.2	5	25.4400	3.91	29	496.8

Note: † P stands for pressure, Ms for mass of polymer matrix, C for initial concentration of Wilkinson's catalyst in HNBR matrix, Time for extraction duration, I for ICP results, Ext. for extraction ratio, Residue for the concentration of Wilkinson's catalyst remaining in HNBR matrix after extraction treatment, θ for the thickness of the HNBR film

Table A-2 Experimental parameters and extraction results obtained under various pressures (20, 40, 60, 100, 150 and 200 bar) at 80 °C on the samples with a thickness of 0.3 or 0.6 mm†

θ (mm)	P (bar)	M_s (g)	C (ppm)	Time (h)	M_d (g)	I (ppm)	Ext. (wt%)	Residue (ppm)
0.3	20	0.2005	694.3	1	23.9693	3.12	46	372.9
		0.2002	694.3	2	24.5179	2.72	52	333.1
		0.2002	694.3	3	24.9179	2.48	56	308.5
		0.2005	694.3	4	24.0603	2.33	60	279.3
		0.2000	694.3	5	25.6275	2.13	61	272.9
	40	0.2001	700.1	1	23.1539	3.38	44	391.6

		0.2003	700.1	2	21.6365	3.24	50	350.0
		0.2003	700.1	3	23.1398	2.86	53	330.4
		0.2003	700.1	4	22.5037	2.76	56	310.0
		0.2000	700.1	5	23.2682	2.59	57	301.0
	60	0.1999	701.5	1	23.0675	2.81	54	323.9
		0.2001	701.5	2	21.4949	2.52	61	271.0
		0.2007	701.5	3	23.0607	2.17	64	249.8
		0.2002	701.5	4	22.1411	2.06	67	228.2
		0.2006	701.59	5	23.2513	1.91	68	222.0
	100	0.2018	705.2	1	21.3639	4.07	39	430.5
		0.2015	705.2	2	20.497	3.55	49	360.9
		0.2035	705.2	3	20.3329	2.98	58	297.5
		0.2046	705.2	4	22.2346	2.69	59	292.3
		0.2040	705.2	5	23.1909	2.52	59	286.9
	150	0.2000	697.8	1	25.2364	3.52	36	443.7
		0.2003	697.8	2	24.519	3.00	47	367.8
		0.2003	697.8	3	23.3502	2.65	56	309.6
		0.2000	697.8	4	24.2347	2.47	57	299.4
		0.2000	697.8	5	24.3503	2.45	57	298.1
	200	0.2004	705	1	23.5021	3.02	50	354.9
		0.2002	705	2	25.8073	2.27	58	292.9
		0.2001	705	3	25.5133	2.28	59	290.3
		0.2000	705	4	25.0492	2.31	59	289.6
		0.2000	705	5	23.7131	2.43	59	288.2
0.6	20	0.2001	701.7	1	23.4547	5.19	13	608.4
		0.2003	701.7	2	22.1825	5.15	19	570.8
		0.2005	701.7	3	22.4107	4.50	28	503.4
		0.2005	701.7	4	23.5276	3.76	37	441.1
		0.2005	701.7	5	24.2176	3.62	38	437.3
	40	0.2001	701.7	1	23.4946	4.88	18	573.5
		0.2002	701.7	2	23.9866	4.30	27	514.9

	0.2001	701.7	3	24.1178	3.82	34	460.7
	0.2005	701.7	4	24.982	3.33	41	414.9
	0.2005	701.7	5	24.8938	3.29	42	408.9
60	0.2003	701.7	1	24.9301	4.15	26	516.6
	0.2000	701.7	2	23.6785	3.66	38	433.6
	0.2000	701.7	3	23.5185	3.22	46	378.8
	0.2001	701.7	4	24.2279	2.81	51	340.9
	0.2005	701.7	5	24.0382	2.84	51	340.6
100	0.2005	704.2	1	25.0432	4.67	17	583.2
	0.2005	704.2	2	24.8594	3.75	34	464.8
	0.2005	704.2	3	24.1911	3.40	42	409.7
	0.2005	701.2	4	23.5921	3.39	43	399.0
	0.2005	701.2	5	24.7742	3.10	45	382.5
150	0.2000	697.8	1	25.2364	4.17	24	526.8
	0.2003	697.8	2	24.5190	3.57	37	436.7
	0.2003	697.8	3	23.3502	3.15	47	367.5
	0.2000	697.8	4	24.2347	2.93	49	355.5
	0.2000	697.8	5	24.3503	2.91	49	354.0
200	0.2005	704.2	1	23.7554	5.12	14	606.8
	0.2003	704.2	2	25.6420	3.84	30	491.7
	0.2005	704.2	3	24.9431	3.18	44	395.8
	0.2005	704.2	4	23.8688	3.28	44	390.7
	0.2000	704.2	5	23.2026	3.34	45	387.7

Notes: † refer to Table A-1, θ stands for the thickness of the HNBR film.

Table A-3 Experimental parameters and extraction results obtained under various pressures (0, 20, 40, 60, 100, 200 bar) and temperatures (40, 50, 60, 70, 80, 90, and 100 °C)†

P (bar)	T (°C)	ρ (g/mL)	Ms (g)	C_0 (ppm)	Time (h)	M_d (g)	I (ppm)	Ext. (wt%)	Residue (ppm)
atm	40	0	0.2000	694.3	1	23.8541	5.67	3	675.8
			0.2005	694.3	2	24.7198	5.15	8	635.5
			0.2002	694.3	3	25.1716	4.83	12	607.8
			0.2003	694.3	4	24.0426	4.83	16	580.3
			0.2003	694.3	5	24.2891	4.67	18	566.2
	50	0	0.2002	704.97	1	25.1004	5.07	10	635.2
			0.2002	704.97	2	24.6595	4.77	17	587.2
			0.2002	704.97	3	23.1238	4.87	20	562.9
			0.2004	704.97	4	23.7586	4.57	23	541.6
			0.2002	704.97	5	24.2923	4.34	25	526.1
	60	0	0.2012	706.0	1	22.5372	5.46	13	611.6
			0.2001	706.0	2	21.9956	5.09	21	559.3
			0.2000	706.0	3	23.9947	4.40	25	528.4
			0.2004	706.0	4	22.9926	4.37	29	501.9
			0.1998	706.0	5	23.4033	4.24	30	496.9
	80	0	0.1999	706.0	1	21.0588	5.47	18	576.7
			0.2002	706.0	2	23.5538	4.23	29	498.2
			0.2005	706.0	3	23.2654	3.81	37	442.7
			0.2014	706.0	4	23.8189	3.41	43	403.2
			0.2010	706.0	5	20.4167	4.01	42	407.3
20	40	0.0371	0.1998	702.1	1	22.0399	6.17	3	680.9
			0.1999	702.1	2	23.2849	5.30	12	617.4
			0.2001	702.1	3	23.3276	4.88	19	569.4
			0.2004	702.1	4	23.5688	4.72	21	554.9
			0.2000	702.1	5	24.0753	4.38	25	527.6
	50	0.0356	0.1999	702.1	1	24.6426	4.72	17	581.4
			0.2005	702.1	2	23.5172	4.26	29	499.7

P (bar)	T (°C)	ρ (g/mL)	Ms (g)	C_0 (ppm)	Time (h)	M_d (g)	I (ppm)	Ext. (wt%)	Residue (ppm)
			0.2000	702.1	3	24.0646	3.85	34	463.7
			0.2005	702.1	4	23.9180	3.78	36	451.0
			0.2000	702.1	5	22.7309	3.74	39	425.1
	60	0.0342	0.2000	702.1	1	23.2808	4.55	25	529.6
			0.2000	702.1	2	23.3052	3.73	38	434.5
			0.2001	702.1	3	24.5209	3.15	45	385.9
			0.2000	702.1	4	23.5353	3.08	48	363.0
			0.2003	702.1	5	22.9476	2.93	52	336.0
	70	0.0330	0.1999	702.1	1	23.6846	3.59	39	425.7
			0.2001	702.1	2	23.3397	3.04	49	355.1
			0.2000	702.1	3	23.8171	2.74	54	326.3
			0.2004	702.1	4	22.7781	2.66	57	302.0
			0.1999	702.1	5	23.9829	2.39	59	286.7
	80	0.0318	0.2005	694.3	1	23.9693	3.12	46	372.9
			0.2002	694.3	2	24.5179	2.72	52	333.1
			0.2002	694.3	3	24.9179	2.48	56	308.5
			0.2005	694.3	4	24.0603	2.33	60	279.3
			0.2000	694.3	5	25.6275	2.13	61	272.9
	90	0.0308	0.2005	700.1	1	23.9064	3.20	46	381.2
			0.2002	700.1	2	23.0818	2.86	53	330.0
			0.2005	700.1	3	22.5711	2.65	57	298.3
			0.2003	700.1	4	23.8750	2.36	60	281.5
			0.2003	700.1	5	23.9041	2.29	61	273.9
	100	0.0298	0.2000	705.4	1	23.6721	3.38	43	400.2
			0.1999	705.4	2	24.7860	2.81	51	348.3
			0.2005	705.4	3	24.0890	2.54	57	305.4
			0.2001	705.4	4	24.7016	2.27	60	280.6
			0.2005	705.4	5	24.8359	2.24	61	277.9
40	40	0.0838	0.2001	704.1	1	25.0168	4.73	16	592.0

P (bar)	T (°C)	ρ (g/mL)	Ms (g)	C_0 (ppm)	Time (h)	M_d (g)	I (ppm)	Ext. (wt%)	Residue (ppm)
			0.2002	704.1	2	23.1910	4.47	26	518.3
			0.2002	704.1	3	24.4154	3.94	32	480.5
			0.1999	704.1	4	23.5433	3.75	37	441.8
			0.2004	704.1	5	22.8860	3.73	39	426.5
	50	0.0789	0.1998	704.1	1	22.7575	4.70	24	535.1
			0.1999	704.1	2	22.7033	3.83	38	435.7
			0.2002	704.1	3	23.5200	3.31	45	389.5
			0.2003	704.1	4	23.7656	3.18	46	377.0
			0.2001	704.1	5	23.0912	2.97	51	343.0
	60	0.0747	0.1999	704.1	1	25.0420	3.92	30	491.6
			0.1999	704.1	2	23.9281	3.23	45	386.7
			0.2001	704.1	3	23.4518	2.95	51	345.9
			0.2001	704.1	4	24.9411	2.63	53	329.0
			0.2005	704.1	5	23.6640	2.50	58	294.9
	70	0.0712	0.2006	704.1	1	23.6805	3.68	38	434.9
			0.2005	704.1	2	22.7733	3.00	52	341.1
			0.2000	704.1	3	23.8355	2.58	56	308.1
			0.2005	704.1	4	23.9493	2.52	57	300.6
			0.2000	704.1	5	23.0787	2.20	64	253.9
	80	0.0680	0.2001	700.1	1	23.1539	3.38	44	391.6
			0.2003	700.1	2	21.6365	3.24	50	350.0
			0.2003	700.1	3	23.1398	2.86	53	330.4
			0.2003	700.1	4	22.5037	2.76	56	310.0
			0.2000	700.1	5	23.2682	2.59	57	301.0
	90	0.0652	0.2005	700.1	1	22.6772	3.14	49	355.7
			0.2003	700.1	2	24.6234	2.76	51	339.9
			0.2000	700.1	3	24.3114	2.52	56	306.8
			0.2003	700.1	4	24.6745	2.27	60	279.1
			0.2005	700.1	5	23.3089	2.19	64	255.1

P (bar)	T (°C)	ρ (g/mL)	Ms (g)	C_0 (ppm)	Time (h)	M_d (g)	I (ppm)	Ext. (wt%)	Residue (ppm)
	100	0.0627	0.2005	705.4	1	23.4698	3.10	48	363.4
			0.2002	705.4	2	24.9099	2.74	52	340.4
			0.2002	705.4	3	24.573	2.53	56	311.1
			0.2003	705.4	4	24.7098	2.30	60	283.9
			0.2000	705.4	5	23.5008	2.25	62	264.6
60	40	0.1493	0.2002	703.5	1	22.9813	5.12	16	587.5
			0.2009	703.5	2	23.7948	4.57	23	541.8
			0.2007	703.5	3	23.2358	4.47	26	517.7
			0.2003	703.5	4	22.5675	4.50	28	506.9
			0.2003	703.5	5	24.8045	4.09	28	507.2
	50	0.1352	0.2002	695.8	1	23.6689	4.65	21	549.7
			0.2005	695.8	2	24.4417	3.98	30	485.0
			0.2002	695.8	3	25.7544	3.43	37	441.7
			0.2004	695.8	4	24.1280	3.32	43	399.2
			0.2002	695.8	5	25.3339	3.10	44	392.0
	60	0.1249	0.1999	705.6	1	25.4064	3.82	31	485.2
			0.2001	705.6	2	23.8366	3.37	43	402.0
			0.1998	705.6	3	23.1124	3.30	46	382.3
			0.1998	705.6	4	24.4826	2.86	50	351.0
			0.2005	705.6	5	24.9845	2.80	51	348.4
	70	0.1168	0.2001	694.3	1	24.5968	3.47	39	426.4
			0.2005	694.3	2	23.1551	3.05	49	352.2
			0.2	694.3	3	24.0506	2.85	51	342.5
			0.2002	694.3	4	23.4894	2.67	55	313.8
			0.2	694.3	5	23.5438	2.57	56	302.4
	80	0.1101	0.1999	701.5	1	23.0675	2.81	54	323.9
			0.2001	701.5	2	21.4949	2.52	61	271.0
			0.2007	701.5	3	23.0607	2.17	64	249.8
			0.2002	701.5	4	22.1411	2.06	67	228.2

P (bar)	T (°C)	ρ (g/mL)	Ms (g)	C_0 (ppm)	Time (h)	M_d (g)	I (ppm)	Ext. (wt%)	Residue (ppm)
			0.2006	701.5	5	23.2513	1.91	68	222.0
	90	0.1045	0.2009	701.5	1	22.3071	2.49	61	276.1
			0.2005	701.5	2	22.6166	1.95	69	219.7
			0.2000	701.5	3	21.1479	1.98	70	209.9
			0.2000	701.5	4	23.0434	1.65	73	190.4
			0.2002	701.5	5	21.8354	1.59	75	173.5
	100	0.0996	0.2002	698.2	1	24.227	2.18	62	263.3
			0.2003	698.2	2	24.5772	1.81	68	221.7
			0.1998	698.2	3	23.9407	1.68	71	200.9
			0.2002	698.2	4	25.0295	1.45	74	181.3
			0.1998	698.2	5	22.7268	1.47	76	167.7
80	100	0.1413	0.2000	705.0	1	24.6975	2.08	64	256.9
			0.2002	705.0	2	25.0440	1.76	69	220.4
			0.2003	705.0	3	24.0723	1.54	74	184.8
			0.2001	705.0	4	23.3098	1.46	76	169.7
			0.2000	705.0	5	23.7391	1.46	75	173.1
100	40	0.6286	0.2003	703.5	1	22.0863	5.62	12	620.3
			0.2004	703.5	2	22.7613	4.93	20	559.8
			0.2002	703.5	3	24.7508	4.46	22	551.6
			0.2003	703.5	4	22.4283	4.94	21	552.7
			0.2003	703.5	5	23.8182	4.41	25	524.5
	50	0.3843	0.1999	705.2	1	22.0300	5.28	18	581.4
			0.1979	705.2	2	22.5240	4.64	25	528.4
			0.1443	705.2	3	22.1795	3.37	27	517.3
			0.1998	705.2	4	22.3159	4.61	27	514.9
			0.1998	705.2	5	23.3013	4.21	30	491.5
	60	0.2899	0.2037	705.2	1	22.2097	4.73	27	515.4
			0.2019	705.2	2	21.5303	4.35	34	464.2
			0.2002	705.2	3	22.2116	4.03	37	447.3

P (bar)	T (°C)	ρ (g/mL)	Ms (g)	C_0 (ppm)	Time (h)	M_d (g)	I (ppm)	Ext. (wt%)	Residue (ppm)
			0.2008	705.2	4	22.7305	3.81	39	431.8
			0.2006	705.2	5	20.6538	4.07	41	419.5
	70	0.2478	0.2015	705.2	1	21.3738	4.43	33	469.9
			0.2013	705.2	2	21.6466	3.89	41	418.2
			0.2014	705.2	3	20.3832	3.77	46	381.9
			0.205	705.2	4	22.5434	3.31	48	363.6
			0.2048	705.2	5	21.9481	3.27	50	350.3
	80	0.2216	0.2018	705.2	1	21.3639	4.07	39	430.5
			0.2015	705.2	2	20.4970	3.55	49	360.9
			0.2035	705.2	3	20.3329	2.98	58	297.5
			0.2046	705.2	4	22.2346	2.69	59	292.3
			0.204	705.2	5	23.1909	2.52	59	286.9
	90	0.2029	0.1999	708.3	1	24.1445	3.48	41	420.1
			0.2004	708.3	2	24.9277	2.79	51	347.2
			0.2004	708.3	3	22.4710	2.61	59	292.5
			0.2000	708.3	4	23.6520	2.29	62	270.6
			0.2003	708.3	5	24.0330	2.22	62	266.2
	100	0.1886	0.2002	698.2	1	24.8245	3.09	45	383.0
			0.2001	698.2	2	22.6832	2.95	52	334.8
			0.1999	698.2	3	23.0527	2.56	58	295.8
			0.2000	698.2	4	25.3393	2.14	61	271.0
			0.1998	698.2	5	25.4602	2.11	61	268.9
200	40	0.8398	0.2001	695.4	1	23.8001	5.41	8	643.2
			0.2001	695.4	2	24.2808	4.60	20	558.0
			0.2001	695.4	3	24.4070	4.34	24	529.6
			0.2003	695.4	4	23.8923	4.29	26	511.3
			0.2002	695.4	5	25.1416	3.89	30	488.9
	50	0.7843	0.2	695.8	1	23.8424	4.76	18	567.3
			0.2004	695.8	2	24.6312	3.91	31	481.3

P (bar)	T (°C)	ρ (g/mL)	Ms (g)	C_0 (ppm)	Time (h)	M_d (g)	I (ppm)	Ext. (wt%)	Residue (ppm)
			0.2001	695.8	3	23.8383	3.74	36	445.3
			0.2001	695.8	4	23.1321	3.64	39	421.0
			0.2003	695.8	5	22.9517	3.50	42	401.1
	60	0.7237	0.2002	705.6	1	24.7999	3.61	37	446.7
			0.2000	705.6	2	22.6906	3.30	47	374.0
			0.2000	705.6	3	22.2153	3.23	49	359.0
			0.2003	705.6	4	23.2601	2.95	51	342.3
			0.2001	705.6	5	24.8585	2.61	54	324.9
	70	0.6590	0.1999	701.9	1	22.7103	4.28	31	485.9
			0.2002	701.9	2	22.4929	3.96	37	444.9
			0.2000	701.9	3	23.2339	3.60	40	418.5
			0.1999	701.9	4	22.1835	3.55	44	394.6
			0.2004	701.9	5	23.8679	3.15	46	375.8
	80	0.5939	0.2004	705.0	1	23.5021	3.02	50	354.9
			0.2002	705.0	2	25.8073	2.27	58	292.9
			0.2001	705.0	3	25.5133	2.28	59	290.3
			0.2000	705.0	4	25.0492	2.31	59	289.6
			0.2000	705.0	5	23.7131	2.43	59	288.2
	90	0.5332	0.2012	703.5	1	25.1589	2.44	57	305.2
			0.2002	703.5	2	25.4416	2.13	61	271.1
			0.2008	703.5	3	23.7511	2.23	63	263.6
			0.2005	703.5	4	22.6465	2.28	63	257.8
			0.2005	703.5	5	23.6311	2.01	66	237.0
	100	0.4805	0.2005	698.2	1	24.9927	3.20	43	398.8
			0.2002	698.2	2	24.3134	2.59	55	314.1
			0.2003	698.2	3	24.1526	2.60	55	313.5
			0.2004	698.2	4	23.6250	2.62	56	309.0
			0.2001	698.2	5	24.4720	2.48	57	303.5

Notes: † See notes of Table A-1. ρ for the density of CO_2.

Bibliography

[1] P. W. N. M. v. Leeuwen, *Homogeneous Catalysis: Understanding the Art*, Kluwer Academic Publishers, Dordrecht **2000**.

[2] D. J. Cole-Hamilton, R. P. Tooze, *Catalyst Separation, Recovery and Recycling*, Vol. 30, Springer, Dordrecht **2006**.

[3] S. Bhattacharjee, A. K. Bhowmick, B. N. Avasthi, in *Handbook of Engineering Polymeric Materials*, (Ed: N. P. Cheremisinoff), Marcel Dekker, Inc., New York **1997**, 555.

[4] Z. Wei, J. Wu, Q. Pan, G. L. Rempel, *Macromol. Rapid Commun.* **2005**, *26*, 1768.

[5] G. L. Rempel, Q. Pan, J. Wu, *United States Patent 7345115*, **2008**.

[6] A. K. Lele, A. D. Shine, *AlChE J.* **1992**, *38*, 742.

[7] P. D. Condo, D. R. Paul, K. P. Johnston, *Macromolecules* **1994**, *27*, 365.

[8] M. Lee, C. Tzoganakis, C. B. Park, *Adv. Polym. Tech.* **2000**, *19*, 300.

[9] D. L. Tomasko, H. Li, D. Liu, X. Han, M. J. Wingert, L. J. Lee, K. W. Koelling, *Ind. Eng. Chem. Res.* **2003**, *42*, 6431.

[10] S. P. Nalawade, F. Picchioni, L. P. B. M. Janssen, *Prog. Polym. Sci.* **2006**, *31*, 19.

[11] S. Üzer, U. Akman, Ö. Hortaçsu, *J. Supercrit. Fluids* **2006**, *38*, 119.

[12] G. R. Akien, M. Poliakoff, *Green Chem.* **2009**, *11*, 1083.

[13] P. G. Jessop, B. Subramaniam, *Chem. Rev.* **2007**, *107*, 2666.

[14] H. Jin, B. Subramaniam, A. Ghosh, J. Tunge, *AlChE J.* **2006**, *52*, 2575.

[15] J. L. Gohres, C. L. Kitchens, J. P. Hallett, A. V. Popov, R. Hernandez, C. L. Liotta, C. A. Eckert, *J. Phys. Chem. B* **2008**, *112*, 4666.

[16] S. Sicardi, L. Manna, M. Banchero, *J. Supercrit. Fluids* **2000**, *17*, 187.

[17] F. H. Jardine, Ed. *Chlorotris(triphenylphosphine)rhodium(I): Its Chemical and Catalytic Reactions*, Vol. 28, John Wiley & Sons, Inc, New York **1981**.

[18] G. Favero, P. Rigo, *Gazz. Chim. Ital.* **1972**, *102*, 597.

[19] S. J. Anderson, A. H. Horbury, *J. Chem. Soc., Chem. Commun.* **1974**, 37.

[20] F. Faraone, *J. Chem. Soc., Dalton Trans.* **1975**, *6*, 541.

[21] S. Bresadola, B. Longato, *Inorg. Chem.* **1974**, *13*, 539.

[22] S. Bresadola, B. Longato, F. Morandini, *Coord. Chem. Rev.* **1975**, *16*, 19.

[23] B. Çetinkaya, M. F. Lappert, S. Torroni, *J. Chem. Soc., Chem. Commun.* **1979**, 843.

[24] B. Çetinkaya, M. F. Lappert, J. McMeeking, *J. Chem. Soc., Dalton Trans.* **1973**, 1975.

[25] R. W. Mitchell, J. D. Ruddick, G. Wilkinson, *J. Chem. Soc. (A)* **1971**, 3224.

[26] J. A. Osborn, F. H. Jardine, J. F. Young, G. Wilkinson, *J. Chem. Soc. (A)* **1966**, *12*, 1711.

[27] D. R. Eaton, S. R. Suart, *J. Am. Chem. Soc.* **1968**, *90*, 4170.

[28] R. H. Grubbs, L. C. Kroll, *J. Am. Chem. Soc.* **1971**, *93*, 3062.

[29] R. H. Grubbs, L. C. Kroll, *Polym. Prepr. (Am. Chem. Soc., Div. Polym. Chem.)* **1971**, *12*, 423.

[30] R. H. Grubbs, L. C. Kroll, E. M. Sweet, *J. Macromol. Sci. Chem.* **1973**, *7*, 1047.

[31] C. U. Pittman, L. R. Smith, R. M. Hanes, *J. Am. Chem. Soc.* **1975**, *97*, 1742.

[32] M. Bartholin, C. Graillat, A. Guyot, G. Coudurier, J. Bandiera, C. Naccache, *J. Mol. Catal.* **1977**, *3*, 17.

[33] E. Bayer, V. Schurig, *Angew. Chem. Int. Ed.* **1975**, *14*, 493.

[34] P. Blond, A. Rio, G. Cordier, G. Edelga, Y. Sangouard, *J. Mol. Catal.* **1978**, *4*, 181.

[35] T. D. Madden, P. J. Quinn, *Biochem. Soc. Trans.* **1978**, *6*, 1345.

[36] M. A. Bennett, T. W. Turney, *Aust. J. Chem.* **1973**, *26*, 2321.

[37] J. F. Nixon, M. Kooti, *J. Organomet. Chem.* **1978**, *149*, 71.

[38] T. Nishiguchi, K. Tachi, K. Fukuzumi, *J. Org. Chem.* **1975**, *40*, 240.

[39] M. C. Baird, D. N. Lawson, J. T. Mague, J. A. Osborn, G. Wilkinson, *Chem. Commun.* **1966**, 129.

[40] M. C. Baird, G. J. Hartwell, R. Mason, A. I. M. Rae, G. G. Wilkinson, *Chem. Commun.* **1967**, 92.

[41] M. C. Baird, G. Wilkinson, *J. Chem. Soc. (A)* **1967**, 865.

[42] D. Chapman, P. J. Quinn, *PNAS* **1976**, *73*, 3971.

[43] R. Grigg, F. Heaney, J. Idle, A. Somasunderam, *Tetrahedron Lett.* **1990**, *31*, 2767.

[44] T. Nishiguchi, K. Tachi, K. Fukuzumi, *J. Org. Chem.* **1975**, *40*, 237.

[45] P. Li, W. Thitsartarn, S. Kawi, *Ind. Eng. Chem. Res.* **2009**, *48*, 1824.

[46] V. V. Grushin, H. Alper, *Organometallics* **1993**, *12*, 3846.

[47] B. Marciniec, *Silicon Chemistry* **2002**, *1*, 155.

[48] M. Capka, J. Hetflejs, V. M. Vdovin, V. E. Fedorov, N. A. Pritula, G. K. Fedorova, *React. Kinet. Catal. Lett.* **1986**, *31*, 41.

[49] J. Hagen, *Industrial Catalysis: A Practical Approach*, WILEY-VCH Verlag GmbH&Co. KGaA, Weinheim **2006**.

[50] D. L. Beach, K. W. Barnett, *J. Organomet. Chem.* **1977**, *142*, 225.

[51] W. J. Dejarlais, E. A. Emken, *Lipids* **1976**, *11*, 594.

[52] J. Kramer, E. Nöllen, W. Buijs, W. L. Driessen, J. Reedijk, *React. Funct. Polym.* **2003**, *57*, 1.

[53] J. Kramer, J. A. Erkelens, A. R. García, W. L. Driessen, J. Reedijk, *New J. Chem.* **2002**, *26*, 822.

[54] A. T. Bell, *Science* **2003**, *299*, 1688.

[55] A. Kirschning, W. Solodenko, K. Mennecke, *Chem. Eur. J.* **2006**, *12*, 5972.

[56] D. J. Cole-Hamilton, *Science* **2003**, *299*, 1702.

[57] M. D. Jones, R. Raja, J. M. Thomas, B. F. G. Johnson, *Top. Catal.* **2003**, *25*, 71.

[58] J. M. Thomas, R. Raja, D. W. Lewis, *Angew. Chem. Int. Ed.* **2005**, *44*, 6456.

[59] D. E. D. Vos, M. Dams, B. F. Sels, P. A. Jacobs, *Chem. Rev.* **2002**, *102*, 3615.

[60] C. E. Song, S.-g. Lee, *Chem. Rev.* **2002**, *102*, 3495.

[61] C. A. McNamara, M. J. Dixon, M. Bradley, *Chem. Rev.* **2002**, *102*, 3275.

[62] M. Benaglia, A. Puglisi, F. Cozzi, *Chem. Rev.* **2003**, *103*, 3401.

[63] R. v. Heerbeek, P. C. J. Kamer, P. W. N. M. v. Leeuwen, J. N. H. Reek, *Chem. Rev.* **2002**, *102*, 3717.

[64] A. P. Wight, M. E. Davis, *Chem. Rev.* **2002**, *102*, 3589.

[65] M. H. Valkenberg, W. F. Hölderich, *Cat. Rev. - Sci. Eng.* **2002**, *44*, 321.

[66] L. Alaerts, J. Wahlen, P. A. Jacobs, D. E. D. Vos, *Chem. Commun.* **2008**, 1727.

[67] R. H. Grubbs, E. M. Sweet, *J. Mol. Catal.* **1977/78**, *3*, 259.

[68] V. Fiandanese, P. Mastrorilli, C. F. Nobile, A. Punzi, *J. Mol. Catal. A: Chem.* **1998**, *136*, 111.

[69] R. Giannandrea, P. Mastrorilli, G. Zaccaria, C. F. Nobile, *J. Mol. Catal. A: Chem.* **1996**, *109*, 113.

[70] A. J. Wright, S. Reynier, S. Skonieczny, L. L. Diosady, *IJASE* **2003**, *1,2*, 89.

[71] L. Wang, M. Jia, S. Shylesh, T. Philippi, A. Seifert, S. Ernst, A. P. Singh, W. R. Thiel, *ChemCatChem* **2010**, *2*, 1477.

[72] M. Bartholin, J. Conan, A. Guyot, *J. Mol. Catal.* **1977**, *2*, 307.

[73] K. Kochloefl, W. Liebelt, *J. Chem. Soc., Chem. Commun.* **1977**, 510.

[74] D. Cauzzi, M. Lanfranchi, G. Marzolini, G. Predieri, A. Tiripicchio, M. Costa, R. Zanoni, *J. Organomet. Chem.* **1995**, *488*, 115.

[75] D. Cauzzi, M. Costa, L. Gonsalvi, M. A. Pellinghelli, G. Predieri, A. Tiripicchio, R. Zanoni, *J. Organomet. Chem.* **1997**, *541*, 377.

[76] M. Bartók, G. Szöllösi, Á. Mastalir, I. Dékány, *J. Mol. Catal. A: Chem.* **1999**, *139*, 227.

[77] P. R. Rony, J. F. Roth, *J. Mol. Catal.* **1975/76**, *1*, 13.

[78] S. Banerjee, S. S. Wong, *J. Am. Chem. Soc.* **2002**, *124*, 8940.

[79] P. Mastrorilli, A. Rizzuti, G. P. Suranna, C. F. Nobile, *Inorg. Chim. Acta* **2000**, *304*, 17.

[80] R. V. Chaudhari, A. Bhattacharya, B. M. Bhanage, *Catal. Today* **1995**, *24*, 123.

[81] F. Raynal, R. Barhdadi, J. Périchon, A. Savall, M. Troupel, *Adv. Synth. Catal.* **2002**, *344*, 45.

[82] M. Yuan, H. Chen, R. Li, Y. Li, X. Li, *Appl. Catal., A* **2003**, *251*, 181.

[83] V. Kotzabasakis, E. Georgopoulou, M. Pitsikalis, N. Hadjichristidis, G. Papadogianakis, *J. Mol. Catal. A: Chem.* **2005**, *231*, 93.

[84] V. Kotzabasakis, N. Hadjichristidis, G. Papadogianakis, *J. Mol. Catal. A: Chem.* **2009**, *304*, 95.

[85] G. L. Rempel, Q. Pan, J. Wu, *United Sates Patent 7385010*, **2008**.

[86] A. Bouriazos, K. Mouratidis, N. Psaroudakis, G. Papadogianakis, *Catal. Lett.* **2008**, *121*, 158.

[87] E. Wiebus, B. Cornils, in *Catalyst Separation, Recovery and Recycling*, Vol. 30 (Eds: D. J. Cole-Hamilton, R. P. Tooze), Springer, Dordrecht **2006**, 105.

[88] I. T. Horváth, J. Rábai, *Science* **1994**, *266*, 72.

[89] D. F. Foster, D. Gudmunsen, D. J. Adams, A. M. Stuart, E. G. Hope, D. J. Cole-Hamilton, G. P. Schwarz, P. Pogorzelec, *Tetrahedron* **2002**, *58*, 3901.

[90] C. C. Tzschucke, *Angew. Chem. Int. Ed.* **2002**, *41*, 3964.

[91] G. Pozzi, I. Shepperson, *Coord. Chem. Rev.* **2003**, *242*, 115.

[92] A. P. Dobbs, M. R. Kimberley, *J. Fluorine Chem.* **2002**, *118*, 3.

[93] B. Croxtall, J. Fawcett, E. G. Hope, A. M. Stuart, *J. Chem. Soc., Dalton Trans.* **2002**, 491.

[94] E. G. Hope, R. D. W. Kemmitt, D. R. Paige, A. M. Stuart, D. R. W. Wood, *Polyhedron* **1999**, *18*, 2913.

[95] I. Horváth, G. Kiss, R. A. Cook, J. E. Bond, P. A. Stevens, J. Rabai, E. J. Mozeleski, *J. Am. Chem. Soc.* **1998**, *120*, 3133.

[96] D. Sinou, D. Maillard, A. Aghmiz, A. M. M. i-Bultó, *Adv. Synth. Catal.* **2003**, *345*, 603.

[97] B. Richter, E. d. Wolf, G. v. Koten, B.-J. Deelman, *J. Org. Chem.* **2000**, *65*, 3885.

[98] E. Wolf, A. J. M. Mens, O. L. J. Gijzeman, J. H. v. Lenthe, L. W. Jenneskens, B.-J. Deelman, G. v. Koten, *Inorg. Chem.* **2003**, *42*, 2115.

[99] M.-A. Guillevic, C. Rocaboy, A. M. Arif, I. T. Horváth, J. A. Gladysz, *Organometallics* **1998**, *17*, 707.

[100] E. G. Hope, R. D. W. Kemmitt, D. R. Paige, A. M. Stuart, *J. Fluorine Chem.* **1999**, *99*, 197.

[101] T. Welton, *Chem. Rev.* **1999**, *99*, 2071.

[102] P. Wasserscheid, W. Keim, *Angew. Chem. Int. Ed.* **2000**, *39*, 3772.

[103] P. Wasserscheid, T. Welton, Eds., *Ionic Liquids in Synthesis*, Wiley-VCH, Weinheim **2002**.

[104] J. D. Holbrey, A. E. Visser, R. D. Rogers, Eds., *Solubility and Solvation in Ionic Liquids* Wiley-VCH, Weinheim **2003**.

[105] T. Welton, Ed. *Polarity*, Wiley-VCH, Weinheim **2003**.

[106] P. Wasserscheid, H. Waffenschmidt, P. Machnitzki, K. W. Kottsieper, O. Stelzer, *Chem. Commun.* **2001**, 451.

[107] F. Favre, H. Olivier-Bourbigou, D. Commereuc, L. Saussine, *Chem. Commun.* **2001**, 1360.

[108] J. Sirieix, M. Ossberger, B. Betzemeier, P. Knochel, From, *Synlett* **2000**, 1613.

[109] K. W. Kottsieper, O. Stelzer, P. Wasserscheid, *J. Mol. Catal. A: Chem.* **2001**, *175*, 285.

[110] L. A. Blancard, D. Hancu, E. J. Beckman, J. F. Brennecke, *Nature* **1999**, *399*, 28.

[111] P. G. Jessop, W. leitner, in *Chemical Synthesis Using Supercritical Fluids*, (Eds: P. G. Jessop, W. leitner), WILEY-VCH Verlag GmbH, Weinheim **1999**.

[112] F. Liu, M. B. Abrams, R. T. Baker, W. Tumas, *Chem. Commun.* **2001**, 433.

[113] R. A. Brown, P. Pollet, E. McKoon, C. A. Eckert, C. L. Liotta, P. G. Jessop, *J. Am. Chem. Soc.* **2001**, *123*, 1254.

[114] M. F. Sellin, P. B. Webb, D. J. Cole-Hamilton, *Chem. Commun.* **2001**, 781.

[115] A. I. Cooper, *J. Mater. Chem.* **2000**, *10*, 207.

[116] J. A. Darr, M. Poliakoff, *Chem. Rew.* **1999**, *99*, 495.

[117] M. A. McHugh, V. Krukonis, *Supercritical Fluid Extraction: Principals and Practice*, Butterworth-Heinemann, Toronto **1994**.

[118] J. ke, B. Han, M. W. George, H. Yan, M. Poliakoff, *J. Am. Chem. Soc.* **2001**, *123*, 3661.

[119] T. Sarbu, T. Styranec, E. J. Beckman, *Nature* **2000**, *405*, 165.

[120] K. Zosel, *Angew. Chem. Int. Ed.* **1978**, *17*, 702.

[121] S. Kainz, P.-D. Daniel Koch, W. Leitner, W. Baumann, *Angew. Chem. Int. Ed.* **1997**, *36*, 1628.

[122] G. Franciò, W. Leitner, *Chem. Commun.* **1999**, 1663.

[123] D. J. Adams, W. Chen, E. G. Hope, S. Lange, A. M. Stuart, A. West, J. Xiao, *Green Chem.* **2003**, *5*, 118.

[124] G. Franciò, K. Wittmann, W. Leitner, *J. Organomet. Chem.* **2001**, *621*, 130.

[125] E. L. V. Goetheer, A. W. Verkerk, L. J. P. v. d. Broeke, E. d. Wolf, B.-J. Deelman, G. v. Koten, J. T. F. Keurentjes, *J. Catal.* **2003**, *219*, 126.

[126] M. J. Burk, S. Feng, M. F. Gross, W. Tumas, *J. Am. Chem. Soc.* **1995**, *117*, 8277.

[127] S. Kainz, A. Brinkmann, W. Leitner, A. Pfaltz, *J. Am. Chem. Soc.* **1999** *121*, 6421.

[128] S. Lange, A. Brinkmann, P. Trautner, K. Woelk, J. Bargon, W. Leitner, *Chirality* **2000**, *12*, 450.

[129] O. R. Davies, A. L. Lewis, M. J. Whitaker, H. Tai, K. M. Shakesheff, S. M. Howdle, *Adv. Drug Del. Rev.* **2008**, *60*, 373.

[130] I. Kikic, F. Vecchione, *Curren. Opin. Solid ST. M.* **2003**, *7*, 399.

[131] I. Tsivintzelis, A. G. Angelopoulou, C. Panayiotou, *Polymer* **2007**, *48*, 5928.

[132] J. P. Hallett, J. W. Ford, R. S. Jones, P. Pollet, C. A. Thomas, C. L. Liotta, C. A. Eckert, *Ind. Eng. Chem. Res.* **2008**, *47*, 2585.

[133] M. C. McLeod, M. Anand, C. L. Kitchens, C. B. Roberts, *Nano Lett.* **2005**, *5*, 461.

[134] D. J. Dixon, K. P. Johnston, R. A. Bodmeier, *AlChE J.* **1993**, *39*, 127.

[135] A. M. Scurto, K. W. Hutchenson, B. Subramaniam, Eds., *Gas-Expanded Liquids: Fundamentals and Applications*, Vol. 1006, ACS Symposium Series, Washington D. C. **2009**.

[136] K. W. Hutchenson, A. M. Scurto, B. Subramaniam, *Gas-Expanded Liquids and Near-Critical Media*, Vol. 1006, **2009**.

[137] I.-H. Lin, C.-S. Tan, *J. Supercrit. Fluids* **2008**, *46*, 112.

[138] V. T. Wyatt, D. Bush, J. Lu, J. P. Hallett, C. L. Liotta, C. A. Eckert, *J. Supercrit. Fluids* **2005**, *36*, 16.

[139] C. L. Shukla, J. P. Hallett, A. V. Popov, R. Hernandez, C. L. Liotta, C. A. Eckert, *J. Phys. Chem. B* **2006**, *110*, 24101.

[140] J. L. Gohres, A. V. Popov, R. Hernandez, C. L. Liotta, C. A. Eckert, *JCTC* **2009**, *5*, 267.

[141] J. L. Gohres, A. T. Marin, J. Lu, C. L. Liotta, C. A. Eckert, *Ind. Eng. Chem. Res.* **2009**, *48*, 1302.

[142] R. R. Weikel, J. P. Hallett, C. L. Liotta, C. A. Eckert, *Ind. Eng. Chem. Res.* **2007**, *46*, 5252.

[143] J. P. Hallett, P. Pollet, C. L. Liotta, C. A. Eckert, *Acc. Chem. Res.* **2008**, *41*, 458.

[144] X. Xie, C. L. Liotta, C. A. Eckert, *Ind. Eng. Chem. Res.* **2004**, *43*, 2605.

[145] Y.-C. Chen, C.-S. Tan, *J. Supercrit. Fluids* **2007**, *41*, 272.

[146] J. S. Parent, *Catalytic Hydrogenation of Butadiene Copolymers*, Ph.D, Chemical Engineering Department, University of Waterloo, Waterloo **1996**.

[147] C. B. Ojeda, F. S. Rojas, *Talanta* **2007**, *71*, 1.

[148] D. R. Palo, C. Erkey, *J. Chem. Eng. Data* **1998**, *43*, 47.

[149] D. R. Palo, C. Erkey, *Ind. Eng. Chem. Res.* **1998**, *37*, 4203.

[150] J. M. Desimone, Z. Guan, C. S. Elsbernd, *Science* **1992**, *257*, 945.

[151] K. E. Laintz, E. Tachikawa, *Anal. Chem.* **1994**, *66*, 2190.

[152] Z. Marczenko, E. kowalczyk, *Anal. Chim. Acta* **1979**, *108*, 261.

[153] J. R. Hart, "Ethylenediaminetetraacetic Acid and Related Chelating Agents" in *Ullmann's Encyclopedia of Industrial Chemistry*, Wiley-VCH Verlag GmbH & Co. KGaA, **2000**.

[154] K. Eller, E. Henkes, R. Rossbacher, H. Höke, "Amines, Aliphatic" in *Ullmann's Encyclopedia of Industrial Chemistry*, Wiley-VCH Verlag GmbH & Co. KGaA, **2000**.

[155] G. Fraenkel, "N,N,N',N',N"-pentamethyldiethylenetriamine" in *e-EROS Encyclopedia of Reagents for Organic Synthesis*, New York: John Wiley & Sons Ltd., Wiley InterScience (Online service) **2001**.

[156] R. K. Haynes, S. C. Vonwiller, "Tetramethylethylenediamine" in *e-EROS Encyclopedia of Reagents for Organic Synthesis*, New York: John Wiley & Sons Ltd., Wiley InterScience (Online service) **2006**.

[157] F. L. Garvan, Ed. *Metal Chelates of Ethylenediaminetetraacetic Acid and Related Substances*, Academic Press Inc., New York **1964**.

[158] C. F. Bell, *Principles and Applications of Metal Chelation*, Oxford University Press, Oxford **1977**.

[159] E. Brunner, *J. Chem. Thermodyn.* **1985**, *17*, 671.

[160] A.-D. Leu, S. Y.-K. Chung, D. B. Robinson, *J. Chem. Thermodynamics* **1991**, *23*, 979.

[161] S.-D. Yeo, S.-J. Park, J.-W. Kim, J.-C. Kim, *J. Chem. Eng. Data* **2000**, *45*, 932.

[162] M. L. Clarke, D. Ellis, K. L. Mason, A. G. Orpen, P. G. Pringle, R. L. Wingad, D. A. Zaher, R. T. Baker, *Dalton* **2005**, 1294.

[163] N. von Solms, J. Kristensen, *Int. J. Refrig.* **2010**, *33*, 19.

[164] N. A. Mohammadi, G. L. Rempel, *Macromolecules* **1987**, *20*, 2362.

[165] J. S. Parent, N. T. MacManus, G. L. Rempel, *Ind. Eng. Chem. Res.* **1996**, *35*, 4417.

[166] W. G. Chapman, K. E. Gubbins, G. Jackson, M. Radosz, *Ind. Eng. Chem. Res.* **1990**, *29*, 1709.

[167] J. Gross, G. Sadowski, *Ind. Eng. Chem. Res.* **2002**, *41*, 5510.

[168] N. v. Solms, M. L. Michelsen, G. M. Kontogeorgis, *Ind. Eng. Chem. Res.* **2003**, *42*, 1098.

[169] J. Gross, G. Sadowski, *Ind. Eng. Chem. Res.* **2001**, *40*, 1244.

[170] J. Gross, G. Sadowski, *Ind. Eng. Chem. Res.* **2002**, *41*, 1084.

[171] F. Tumakaka, J. Gross, G. Sadowski, *Fluid Phase Equilib.* **2002**, *194-197*, 541.

[172] J. Gross, O. Spuhl, F. Tumakaka, G. Sadowski, *Ind. Eng. Chem. Res.* **2003**, *42*, 1266.

[173] I. A. Kouskoumvekaki, N. v. Solms, T. Lindvig, M. L. Michelsen, G. M. Kontogeorgis, *Ind. Eng. Chem. Res.* **2004**, *43*, 2830.

[174] F. Becker, M. Buback, H. Latz, G. Sadowski, F. Tumakaka, *Fluid Phase Equilib.* **2004**, *215*, 263.

[175] M. Kleiner, F. Tumakaka, G. Sadowski, H. Latz, M. Buback, *Fluid Phase Equilib.* **2006**, *241*, 113.

[176] L. A. Román-Ramírez, F. García-Sánchez, C. H. Ortiz-Estrada, D. N. Justo-García, *Ind. Eng. Chem. Res.* **2010**, *49*, 12276.

[177] J.-H. Yoon, H.-S. Lee, H. Lee, *J. Chem. Eng. Data* **1993**, *38*, 53.

[178] E. Brunner, W. Hültenschmidt, G. Schlichtharle, *J. Chem. Thermodyn.* **1987**, *19*, 273.

[179] S. H. Page, S. R. Goates, M. L. Lee, *J. Supercrit. Fluids* **1991**, *4*, 109.

[180] K. Ohgaki, T. Katayama, *J. Chem. Eng. Data* **1976**, *21*, 53.

[181] C. J. Chang, C.-Y. Day, C.-M. Ko, K.-L. Chiu, *Fluid Phase Equilib.* **1997**, *131*, 243.

[182] K. Suzuki, H. Sue, *J. Chem. Eng. Data* **1990**, *35*, 63.

[183] P. B. Zetterlund, F. Aldabbagh, M. Okubo, *J. Polym. Sci., Part A: Polym. Chem.* **2009**, *47*, 3711.